International Journal of Biological Macromolecules

Designing Sustainable Soil Conditioners: Nanocomposite-Based Thermoplastic Starch for Enhanced Soil Health and Crop Performance

--Manuscript Draft--

Manuscript Number:	IJBIOMAC-D-24-29188R1
Article Type:	Research Paper
Section/Category:	Carbohydrates, Natural Polyacids and Lignins
Keywords:	Soil water retention, NPK absorption, UV-C degradation resistance, Sustainable agriculture
Corresponding Author:	Marystela Ferreira UFSCar - Campus Sorocaba Sorocaba, SP BRAZIL
First Author:	Jéssica Rodrigues
Order of Authors:	Jéssica Rodrigues
	Amanda de Freitas
	Henrique Vieira
	Lívia Emidio
	Stefanny Amaro
	Mariana Azevedo
	Iolanda Duarte
	Vagner Botaro
	Leonardo Fraceto
	Marystela Ferreira
Abstract:	The growing demand for sustainable solutions in agriculture, driven by global population growth and increasing soil degradation, has intensified the search for sustainable soil conditioners. This study investigated the impact of adding nanoclay (NC) and nano lignin (NL) to thermoplastic starch (TPS) on its physical, chemical, and thermal properties, its effectiveness as a soil conditioner, and its resistance to UV-C degradation. TPS nanocomposites were prepared with varying NC (3%, 5%, 7%) and NL (0.3%, 0.5%, 0.7%) proportions and characterized by FTIR, SEM, TGA, and DSC. Swelling tests, phosphate buffer solubility, cation exchange capacity (CEC), and UV-C degradation resistance were evaluated. Results indicated that incorporating 7% NC (TPS/NC7%) significantly improved TPS's CEC and swelling properties. Adding 0.3% NL (TPS/NC7%/NL0.3%) improved photodegradation resistance and thermal stability. The TPS/NC7%/NL0.3% nanocomposites also demonstrated superior water retention in soil, efficient absorption and controlled release of nitrogen, phosphorus and potassium (NPK) fertilizer, significant reduction in the leaching of ions, and antimicrobial activity against both Gram-positive and Gram-negative bacteria, highlighting their biodegradability and potential as soil conditioners to promote agricultural sustainability. Additionally, tests conducted on cherry tomatoes confirmed the effectiveness of these nanocomposites under real cultivation conditions, with improved seedling development when using the TPS/NC7%/NL0.3% soil conditioner.
Suggested Reviewers:	Pascal Wong-Wah-Chung pascal.wong-wah-chung@univ-amu.fr
	Xuetao Guo guoxuetao2005@nwafu.edu.cn
	Jean-Luc Gardette luc.gardette@univ-bpclermont.fr
Opposed Reviewers:	

Response to Reviewers:	Sorocaba, SP, Brazil, January 03, 2025 Dr. Mario M Martinez Editor International Journal of Biological Macromolecules Ref: Revised version – IJBIOMAC-D-24-29188 The authors thank the Reviewers for their valuable comments and remarks regarding this manuscript. We have addressed all comments and suggestions adequately. The requested alterations/corrections have been inserted directly into the manuscript (significant changes are highlighted in yellow) and are described below. Yours sincerely, Dr. Marystela Ferreira, Corresponding author Designing Sustainable Soil Conditioners: Nanocomposite-Based Thermoplastic Starch for Enhanced Soil Health and Crop Performance Jéssica S. Rodriguesa1, Amanda S. M de Freitasa,b1, Henrique O. S. Vieirab, Lívia S. Emidiob, Stefanny F. Amarob, Mariana A. Azevedob, Iolanda C. S. Duarteb, Vagner R. Botarob, Leonardo F. Fracetoa, Marystela Ferreirab aInstitute of Science and Technology of Sorocaba, São Paulo State University (UNESP), Av.Três de Março 511, 18087-180, Sorocaba, SP, Brazil. b Science and Technology Center for Sustainability (CCTS), Federal University of São Carlos (UFSCar), João Leme dos Santos, km 110, 18052-780, Sorocaba, SP, Brazil. 1 These authors contributed equally to the manuscript Corresponding author: marystela@ufscar.br Response Letter Reviewer #1: 1. Abstract should be more exact concerning the statements, such as "enhanced swelling properties" (line27), where it is not clear whether it should be higher or lower Answer: The sentence was modified: “Results indicated that incorporating 7% NC (TPS/NC7%) significantly improved the CEC and the swelling properties of TPS.” 2. The abbreviation NPK is not explained. Answer: The acronym NPK was explained as “…nitrogen, phosphorus and potassium (NPK) fertilizer.” 3. In keywords "biodegradability" is mentioned, however, this is in contradiction with some standards, requiring maximum amount of nonbiodegradable components being 5 wt %, while in all samples the montmorillojnite content is 7 wt %. Answer: We appreciate the observation regarding the standards that limit the content of non-biodegradable components to 5% by weight. Although the 7% content exceeds the mentioned limit, the material maintains predominant biodegradability characteristics due to the biodegradable polymer matrix. However, to avoid conceptual errors, this keyword has been removed. 4. L. 52 - what is polystyreneplored? Answer: This word doesn't make sense in the sentence; it must have been a typo. The

sentence has been corrected: “Materials such as starch, lignin, and clay are now recognized as innovative and accessible solutions to enhance agricultural productivity.”

5. L. 63 - what means one-dimensional particles?
Answer: Thank you for your question about "one-dimensional particles." In this context, "one-dimensional particles" refer to materials that exhibit nanoscale dimensions in one direction while having much larger dimensions in the other two. Specifically, these particles are typically characterized by their high aspect ratio, meaning their length and width are significantly greater than their thickness.
Clay nanoparticles, such as montmorillonite, are considered one-dimensional because they exist as platelets or sheets with nanometer-scale thickness (typically 1-2 nm) but lateral dimensions in the range of several micrometers. This unique geometry allows them to interact effectively with organic monomers and polymers, creating clay-polymer nanocomposites with enhanced properties.
The term highlights their structural uniqueness, crucial for the improvements observed in modulus, mechanical strength, flame resistance, heat resistance, and barrier properties when these nanoparticles are incorporated into a polymer matrix.

6. L. 76 what is the reason for plant ability to enhanced water and nutrients abruption?
Answer: Thank you for your question about the mechanism behind the plant's increased ability to absorb water and nutrients when lignin is applied. We have inserted a paragraph to enrich this discussion due to its relevance to the manuscript. “This improvement can be attributed to several factors. Lignin acts as a biostimulant, promoting root growth and increasing root surface area, which improves soil exploration and nutrient uptake [15]. Additionally, lignin derivatives can enhance soil structure, improve water retention, and facilitate root nutrient access. Its bioactive compounds, such as phenolics, stimulate enzymatic and metabolic activities in plants, optimizing absorption processes [16].”

7. Ls 89-90, mentioning the increased reactivity is vague, in my view the reactivity is the same just the surface increase leads to an increase of reactive sites.
Answer: In fact, the term "increased reactivity" may seem vague in this context, so the text was more precisely formulated. “This enhanced availability of reactive sites makes processes more efficient, enabling the use of smaller quantities of material and reducing costs.”

8. L. 123, mentioning Morsali (2022) seems as a quotation, it should be properluy numbers and inserted among the literature. I remember there was also another similar item somewhere.
Answer: All text has been reviewed and corrected in 3 different places. Thank you for noticing.
Morsali et al. (2022)[26], Kharissova et al. (2021)[33], Levana et al. (2023)[32], Macedo et al. (2023)[44]

9. L. 132, PD preparation, usually a kind of sheasr is applied to get thermoplastic starch.
Answer: In our study, thermoplastic starch was obtained using only heat, degreasing, and the combination of the plasticizing agent’s glycerol and water. The material obtained presented the plating characteristics.

10. L. 161 Thermal events are mentioned to take as the second scan. The used sentence means that this was done also for TGA, that would be really strange to discuss TGA second run.
Answer: The sentence was modified to highlight that the second heating was used only for DSC analysis. “Thermal events were identified and quantified during the second heating scan for DSC analyses, supported by TRIOS® software.”

11. L. 167 - 168, for 30 and 60 minutes until a constant mass was reached - TOTALLY UNCLEAR. Pls be more exact whemn describing the procedure.
Answer: The sentence was modified: “Approximately 0.1 g of the nanocomposite was added to 10 mL beakers containing 5 mL of phosphate buffer solution (pH 5, 7, and 9) for 30 min.”

12. Solubility - total mess. First in Hnadbooks solubility of various materials is listed, in that case usually the content of the material forming saturated solution is published, it is needed to give temperature and pressure. I guess you are determining the soluble or extractable portion, not solubility
Answer: Thank you for your observation. You are correct that our methodology evaluates the soluble or extractable fraction of the material, not the solubility in the classical sense (e.g., the concentration of the material in a saturated solution at a specific temperature and pressure). We have revised the text accordingly to clarify this distinction and avoid any potential misinterpretation. The revised term "soluble fraction determination" better describes the method and results.
Soluble Fraction Determination: The determination of the soluble fraction of the samples in phosphate buffer solutions (pH 5.0, 7.0, and 9.0) was performed following the method of Gontard, Guilbert, and Cuq (1992)[28], with some adaptations. Initially, the dry matter percentage of the samples was determined by weighing them after drying in an oven at 70°C for 2 h. The samples were then immersed in 20 mL of phosphate buffer solution (pH 5.0, 7.0, and 9.0) and maintained under slow agitation at 38°C for 24 h. After this period, each solution was filtered, and the retained material was dried in an oven at 70°C for 24 h until a constant mass was achieved. The amount of non-soluble dry matter was determined using Equation 2
Soluble Fraction (%) =(Wi - Wf)/Wf x 100 (Equation 2)
Where: Wi = initial mass of dry material and Wf = final mass of non-solubilized dry material.

13. The data in the Table 1 seem to show interestin and perhaps important results. However, the Table is almost useless for most readers since it does not explain the individual columns, such as TR, R600, etc. In fact for all Fugures and Tables the description should enable to understand the information without necessity to read the text of the publication.
Answer: A caption has been added to the table to explain the columns and facilitate understanding of the data: “aInitial degradation temperature of 5%; bTemperature of the maximum degradation rate; cMass loss rate up to Tmax; dFinal degradation temperature; e Temperature difference associated with thermal transition; fThe coal amount at the end of degradation process in 600°C.”

14. In fact, insufficient explanation is given for changes of data in Table 1 with changing the concentrations. In some case it is logical, in others it is random, no trend, or even opposite regarding the expectation, e.g. for T5%.
Answer: Thank you for your observation. We have revised and expanded the section to explain better the variations in the thermal parameters presented in Table 1. The lack of a clear trend in some samples can be attributed to factors such as:
Heterogeneity in the dispersion of the nanocomposites: The interaction between the components can vary due to differences in the compatibility and distribution of lignin (NL) in the polymer matrix.
Trade-offs between thermal stabilization and degradation of additives: The initial increase in T5% (as observed at 0.3% NL) can be due to the formation of strong interactions between the NC, NL, and the matrix. However, higher concentrations (0.7% NL) can lead to saturation or agglomeration, impairing homogeneous heat transfer.

In the text, we have explained how intermolecular interactions and NL dispersion impact the observed thermal parameters.
“The variability observed in the T5% values, as shown in Table 1, is attributed to the complexity of the thermal decomposition process in these composite systems. The interaction between TPS, NC, and NL introduces multiple decomposition mechanisms influenced by the proportion of each component. While the sample with 0.3% NL displayed the highest T5% (190°C), indicating improved initial thermal resistance, the samples with 0.5% and 0.7% NL exhibited lower values (165°C and 98°C, respectively). This lack of a consistent trend can be explained by potential phase segregation or non-uniform dispersion of the nanoaditives in the matrix, which could reduce the effectiveness of thermal stabilization in some cases. This is consistent with findings in similar systems, where optimal properties are often achieved at specific additive concentrations due to balanced interactions within the composite matrix [36].

Tmax also varied among the samples, reflecting thermal resistance during decomposition. The TPS/NC7% sample showed a Tmax of 350°C, while the NL-added samples exhibited values of 362°C (TPS/NC7%/NL0.3%), 390°C (TPS/NC7%/NL0.5%), and 364°C (TPS/NC7%/NL0.7%). The highest Tmax was observed in TPS/NC7%/NL0.5%, indicating superior thermal resistance, possibly due to greater interaction between the polymer matrix and the nanoaditives [13]. Δm at Tmax also displayed variations. The TPS/NC7% sample experienced a mass loss of 49%, while the NL-containing samples showed losses of 47% (TPS/NC7%/NL0.3%), 59% (TPS/NC7%/NL0.5%), and 52% (TPS/NC7%/NL0.7%). The high mass loss observed in the sample TPS/NC7%/NL0.5% might indicate that at this specific composition, the thermal decomposition is dominated by the degradation of NL, which is consistent with its higher Tmax.
The Tf was derived from the TGA curves, with the TPS/NC7% sample showing the highest Tf of 542°C. The modified samples showed slightly lower Tf values: 539°C for TPS/NC7%/NL0.3%, 532°C for TPS/NC7%/NL0.5%, and 511°C for TPS/NC7%/NL0.7%. These reductions indicate that the presence of nanocomposites can influence the temperature at which decomposition ends. The ΔT varied from 458°C for TPS/NC7% to 342°C for TPS/NC7%/NL0.3%, 370°C for TPS/NC7%/NL0.5%, and 414°C for TPS/NC7%/NL0.7%. The TPS/NC7% sample exhibited the largest ΔT, indicating a broader decomposition range, while the addition of NL resulted in narrower decomposition ranges. Finally, the R600°C was higher in the samples containing NL, with values of 17% (TPS/NC7%/NL0.3%), 16% (TPS/NC7%/NL0.5%), and 15% (TPS/NC7%/NL0.7%), compared to 12% for the TPS/NC7% sample. This suggests that NL promotes the formation of a stable carbonaceous structure, likely due to its aromatic composition, which resists complete degradation."

15. L. 456 - phase transition or specific degradation process, obviously the authors have no idea whats going on.
Answer: We appreciate the constructive critique. We have revisited this section and expanded the analysis to justify the peaks observed in the DSC curves. These peaks were associated with specific phase transitions, such as the glass transition of starch (70°C), and structural changes promoted by NL, including matrix reorganizations and potential chemical interactions. Previous studies support the notion that the presence of lignin, with its complex and highly aromatic structure, can induce additional thermal events due to its initial degradation or structural rearrangement. The revised text now clearly explains that the observed thermal events are related to the intrinsic properties of starch and the effects of varying NL concentrations.

16. L. 455 the number of decimal points is too optimistic. I wonder what is the statter of the values if you would repeat each measurement on DSC three times.
Answer: We acknowledge the reviewer's concern about the decimal points. The values in this manuscript represent the average of three measurements, and the deviation between replicates was less than 0.5°C, ensuring the reliability of the reported results. For clarity, we will simplify the decimal points to two significant figures in the revised manuscript.

17. Following statements should be made more clear
- L. 207 - sieves? Ensuer homogeneity? L. 224 tops of the PETs? L. 231-232, 273-274?
- L. 352 lower water solubility, 353 more significant awelling?
- L. 471-472 impossible to understand, shat you mean with similar behaviour?
- L. 545 Leached weakly - another puzzle?
- L. 554 – unclear
Answer: As requested, the necessary alterations were made to the text, and the changes have been highlighted in yellow for your review.

18. Concerning the effect of NL on TGA data, I recommend to run TGA of virgin NL.
Answer: We appreciate the suggestion; running TGA on virgin NL is not essential for this study. The thermal behavior of lignin, including its degradation temperature and char residue formation, has been extensively characterized in the literature and is well-documented. In this study, our focus was on understanding the impact of NL when incorporated into the TPS/NC matrix. The observed thermal improvements, such as increased T5% and Tmax, strongly suggest the formation of new interactions between the matrix and NL. These interactions, rather than the standalone thermal properties of

NL, are the primary contributors to the improved thermal stability of the composites. By referring to established data for lignin, we ensured that our analysis remains focused on the synergistic effects within the composite material, aligning with the core objective of this work.

19. Whole part of 3.2.2. is based on the data in Supplementary section. In my view this is incorrect. Either put it in main text or delete whole section
Answer: Thank you for your comment. While we understand your concern regarding the reliance on Supplementary data, we would like to emphasize that we consider Section 3.2.2 to be a crucial part of the manuscript. It provides a detailed analysis of the impact of UV-C exposure on the stability and photodegradation of the nanocomposites, which is central to understanding the behavior of the materials studied. This discussion is essential for the comprehensive interpretation of the results and for the overall relevance of the study.
Therefore, we have decided to retain this section in the manuscript, with the supplementary data included, as the images and figures are essential to illustrating the conclusions discussed in this section. However, we have made efforts to ensure that the main conclusions and key findings of Section 3.2.2 are clearly explained in the main text so that readers can understand the significance of the results, even though the detailed figures are provided in the Supplementary section.

20. L.538 539, permeability and water retention are two different properties, they do not necessarily correspond and must be deiscissed independently. Pls check the definition of permeability.
Answer: Thank you for your insightful comment. Upon review, we realize that the analysis conducted in our study focused on water retention rather than permeability. Therefore, we have revised the section to discuss water retention explicitly, as this was the primary focus of the experimental setup. The revised version of the text now adequately addresses the water retention properties of the nanocomposites and removes any reference to permeability, which was not analyzed in this experiment. We believe this clarification resolves the issue.
‘In Figure S6, the control soil, without additives (Control), showed an initial water retention of around 160%, which was used as a reference. The addition of TPS to the soil increased this retention to approximately 180%, which was attributed to the hygroscopic nature of TPS. The polar groups in TPS strongly interacted with water molecules, forming hydrogen bonds and enhancing water absorption [13]. When NC were added (TPS/NC7%), water retention slightly decreased, reaching around 170%. This suggested that the presence of NC influenced the composite structure, making it denser and reducing its ability to hold moisture, as it became less effective at retaining water.
When NL was added (TPS/NC7%/NL0.3%), water retention was further reduced, down to approximately 150%. This effect was explained by the hydrophobic properties of lignin, which hindered water absorption by the starch and nano clay matrix [42]. NL acted as an additional barrier, reducing the water retention of the composite by decreasing its ability to absorb and retain moisture.”

21. English is in some parts not quite understandable, e.g. L. 68 "significantly benefit plant development".
Answer: Thank you for your comment. We have revised the sentence for clarity. The revised version reads:
"Also, lignin can be used as a soil conditioner due to its physical, chemical, thermal, and biological properties, which greatly enhance plant growth and development [12,13]."

- L. 115, glycerine and glycerol are the two different chemicals? What means P.A.?
Answer: In response to your query, glycerine and glycerol refer to the same chemical compound, $C_3H_8O_3$; sorry for the error. The term "P.A." stands for "Purissimum Analysis," which indicates that the chemical is of analytical grade, meaning it is suitable for laboratory use due to its high purity.

- L 200 Very awkward expression, perhaps something like: The distance between the sample and the lamp…
"The distance between the sample and the lamp was maintained at 20 cm for 21 days."
Answer: Other parts of the manuscript have been revised for clarity in English.

	Reviewer #2: The paper's primary objective requires more nanoparticle characterization studies. Microscopy morphology studies and nanoparticle size distribution are the minimum evidence for nano approval. After that, more studies are needed about the diffusion of nanoparticles as a function of size into the crop via soil. Is there evidence that excess nanoparticles are in crops? Comments: We appreciate your comments and suggestions. However, we would like to clarify that the primary objective of this study was to investigate the effectiveness of thermoplastic starch (TPS)-based nanocomposites with the addition of nanoclay (NC) and nanolignin (NL) as soil conditioners, focusing on their physical, chemical, and thermal properties and their resistance to UV-C degradation. While nanoparticle characterization is an important aspect for further approval in studies of their interactions with soil and plants, the emphasis of this study was on evaluating their effectiveness under practical cultivation conditions and their impact on soil health and plant performance. The novelty of this paper lies precisely in the practical application of nanocomposites as soil conditioners and their direct impact on plant performance and agricultural sustainability. By focusing on the effectiveness of the developed materials as soil conditioners, our results demonstrate how adding NC and NL improves key characteristics such as cation exchange capacity (CEC), water retention, UV-C degradation resistance, and controlled nutrient release. These aspects are crucial for promoting soil health and plant growth, which are the central objectives of this study. In this context, we performed the essential characterizations for the scope of the work, including sample morphology analysis (SEM), particle size distribution (TGA and DSC), soil water retention, cation exchange capacity (CEC), UV-C degradation resistance, and NPK fertilizer absorption and controlled release tests. These tests provide a comprehensive view of how the nanocomposites influence soil structure, water retention, nutrient release, and degradation protection, which are crucial for assessing their effectiveness as soil conditioners. Additionally, we would like to emphasize that the NC used in this study is commercial. Therefore, its characteristics have already been extensively described in the literature, making additional characterization unnecessary. As for the NL, it was developed in other studies in the literature, as mentioned in the manuscript, and its properties have been previously explored, so a further in-depth characterization of these properties was not required for this study. Regarding the additional characterization of nanoparticles, we recognize its importance in specific research contexts. However, based on the scope of this study, we opted not to delve into the diffusion of nanoparticles in plants, as this study focused primarily on the beneficial effects of the nanocomposites on the soil and plant health without directly exploring the migration of nanoparticles to the crops. Existing literature suggests that NL and NC have properties that allow plants to modulate soil characteristics and nutrient uptake, as observed in the tomato plant tests. Furthermore, we did not observe any evidence of adverse effects on plant development or excessive accumulation of nanoparticles in the crops tested, suggesting that the nanoparticles do not accumulate in the plants in a harmful way. A more detailed analysis of nanoparticle safety and behavior in plants can be addressed in future studies, but it was beyond the scope and objectives of the current work. Therefore, we believe that the characterizations conducted were adequate for the objectives of this study and provided valuable insights into the potential of nanocomposites as sustainable soil conditioners. The suggestion to include more studies on nanoparticle diffusion into plants, while relevant in another context, falls outside the central theme of this study, which focuses on the application of the nanocomposites in soil and their impact on soil properties and plant growth.

Designing Sustainable Soil Conditioners: Nanocomposite-Based Thermoplastic Starch for Enhanced Soil Health and Crop Performance

Jéssica S. Rodrigues[a1], Amanda S. M de Freitas[a,b1], Henrique O. S. Vieira[b], Lívia S. Emidio[b], Stefanny F. Amaro[b], Mariana A. Azevedo[b], Iolanda C. S. Duarte[b], Vagner R. Botaro[b], Leonardo F. Fraceto[a], Marystela Ferreira[b]

[a]Institute of Science and Technology of Sorocaba, São Paulo State University (UNESP), Av.Três de Março 511, 18087-180, Sorocaba, SP, Brazil.

[b] Science and Technology Center for Sustainability (CCTS), Federal University of São Carlos (UFSCar), João Leme dos Santos, km 110, 18052-780, Sorocaba, SP, Brazil.

[1] These authors contributed equally to the manuscript

Corresponding author: marystela@ufscar.br

ABSTRACT

The growing demand for sustainable solutions in agriculture, driven by global population growth and increasing soil degradation, has intensified the search for sustainable soil conditioners. This study investigated the impact of adding nanoclay (NC) and nano lignin (NL) to thermoplastic starch (TPS) on its physical, chemical, and thermal properties, its effectiveness as a soil conditioner, and its resistance to UV-C degradation. TPS nanocomposites were prepared with varying NC (3%, 5%, 7%) and NL (0.3%, 0.5%, 0.7%) proportions and characterized by FTIR (Fourier Transform Infrared Spectroscopy), SEM (Scanning Electron Microscopy), TGA (Thermogravimetric Analysis), and DSC (Differential Scanning Calorimetry). Swelling tests, phosphate buffer solubility, cation exchange capacity (CEC), and UV-C degradation resistance were evaluated. Results indicated that incorporating 7% NC (TPS/NC7%) significantly improved TPS's CEC and swelling properties. Conversely, adding 0.3% NL (TPS/NC7%/NL0.3%) improved photodegradation resistance and thermal stability. The TPS/NC7%/NL0.3% nanocomposites also demonstrated superior water retention in soil, efficient absorption and controlled release of nitrogen, phosphorus and potassium (NPK) fertilizer, significant reduction in the leaching of NH_4^+, $H_2PO_4^-$, and K^+ ions, and antimicrobial activity against both Gram-positive and Gram-negative bacteria, highlighting their biodegradability and potential as soil conditioners to promote agricultural sustainability. Additionally, tests conducted on cherry tomatoes confirmed the effectiveness of these nanocomposites under real cultivation conditions, with improved seedling development when using the TPS/NC7%/NL0.3% soil conditioner.

Keywords: Soil water retention, NPK absorption, UV-C degradation resistance, sustainable agriculture.

1. Introduction

The rapid population growth and increasing demand for agricultural land drive the need for higher food production, particularly as the global population reaches 8 billion [1,2]. This puts significant pressure on agricultural systems, creating major challenges for global food security while negatively impacting soils, with severe consequences for human health and ecosystem sustainability [3]. In this context, seeking innovative and efficient techniques to mitigate these damages becomes crucial, with the conversion of waste into soil conditioners emerging as a highly effective approach [1,2].

Soil conditioners are crucial in promoting plant growth, enhancing soil health, and reducing the need for chemical fertilizers [4]. Recently, a notable effort has been to incorporate microorganisms into soil conditioners to boost carbon sequestration. Using living organisms, such as earthworms, to produce vermicompost - a nutrient-rich organic fertilizer - has emerged as a beneficial approach [5]. At the same time, nanotechnology has gained traction in agriculture, showing promising results [6], suggesting that nanoscale materials can be effective agents in soil conditioners. Materials such as starch, lignin, and clay are now recognized as innovative and accessible solutions to enhance agricultural productivity. Beyond their critical role in agriculture, these composites are applied across various sectors, including aerospace, construction, sports, marine, and personal protection [7].

Thermoplastic starch (TPS) is a promising biopolymer that can replace conventional polymers, mainly when derived from cassava starch combined with a selected plasticizer [8,9]. This material can absorb fluids, respond readily to water, and excel in soil moisture retention. Meanwhile, clay, an essential element for soil fertility, plays a pivotal role in sustainable soil management [10]. Its cation exchange capacity (CEC) influences ion exchange, pollutant migration, and nutrient availability. In this context, nanoclay (NC) enhances the properties of traditional clay. These nanoscale, one-dimensional particles can be modified to form clay complexes compatible with organic monomers and polymers [11], offering benefits such as significant improvements in modulus, mechanical strength, flame resistance, heat resistance, and barrier properties.

In addition, lignin can be used as a soil conditioner due to its physical, chemical, thermal, and biological properties, greatly enhancing plant growth and development [12,13]. It improves soil structure by increasing its porosity and water retention capacity. Additionally, lignin's functional groups, such as carboxyl and phenolic, enhance the soil's CEC. This helps improve the availability of essential nutrients like potassium, calcium, and magnesium while reducing nutrient leaching. Lignin achieves this by forming complexes with these nutrients,

preventing them from being rapidly washed away by irrigation or rainwater [14]. Lignin can also serve as a substrate for beneficial soil microorganisms, as its gradual decomposition increases the organic matter content in the soil, which is essential for soil fertility. Furthermore, lignin acts as a biostimulant, promoting root growth and enhancing the plant's ability to absorb water and nutrients. This improvement can be attributed to several factors. Lignin acts as a biostimulant, promoting root growth and increasing root surface area, which improves soil exploration and nutrient uptake [15].

Additionally, lignin derivatives can enhance soil structure, improve water retention and facilitating root access to nutrients. Its bioactive compounds, such as phenolics, stimulate enzymatic and metabolic activities in plants, optimizing absorption processes [16]. Its antioxidant properties also play a crucial role in protecting plants from oxidative stress caused by adverse conditions such as drought, salinity, or pathogen attacks [17].

Lignin's role as a UV blocker has shown positive results in protecting certain groups of microorganisms and promoting their growth [9]. Studies have demonstrated that lignin can protect bacteria, fungi, and specific viruses used in pest control when added to pesticide formulations [18]. Lignin also preserves *Pichia anomala* (strain K) and other antagonistic yeasts used as biocontrol agents against post-harvest diseases from UV radiation. Furthermore, adding lignin, especially in its nanostructured form, plays a vital role in protecting *Escherichia coli* from UV-induced mortality, with enhanced results when nano lignin are employed [19].

Nanoscale materials, such as nano lignin (NL), have garnered significant interest from researchers due to their unique properties and ability to enhance particle reactivity through a high surface area [20]. This improved availability of reactive sites makes processes more efficient, enabling the use of smaller quantities of material and reducing costs. In addition to its well-known applications, nano lignin has recently been used as a reinforcing agent in composites and hybrid nanocomposites across a wide range of applications. Its ability to bind tightly with various biopolymers significantly improves materials' thermal and mechanical properties [21].

This study investigated the combined effects of TPS, NC, and NL as soil conditioners. Previous studies had demonstrated the individual benefits of TPS when combined with NL and NC, highlighting enhancements in mechanical and thermal strength, increased water retention capacity, and good biodegradability [22–25]. However, more research is needed to address the synergistic interaction of these three components in a single nanocomposite and their combined impact on soil quality. The simultaneous inclusion of NL, known for its antioxidant, antimicrobial, and UV-blocking properties, along with NC, which enhances CEC, offered

substantial potential to optimize soil conditioners' physical and chemical properties and improve nutrient availability and soil aeration. Moreover, the effectiveness of these nanocomposites was tested on red cherry tomatoes, providing proof of concept in greenhouse conditions. Thus, this study sought valuable insights into how these nanocomposites could improve soil quality and contribute to more sustainable agricultural practices.

2. Materials and methods

2.1 Materials

The lignin used in this research was extracted from *Eucalyptus urograndis* through the kraft process in the production of cellulose and paper, supplied by the company Suzano, located in the state of São Paulo, Brazil. The soluble starch (ACS), ammonium acetate ($NH_4C_2H_3O_2$), barium chloride ($BaCl_2$), and potassium hydroxide (KOH) were provided by Êxodo Científica. Anidrol supplied the glycerol ($C_3H_8O_3$). The NC used was hydrophilic bentonite (Montmorillonite), and potassium chloride (KCl) were obtained from Sigma-Aldrich. Acetone (C_3H_6O), hydrochloric acid (HCl), and phenolphthalein ($C_{20}H_{14}O_4$) were sourced from Synth. The NPK fertilizer used in the soil conditioner evaluation was Fertilizante Mineral Misto 10-10-10+micros (Boron (0.06%), Sulfur (1%), Iron (0.03%), Magnesium (0.03%), and Zinc (0.10%)) from Dimy®, and the soil used was from Forth®. The red cherry tomato seeds were obtained from Feltrin Sementes®. Mueller Hinton Broth was supplied by Difco.

2.2 Lignin Nanoparticles Synthesis

NL was synthesized using the antisolvent precipitation method, as detailed by Morsali *et al.* (2022)[26]. Initially, 0.5 g of pre-dried kraft lignin (KL) was dissolved in a solution containing 30 g of acetone and 10 g of deionized water under constant stirring for 3 h at room temperature. The solution was filtered through a 0.45 μm pore membrane (Millipore) to remove undissolved solids. To form a colloidal dispersion of KL, 120 g of deionized water was added to the stirring solution. Finally, the acetone was removed using a rotary evaporator under reduced pressure at a temperature of 40°C.

2.3 Sample Preparation

A mixture of 110 g of ultrapure water, 30 g of soluble starch, and 10 g of glycerol was heated under stirring until it reached approximately 80°C. This condition was maintained for 5 min to prepare the TPS sample. The exact composition was used to prepare the TPS/NC nanocomposites, but with the addition of 3%, 5%, and 7% (w/w) of NC relative to the starch mass, respectively. The addition of NC was strategically performed to enhance cation exchange capacity, soil structure stability, and controlled nutrient release. The most effective TPS/NC

(7%) composition was selected to prepare nanocomposites with NL, termed TPS/NC/NL, in proportions of 0.3%, 0.5%, and 0.7% of NL relative to the starch mass.

The solutions were transferred into Falcon tubes, each filled to approximately one-third of their total volume (~15 mL). The tubes were sealed and placed in a freezer at -18°C for 24 h. After freezing, the samples were lyophilized using a bench-top freeze dryer, Enterprise IB model from Terroni®, for 24 h at a pumping speed of 250 L/min and a temperature of -55°C. Once removed from the lyophilizer, the samples were ground using a mortar and pestle and then sieved.

2.4 Nanocomposites Characterization

Structural and Morphological Analysis: Structural characterization of the nanocomposites was performed using a Nicolet Summit IR 200 spectrometer in Attenuated Total Reflectance (ATR) mode, with 126 scans, a nominal resolution of 4.0 cm^{-1}, and a range of 4000 to 400 cm^{-1}. Morphological analysis was conducted using a Field Emission Gun Scanning Electron Microscope (JSM 7200F Japan Electron Optics Ltd.), operating in InLens mode, with an emission energy beam of 2 kV and a working distance of approximately 7 mm. The samples were coated with iridium via sputtering.

Thermal Analysis: Thermal characterization of the composites was carried out using a Perkin Elmer Pyris1 TGA with a constant heating rate of 20 °C/min up to 900°C, maintained in an inert atmosphere with a nitrogen flow rate of 20 mL/min. Thermal measurements were also conducted using a Differential Scanning Calorimeter (DSC), model Q10 from TA Instruments, USA, equipped with a RCS 40 cooling system. The samples were preheated to 100°C with a 5-minute isothermal hold to eliminate thermal history. They were then cooled to -10°C, followed by a second heating to 200°C at a rate of 20 °C/min. All measurements were performed under a 250 mL/min nitrogen flow, with sample masses maintained around 4-7 mg. Thermal events were identified and quantified during the second heating scan for DSC analyses, supported by TRIOS® software.

2.4.1 Physical Properties

Swelling: The swelling capacity in the buffer was assessed according to a method adapted from PAL and PAL (2006)[27]. Approximately 0.1 g of the nanocomposite was added to 10 mL beakers containing 5 mL of phosphate buffer solution (pH 5, 7, and 9) for 30 min. Initially, the samples were weighed dry (Ws, dry mass). After each immersion period, the samples were carefully removed, dried with absorbent paper, and weighed again (Wu, wet weight). The immersion, removal, drying, and weighing process was repeated in triplicate for each time interval. The swelling capacity was calculated according to Equation 1.

$$Swelling\ (\%)\ = \frac{Wu - Ws}{Ws}\ x\ 100 \qquad \text{(Equation 1)}$$

Soluble Fraction Determination: The determination of the soluble fraction of the samples in phosphate buffer solutions (pH 5.0, 7.0, and 9.0) was performed following the method of Gontard, Guilbert, and Cuq (1992)[28], with some adaptations. Initially, the dry matter percentage of the samples was determined by weighing them after drying in an oven at 70°C for 2 h. The samples were then immersed in 20 mL of phosphate buffer solution (pH 5.0, 7.0, and 9.0) and maintained under slow agitation at 38°C for 24 h. After this period, each solution was filtered, and the retained material was dried in an oven at 70°C for 24 h until a constant mass was achieved. The amount of non-soluble dry matter was determined using Equation 2

$$Soluble\ Fraction\ (\%)\ = \frac{Wi - Wf}{Wf}\ x\ 100 \qquad \text{(Equation 2)}$$

Where: Wi = initial mass of dry material and Wf = final mass of non-solubilized dry material.

2.4.2. Cation Exchange Capacity

The study of CEC was conducted following the Ammonium Acetate Method established by the Instituto Geográfico Agustín Codazzi.[29] 1 g of the nanocomposite was mixed with 15 mL of ammonium acetate solution (1.0 M), agitated for 20 min, and allowed to stand for 16 h to initiate cation exchange reactions. After this period, the sample was filtered and washed with a diluted ammonium acetate solution (0.01 M). Subsequently, 15 mL of KCl extraction solution (1.0 M) was added, agitated vigorously for 1 h, and filtered again. The amount of exchanged ammonium was then determined by titration with HCl (0.1 M).

2.4.3. UV-C Exposure

Photodegradation tests of the nanocomposites were conducted to assess their degradation behavior under UV-C radiation. The materials were exposed to UV-C radiation in a lab-made chamber. The lamps used were fluorescent, germicidal, 15 W in power, with a maximum emission wavelength of 254 nm, and an incident energy of 610 ± 10 μW/cm². The distance between the sample and the lamp was 20 cm for 21 days. Degradation was monitored through FTIR analyses, with measurements taken at the beginning and end of the exposure period (0 and 21 days).

2.5. Soil Conditioner Evaluation Tests

2.5.1. Soil Water Retention

To calculate water retention, 10 g of characterized soil (Supplementary Information - S1) was initially used, dried at 105°C for 24 h, and screened through a 2 mm sieve to ensure homogeneity. The soil was mixed with 2.5 g of nanocomposite (TPS, TPS/NC7%, and TPS/NC7%/NL0.3%), maintaining a ratio of 75% soil and 25% nanocomposite (V_{s+n}). This mixture was placed in a 200 mL system made from recycled PET bottles (Polyethylene Terephthalate), with drainage holes at the bottom and perforations at the top to allow airflow. Water was gradually added until the mixture was completely saturated, and the excess water drained was collected and measured. After drainage, the bottles were weighed to determine the saturated soil mass (S_s). The samples were then dried at 105°C for 24 h and weighed again to obtain the mass of the dry soil (D_s). The water retention capacity was calculated using Equation 3. The results were compared with pure soil samples to assess the effectiveness of the nanocomposites in water retention.

$$Water\ retention\ (\%) = \frac{Ss - Ds}{Vs+n}\ x\ 100 \qquad \text{(Equation 3)}$$

2.5.2 Evaluation of NPK Ion by Leaching

Leaching tests were conducted in triplicate at room temperature and neutral pH, adapting the method described by Himmah *et al.*[30] This method aimed to simulate real soil leaching conditions using the soil-film systems mentioned in Section 3.5.2. Over 9 weeks, the concentrations of N (NH_4^+), P ($H_2PO_4^-$), and K (K^+) ions present in the leaching systems were monitored. Weekly, 50 mL of distilled water was poured onto the tops of the PETs, and the collected leachate was analyzed using UV-vis spectrophotometry. A flame photometer was used for K ion release. Additional details can be found in Supplementary Files S2.

2.5.3 Soil Biodegradation

Accelerated biodegradation tests were conducted using Bartha respirators. Each unit contained 50 g of soil and 0.5 g of nanocomposites. To capture the carbon dioxide (CO_2) produced from aerobic microbial activity, 10 mL of 0.2 M KOH solution was placed in the side arm of each respirator. At least three times a week, the KOH solution from the side arm was carefully removed, transferred to an Erlenmeyer flask, and mixed with 1 mL of $BaCl_2$ (1 M) solution to precipitate the carbonate formed. The remaining KOH in the flask was titrated with a standardized HCl (0.1 M) solution to quantify the captured CO_2. Before refilling the side arm

with fresh KOH solution, it was rinsed with 10 mL of CO_2-free deionized water. The biodegradation of the materials was monitored over 50 days at 28°C, following NBR 14283 [31], with samples analyzed in triplicate and results compared to blank triplicates to measure background CO_2 levels.

2.5.4 Antimicrobial Activity

The bacterial viability was evaluated by assessing the growth of Gram-positive and Gram-negative strains, Staphylococcus aureus (ATCC 6538) and Escherichia coli (ATCC 25922), respectively, in the presence of the synthesized hybrid composites. To conduct this, 0.5 g of the material was added to 9.0 mL of Mueller Hinton Broth (MHB). Then, 1.0 mL of bacterial dispersion was standardized to 0.5 at an optical density of 600 nm (OD600), equivalent to 1×10^5 colony-forming units (CFU)·mL^{-1}, and added to the MHB. The mixtures were incubated for 24 h at 35°C. Finally, the quantification of CFU in each experimental batch was determined using a spectrophotometer (OD600). All experiments were conducted in triplicate.

2.6 Effectiveness of Soil Conditioners in Red Cherry Tomato Cultivation

To evaluate the effectiveness of soil conditioners in NPK release, five distinct compositions were tested in 1 L pots using red cherry tomatoes as the model crop. The nanocomposites evaluated were: TPS, TPS/NC7%, and TPS/NC7%/NL0.3%. A total of 6 g of each nanocomposite was swollen with 12 mL of liquid NPK solution (10-10-10). Additionally, two control groups were included: one consisting of only soil (Control) and another with soil plus 12 mL of commercial liquid NPK. Two red cherry tomato seeds were planted in pots containing 500 g of pre-homogenized soil. Each pot received one of the treatments as specified, ensuring all plants were subjected to similar conditions, except for the different soil conditioners applied. To ensure reproducibility, each treatment was replicated in six pots.

Throughout the experiment, plants were monitored weekly to assess their growth, development, and the effectiveness of soil conditioners. Measurements of plant height, number of leaves, and fruit development were recorded weekly. Plant health was observed, including any signs of nutritional deficiencies or stress. Irrigation was controlled to ensure all plants received the same amount of water, avoiding variations that could affect the results.

2.7 Statistical Data Analysis

Statistical analysis was performed on the numerical results obtained from some of the analyses to compare sets of results and identify significant differences between the studied populations. The one-way ANOVA test was used, a variance analysis technique to compare means of multiple independent populations. Among the results from the test, the p-value was used to determine significant statistical differences between sample sets, with significance set at 5% ($p<0.05$). For p-values less than 0.05, a Tukey's Honest Significant Difference test was subsequently conducted to identify significant differences between pairs of sample sets.

3. Results and Discussions

3.1. TPS/NC Characterization

Initially, the effects of adding different concentrations of NC (3, 5, and 7%) on the swelling properties of TPS were examined. Figure 1A presents the FTIR analysis conducted to characterize the structural components of the nanocomposites, both with and without the addition of NC, and to verify the interaction between these materials. In the spectrum attributed to TPS (Figure S3), we observed O-H stretching vibrations at approximately 3300 cm^{-1}. The 2931 and 2881 cm^{-1} bands were assigned to C-H axial deformation. The band at 1632 cm^{-1} is characteristic of OH angular deformation in water and appeared in the samples with the addition of NC. Additionally, the spectrum showed bands at 1409 and 1331 cm^{-1}, related to COH groups, characteristic of TPS. At 995 cm^{-1}, a band corresponding to C-O deformation was observed, where an increase in intensity in the TPS spectrum was noted due to interactions between the plasticizer glycerol and the starch [9,32].

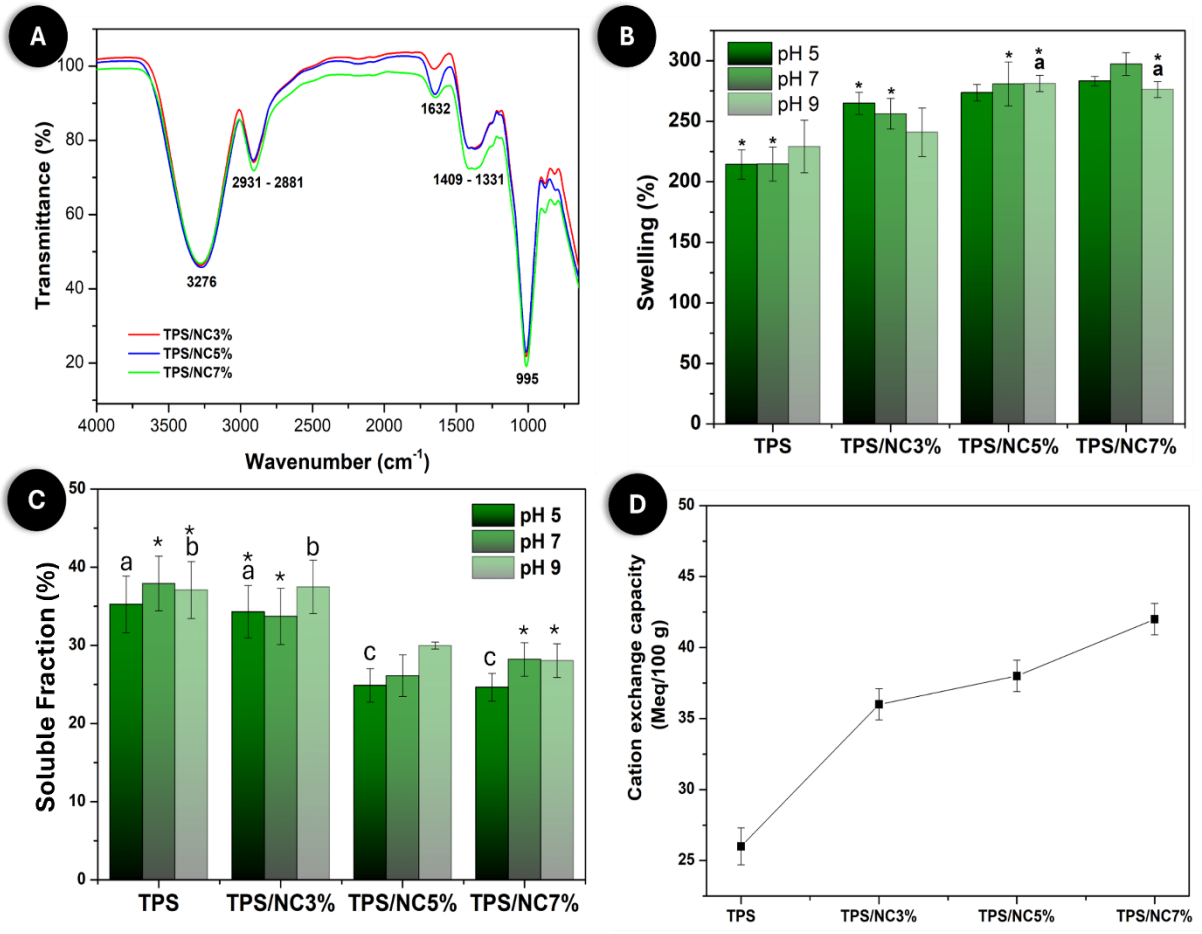

Figure 1. A. FTIR Spectrum. B. Swelling vs. pH Variation (5, 7, and 9). C. Soluble Fraction vs. pH Variation (5, 7, and 9). D. Cation Exchange Capacity for the TPS, TPS/NC3%, TPS/NC5%, and TPS/NC7%. Statistically similar samples: $^{a\text{-}c}$ for the same pH value among different samples; * for the same sample at various pH values.

For the spectrum attributed to NC (Figure S3), characteristic bands were observed between 3600 and 3300 cm^{-1}, corresponding to the stretching vibrations of hydroxyl groups in the silicate layers of NC. In a study by Mert *et al.*[12], where NC was incorporated into macroporous polymers modeled in emulsion (PolyHIPEs), a band between 2230 and 2150 cm^{-1} was attributed to surface groups of NC. This explains the 2359 cm^{-1} band in NC, linked to asymmetric C–H (aliphatic) stretches from surface-modifying groups, absent in the TPS samples. At 1632 cm^{-1}, associated with OH angular deformation in water, NC had a more intense peak than TPS. The TPS/NC7% spectrum closely resembled that of NC, suggesting changes in bonding and structure with increased NC content.

Additionally, the band at 995 cm^{-1}, indicative of C-O deformation, was stronger in NC, possibly due to the vibration of Si-O groups in the NC [33]. The spectra of TPS/NC nanocomposites showed similarities to pure TPS, particularly in the 3300 to 2881 cm^{-1} range, corresponding to O-H stretching and C-H axial deformations, and in the 1409 to 1331 cm^{-1}

range, linked to COH groups. The prominent peaks at 1632 cm^{-1} across the TPS/NC nanocomposites (Figure 1A) and NC may be due to water between the NC layers, with ammonium bromide possibly intercalated between the silicate layers, showing more intensely in the NC spectrum. Furthermore, the 995 cm^{-1} band, besides being related to C-O deformation, may result from the stretching vibration of Si-O groups within the NC.

Adding NC to the nanocomposites enhanced their swelling properties (Figure 1B), attributed to the unique characteristics of this clay, particularly its capacity for expansion and ion exchange. Bentonite, the montmorillonite type, can swell upon contact with water, forming a sandwich-like structure where water molecules are trapped between the clay layers [34]. This considerable expansion significantly increased the volume of the nanocomposite, thereby improving its swelling properties. Based on statistical analysis, no significant difference in swelling was observed for the same sample across different pH levels. It was also noted that increasing the NC content further improved the swelling properties (TPS/NC7% > TPS/NC5% > TPS/NC3% > TPS).

Figure 1C presents soluble fraction analysis vs. pH variation (5, 7, and 9) for TPS and TPS/NC samples (3, 5, and 7%), revealing a behavior opposite to swelling. As the NC concentration in the nanocomposites increased, the soluble fraction decreased. This pattern aligns with NC's water retention ability, as Kharissova *et al.* (2021)[35] highlighted, suggesting that its inclusion in TPS protects the material from dissolution. Notably, samples composed solely of TPS showed significant soluble fraction due to its high affinity for water, which is attributed to the intermolecular hydrogen bonds present in its main components: amylose, characterized by α-(1-4) glycosidic bonds and amylopectin, with α-(1-6) glycosidic bonds [4]. Statistical analysis of the results across different pH levels for the same sample showed no clear behavioral trend, with most groups exhibiting statistically similar samples. TPS and TPS/NC3% had statistically similar soluble fractions for the same pH, while the samples with 5% and 7% NC were also quite similar, particularly at pH 5.

The increase in NC percentage was directly proportional to the rise in CEC, as shown in Figure 1D. Montmorillonite clay exhibits high CEC due to its layered crystalline structure [24]. Cations in the solution surrounding the nanocomposite can move in and out of these layers, allowing for even more significant material expansion. Additionally, CEC influences the interactions between water molecules and clay particles, contributing to the enhanced swelling properties depicted in Figure 1B. These results emphasize the importance of adding montmorillonite to improve the desired properties of the nanocomposites, making them more effective for various applications [4].

The samples exhibited pH levels of 5.7±0.4, 6.9±0.1, 6.5±0.1, 6.6±0.3, and 6.7±0.1 for TPS, NC TPS/NC3%, TPS/NC5%, and TPS/NC7%, respectively. The data showed a trend toward neutral pH, with values ranging between 6 and 7, except for TPS, which was slightly more acidic. This difference can be attributed to the chemical composition of the materials used. NC, being neutral, tends to raise the pH of the samples, while TPS, with its intrinsic acidity, has the opposite effect, lowering the pH. This pH neutrality is important because it allows nanocomposites to be applied across various soil types, regardless of the soil's initial pH [3].

3.2 Nanocomposite added with NL

The TPS/NC7% was selected for its reduced water solubility, which helps minimize the likelihood of leaching, and for exhibiting greater swelling capacity and better CEC compared to the other tested nanocomposites (Figure 1D). In the second phase, the effects of adding different concentrations of NL (0.3%, 0.5%, and 0.7%) on the properties of TPS/NC7% were explored. This approach aims to develop a more effective soil conditioner by leveraging NL's antioxidants, UV-blocking, antimicrobial, and other potential benefits.

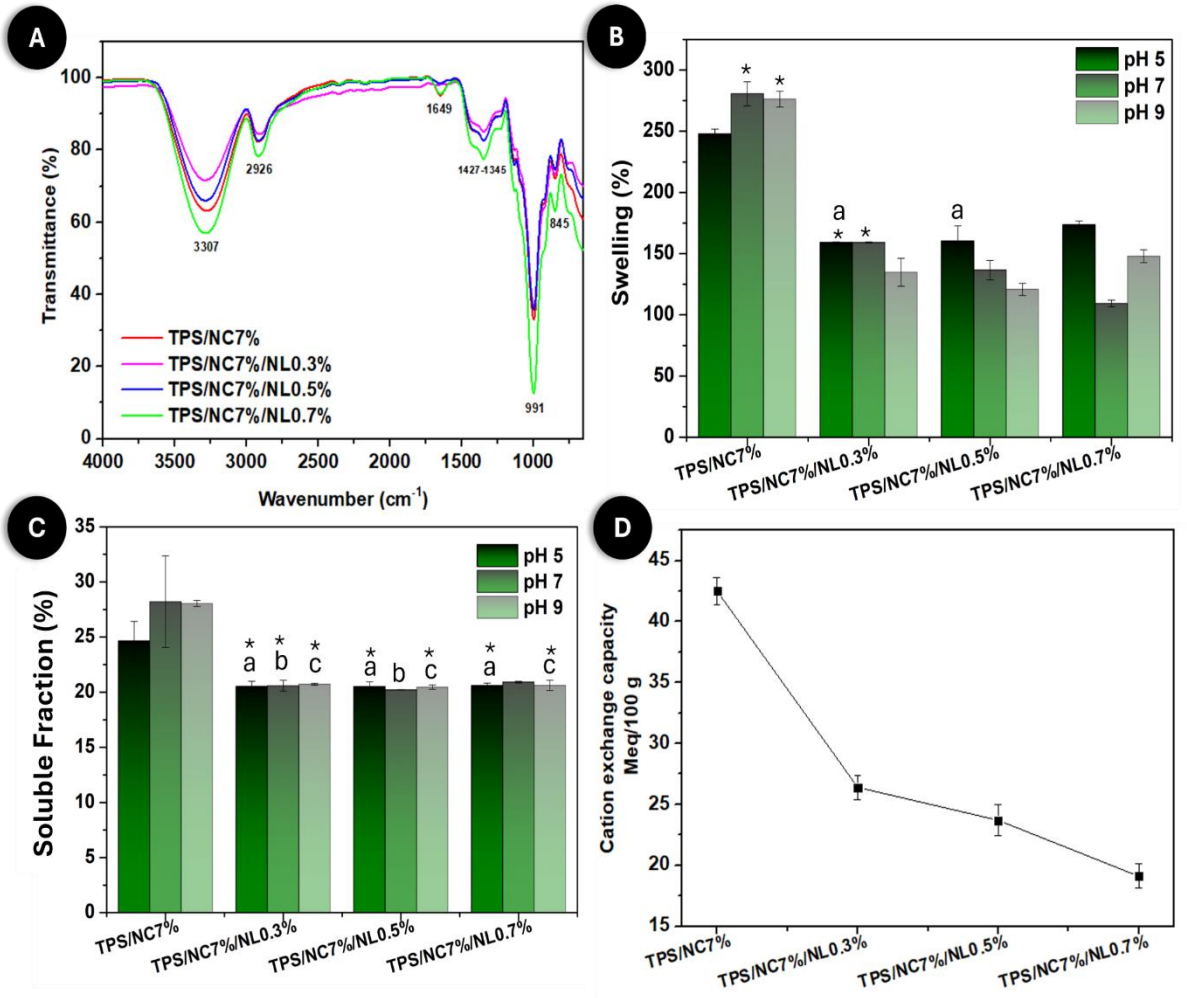

Figure 2. A. FTIR spectrum; B. Swelling vs. pH variation (5, 7, and 9); C. soluble fraction vs. pH variation (5, 7, and 9); and D. Cation exchange capacity for the samples TPS/NC7% and TPS/NC7%/NL (0.3, 0.5, and 0.7%). Statistically similar samples: $^{a\text{-}c}$ for the same pH value among different samples; * for the same sample at various pH values.

Figure 2A presents the FTIR spectra for the three different concentrations of NL. The analysis revealed interactions among the components, indicating that the spectra of the NL-added nanocomposites tend to maintain structures like those of pure TPS and NL (Figure S3). This suggests that these components strongly influence the structure and bonding of the nanocomposite. The band at 2926 cm^{-1} exhibits characteristics like pure TPS, attributed to the axial deformation of C-H, while the band at 1649 cm^{-1} resembles the spectrum of pure NL, corresponding to the vibrations of C=C benzene rings typical of lignin structure. In the case of the TPS/NC7%/NL0.7% nanocomposite, a higher peak is observed, indicating a greater concentration of NL in its composition. The other bands align with those of TPS and NL, except for the band at 991 cm^{-1}, characteristic of NC, which shows a more pronounced peak, especially for TPS/NC7%/NL0.7%. This can be attributed to C-O deformation, stretching vibrations of Si-O groups present in NC, and/or specific structures from NL [13,33].

Figure 2B shows that pH 5 was the most effective for the expansion of materials with NL, with swelling increasing as the concentration of NL rose, where the samples with 0.3% and 0.5% NL were statistically similar. In contrast, at pH 7, there was a trend of decreasing swelling as the concentration of NL increased. At pH 9, a slight decrease in swelling was observed, followed by an increase, remaining relatively constant. In summary, the addition of NL reduced the swelling properties of the nanocomposite compared to TPS/NC7%. This effect can be attributed to NC charges' excellent dispersion and interaction with the TPS matrix. The bonds between TPS, and the various added nanoparticles decreased the polymer chains' mobility, hindering the aqueous medium's permeability through the material. The graph in Figure 2C displayed a soluble fraction trend of around 20% for all samples at the three tested pH levels. Notably, there was a reduction in soluble fraction for all composites compared to the TPS/NC7% sample, indicating lower soluble fraction due to the addition of NL, as anticipated in the literature [21]. This reduction in soluble fraction suggests greater resistance to dissolution in aqueous environments, resulting in more effective protection against leaching. Due to the low mass of NL added, which was less than 1% of the total, the variations in soluble fraction among the different concentrations were minimal.

Figure 2D shows the CEC for the composites TPS/NC7%/NL0.3%, TPS/NC7%/NL0.5%, and TPS/NC7%/NL0.7%. The values indicate a decreasing trend in CEC with increasing NL concentration in the composite. This may be attributed to the greater proportion of NL in the nanocomposite, reducing the available surface area for cations. The pH test revealed values of 6.57±0.06, 5.63±0.02, and 6.25±0.06 for the samples TPS/NC7%/NL0.3%, TPS/NC7%/NL0.5%, and TPS/NC7%/NL0.7%, respectively. These data suggest that the addition of NL, due to its acidic nature, slightly lowered the pH of the samples, except for the composite with 0.5% NL, which had a more acidic pH than the others. However, the overall neutral character was maintained compared to the TPS/NC7% nanocomposites, with pH values ranging from 5.5 to 7. This neutrality makes the TPS/NC7%/NL composites suitable for application in various soils.

3.2.1 Thermal properties

The data from the TGA (Figure 3A) and the DTG (Figure 3B) are compiled in Table 1. This table includes information such as the initial degradation temperature ($T_{5\%}$), which indicates the temperature at which 5% of the initial mass of the analyte was lost; the maximum degradation temperature (T_{max}), obtained from the first derivative of the TGA curves; the mass loss index (Δm), representing the percentage of mass degraded during T_{max}; the final

temperature (T_f), derived from the TGA curves; the decomposition temperature range (ΔT), calculated as the difference between T_f and $T_{5\%}$; and the char residue at 600°C ($R_{600°C}$).

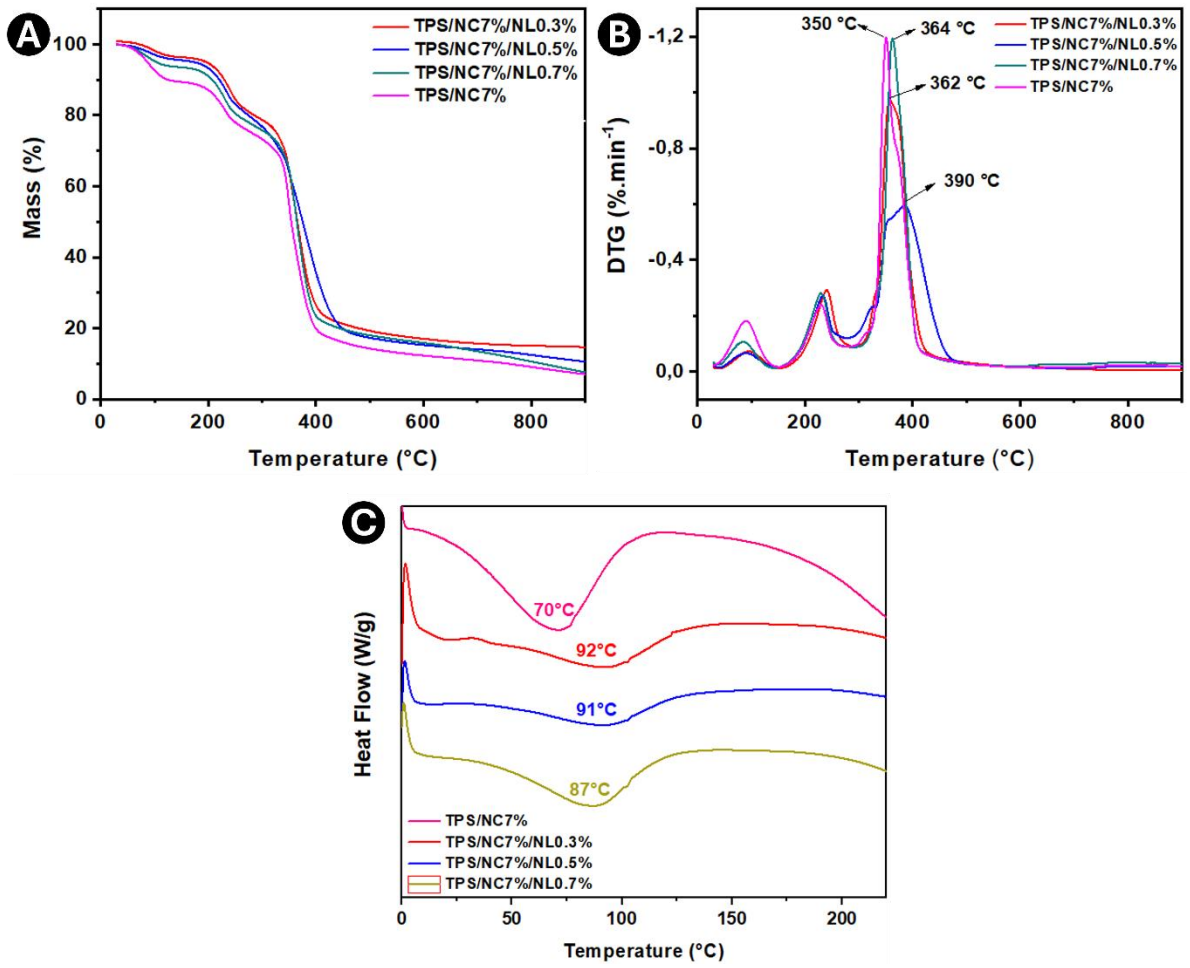

Figure 3. (A) Thermogravimetric (TGA) curves, (B) First Derivative of Thermogravimetric Curves (DTG), and (C) Differential Scanning Calorimetry (DSC) for the samples of TPS/NC7% and TPS/NC7%/NL (0.3, 0.5, and 0.7%).

The variability observed in the $T_{5\%}$ values, as shown in Table 1, is attributed to the complexity of the thermal decomposition process in these composite systems. The interaction between TPS, NC, and NL introduces multiple decomposition mechanisms influenced by the proportion of each component. While the sample with 0.3% NL displayed the highest $T_{5\%}$ (190°C), indicating improved initial thermal resistance, the samples with 0.5% and 0.7% NL exhibited lower values (165°C and 98°C, respectively). This lack of a consistent trend can be explained by potential phase segregation or non-uniform dispersion of the nanoaditives in the matrix, which could reduce the effectiveness of thermal stabilization in some cases. This is consistent with findings in similar systems, where optimal properties are often achieved at specific additive concentrations due to balanced interactions within the composite matrix [36].

T_{max} also varied among the samples, reflecting thermal resistance during decomposition. The TPS/NC7% sample showed a Tmax of 350°C, while the NL-added samples exhibited values of 362°C (TPS/NC7%/NL0.3%), 390°C (TPS/NC7%/NL0.5%), and 364°C (TPS/NC7%/NL0.7%). The highest T_{max} was observed in TPS/NC7%/NL0.5%, indicating superior thermal resistance, possibly due to greater interaction between the polymer matrix and the nanoaditives [13]. Δm at T_{max} also displayed variations. The TPS/NC7% sample experienced a mass loss of 49%, while the NL-containing samples showed losses of 47% (TPS/NC7%/NL0.3%), 59% (TPS/NC7%/NL0.5%), and 52% (TPS/NC7%/NL0.7%). The high mass loss observed in the sample TPS/NC7%/NL0.5% might indicate that at this specific composition, the thermal decomposition is dominated by the degradation of NL, which is consistent with its higher T_{max}.

The T_f was derived from the TGA curves, with the TPS/NC7% sample showing the highest T_f of 542°C. The modified samples showed slightly lower T_f values: 539°C for TPS/NC7%/NL0.3%, 532°C for TPS/NC7%/NL0.5%, and 511°C for TPS/NC7%/NL0.7%. These reductions indicate that the presence of nanocomposites can influence the temperature at which decomposition ends. The ΔT varied from 458°C for TPS/NC7% to 342°C for TPS/NC7%/NL0.3%, 370°C for TPS/NC7%/NL0.5%, and 414°C for TPS/NC7%/NL0.7%. The TPS/NC7% sample exhibited the largest ΔT, indicating a broader decomposition range, while adding NL resulted in narrower decomposition ranges. Finally, the $R_{600°C}$ was higher in the samples containing NL, with values of 17% (TPS/NC7%/NL0.3%), 16% (TPS/NC7%/NL0.5%), and 15% (TPS/NC7%/NL0.7%), compared to 12% for the TPS/NC7% sample. This suggests that NL promotes the formation of a stable carbonaceous structure, likely due to its aromatic composition, which resists complete degradation.

Table 1. Thermal parameters result in TPS/NC7%, TPS/NC7%/NL0.3%, TPS/NC7%/NL0.5%, and TPS/NC7%/NL0.7%.

Samples	$T_{5\%}$ (°C)[a]	$T_{máx}$ (°C)[b]	Δ_m (%)[c]	T_f (°C)[d]	Δ_T (°C)[e]	$R_{600°C}$ (%)[f]
TPS/NC7%	83	350	49	542	458	12
TPS/NC7%/NL0.3%	190	362	47	539	342	17
TPS/NC7%/NL0.5%	165	390	59	532	370	16
TPS/NC7%/NL0.7%	98	364	52	511	414	15

[a]Initial degradation temperature; [b]Temperature of the maximum degradation; [c]Mass loss index up to Tmax; [d]Final degradation temperature; [e]Decomposition temperature range; [f]The amount at the end of degradation process at 600°C.

In the DSC curve (Figure 3C) of TPS/NC7%, a temperature peak at 70°C was identified, associated with the glass transition of starch, suggesting a change in the molecular structure at this point. In the other samples aditivated with NL, only peaks were observed at 92°C for TPS/NC7%/NL0.3%, 91°C for TPS/NC7%/NL0.5%, and 87°C for TPS/NC7%/NL0.7%. These peaks likely represent a combination of phase transitions and specific degradation events related to the interaction between NC and NL in the polymer matrix.

Thus, the addition of NL to TPS/NC7% significantly improved the material's thermal stability. The combination of 7% NC with 0.3% NL exhibited the best results regarding increased initial degradation temperature and amount of charcoal residue, indicating a potential synergy between the components that confers greater thermal resistance to the material. The presence of NC and NL promoted new intermolecular interactions in the composite, with the latter characterized by a complex, highly branched aromatic structure, contributing to the considerable thermal stability of the samples [37].

3.2.2. Impact of UV-C Exposure on the Stability and Photodegradation of the Nanocomposite

It was possible to observe in Figure S4-A that for the samples without UV-C exposure, that is, at 0 days, the higher the percentage of NL added, the greater the intensity of the absorptions at bands 3276 and 2931 cm^{-1} (both corresponding to O-H stretching and C-H axial deformations), 1400 cm^{-1} (associated with COH groups), and 995 cm^{-1} (related to C-O deformation) [32,38,39]. In other words, the concentration of NL is proportional to the increase in band intensity. After 21 days, the TPS and TPS/NC7%/NL0.3% samples exhibited similar UV-C degradation behavior, while the TPS/NC7%/NL0.5% and TPS/NC7%/NL0.7% samples showed improved resistance to photodegradation, indicating that the higher NL concentrations provided better protection against UV-C exposure.

In the bands shown in Figure S4-B, there was a reduction in intensity as the amount of NL added to the sample increased. However, the samples TPS/NC7%/NL0.5% and TPS/NC7%/NL0.7% showed a more significant reduction compared to the TPS and TPS/NC7%/NL0.3% samples. Overall, there is a subtle modification in the samples after exposure to UV-C light due to the low percentage variation ($< 1\%$) of NL analyzed. Thus, there is no predictable behavior for the relationship between NL and photoprotection. Future work aims to conduct this study with higher concentrations of NL.

3.3. Evaluation of the Nanocomposite as a Soil Conditioner

The TPS/NC7%/NL0.3% nanocomposite was selected for soil conditioner evaluation tests due to its superior performance in terms of thermal stability. Additionally, its soluble fraction remained consistent across all tested samples, and it exhibited less variation in swelling at the different pH levels analyzed.

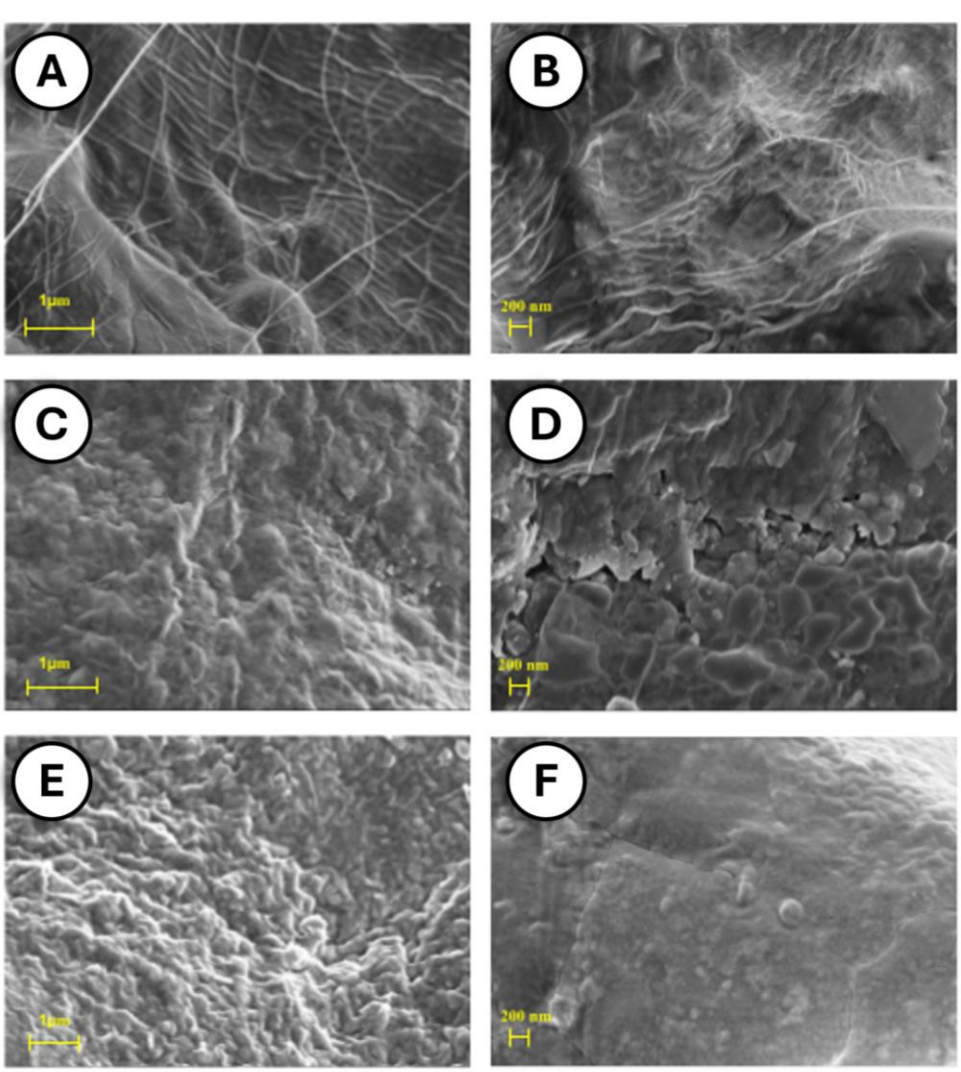

Figure 4. SEM microscopy with the magnification of 35,000 x (right column) and 50,000 x (left column) of the samples TPS (A-B), TPS/NC7% (C-D), and TPS/NC7%/NL0.3% (E-F), respectively.

The SEM micrographs obtained for the samples of TPS (Figures 4A-B), TPS/NC7% (Figures 4C-D), and TPS/NC7%/NL0.3% (Figures 4E-F) were presented at scales of 1 µm and 200 nm. In the micrographs, long filaments characteristic of TPS were identified, reflecting its intrinsic polymeric structure and tendency to form continuous chains [40]. However, with the addition of NC, these filaments were fragmented, resulting in a significantly rougher surface

and a more fragile structural matrix, as evidenced by the formation of tiny pores. This behavior suggests that NC acted as a disruptive agent, interfering with the continuity of the TPS matrix and contributing to a more heterogeneous texture.

The incorporation of NL further intensified the surface roughness of the composite while simultaneously reducing the observed porosity. This decrease in porosity may be attributed to the filling effect of NL, as reported in the literature [40], which possibly infiltrated the existing pores, promoting a compacting effect within the matrix. In the micrographs of the TPS/NC7%/NL0.3% composite (Figures 4E-F), individual components could not be visually distinguished, suggesting strong adhesion and interaction between TPS, NC, and NL. This result indicates an efficient integration of the materials, likely due to robust intermolecular interactions that enhanced the cohesion of the composite structure, corroborating the FTIR analyses.

3.3.1. Antimicrobial Activity

The impact of the soil conditioner on the bacterial growth of *S. aureus* and *E. coli* is illustrated in Figure S5. A more significant bacteriostatic effect was observed for *S. aureus*, with inhibition rates of 68.5% for TPS, 70.76% for TPS/NC7%, and 73.8% for TPS/NC7%/NL0.3%. In the case of *E. coli* (Figure S5), TPS inhibited growth by 38.25%, TPS/NC7% by 59.36%, and TPS/NC7%/NL0.3% by 70.15%. For *S. aureus*, the soil conditioners showed significant differences compared to the control, but there were no significant differences among the treatments themselves. For *E. coli*, significant differences were found between the control and the soil conditioners and between TPS and the other treatments. However, the difference between TPS/NC7% and TPS/NC7%/NL0.3% was insignificant.

The study by Levana *et al*. (2023)[34] with clay-based nanocomposites reported similar inhibition results. The bacteriostatic effect can be attributed to the composition of the soil conditioner. NC is known for its high antibacterial activit. Also, NL has been shown to cause greater inhibition against *S. aureus* than *E. coli*. [41] Overall, the results demonstrated that the soil conditioners have an inhibitory effect on the tested microorganisms.

3.3.2. Water retention in soil

In Figure S6, the control soil, without additives (Control), showed an initial water retention of around 160%, which was used as a reference. The addition of TPS to the soil increased this retention to approximately 180%, which was attributed to the hygroscopic nature

of TPS. The polar groups in TPS strongly interacted with water molecules, forming hydrogen bonds and enhancing water absorption [13]. When NC were added (TPS/NC7%), water retention slightly decreased, reaching around 170%. This suggested that the presence of NC influenced the composite structure, making it denser and reducing its ability to hold moisture, as it became less effective at retaining water.

When NL was added (TPS/NC7%/NL0.3%), water retention was further reduced, down to approximately 150%. This effect was explained by the hydrophobic properties of lignin, which hindered water absorption by the starch and nanoclay matrix [42]. NL acted as an additional barrier, reducing the water retention of the composite by decreasing its ability to absorb and retain moisture.

3.3.4. Leaching of NH_4^+, $H_2PO_4^-$, and K^+ ions

The ability to absorb essential macronutrients, such as N, P, and K, is a crucial parameter for evaluating the effectiveness of nanocomposites in agricultural and environmental applications [43]. Figure 5 presents the graphs of the concentrations of NH_4^+ (Figure 5A), $H_2PO_4^-$ (Figure 5B), and K^+ (Figure 5C) ions, leached weekly, obtained through UV-VIS analysis. This data provided valuable insights into the leaching dynamics of macronutrients and allowed for a critical assessment of the nanocomposite's performance in retaining and releasing these ions. A significant portion of the samples showed statistically similar results over the weeks, such as the control sample, and the graphs highlight the statistically distinct samples for each week among the different compositions.

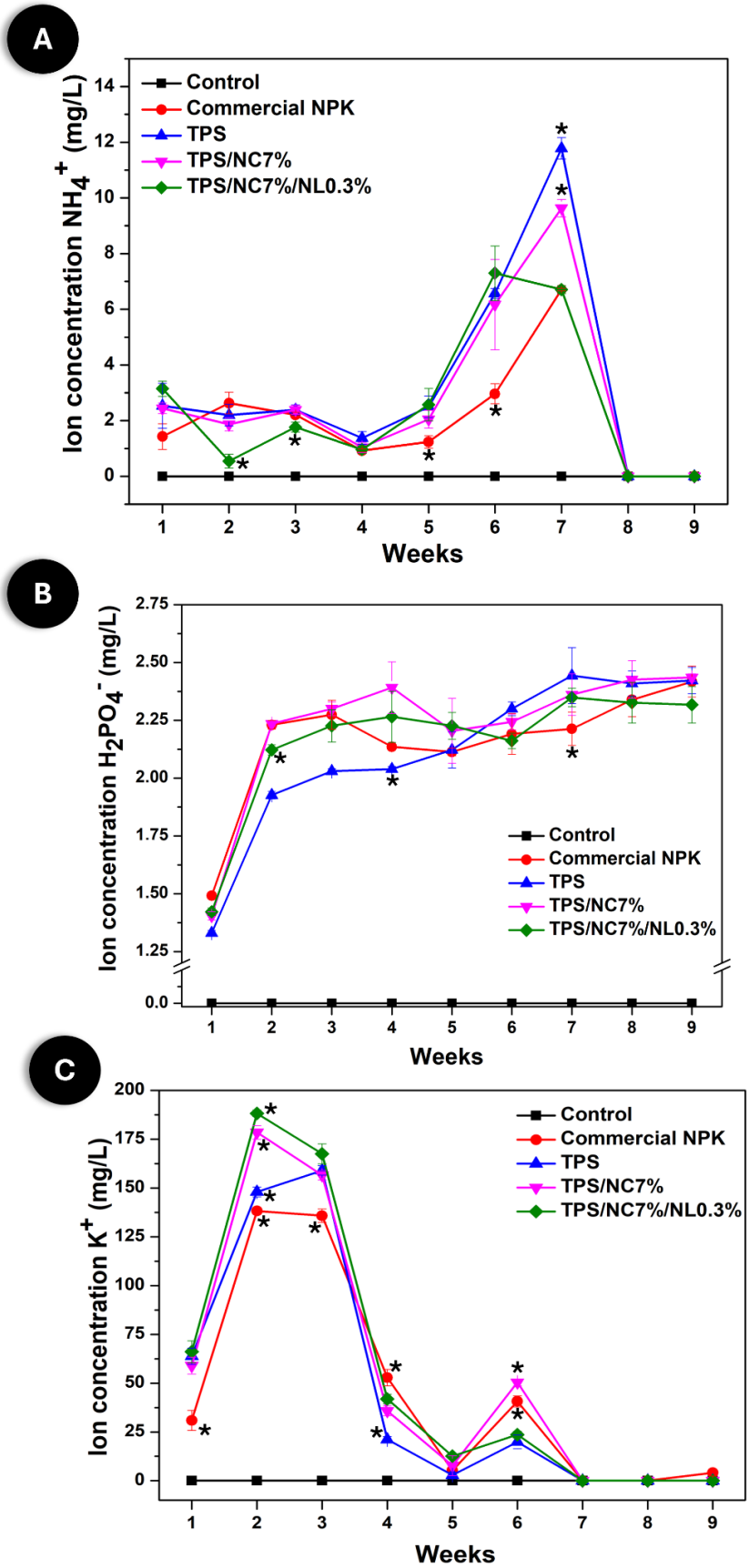

Figure 5. Concentration of NH_4^+ (A), $H_2PO_4^-$ (B), and K^+ (C) ions after leaching in soil. *Statistically distinct samples from the set of samples within the same week interval.

Figure 5A revealed that the leaching behavior of NH_4^+ ions was relatively linear until the fifth week. Overall, the behavior of the samples was quite similar, except for the control, as expected, with the TPS/NC7%/NL0.3% sample being the most statistically distinct, showing lower N leaching compared to the others. From this point, the concentration of ions increased significantly in the sixth week, with the behavior of the nanocomposites being statistically similar. Week 7 saw the maximum leaching, followed by a sharp decline to zero in week 8, which remained consistent throughout week 9. This increase in NH_4^+ leaching can be attributed to microbial activity releasing nitrogenous compounds into the soil [44,45]. The monitoring of leaching for K^+ ions is shown in Figure 5C, where the leached concentration increased significantly by the second week, with statistical differences among all samples. Between weeks 3 and 5, the leached amount drastically decreased, reaching values close to zero by the fifth week, followed by a slight increase in week 6, remaining statistically similar for the TPS and TPS/NC7%/NL0.3% samples. In the final weeks (7, 8, and 9), leaching was zeroed out, considering the measurement error. The behavior observed for K^+ leaching in week 6 may also be related to microbial activity influencing potassium release into the soil.

After the sixth week, only the TPS and TPS/NC7% samples showed an increase in nitrogen leaching, while the nanocomposite TPS/NC7%/NL0.3% exhibited a reduction. This difference can be explained by the fact that TPS served as a food source for microorganisms, whereas NL inhibited microbial activity with its bactericidal properties. This hypothesis was confirmed by the antimicrobial activity test results, which demonstrated a greater inhibitory capacity against bacteria for the TPS/NC7%/NL0.3% compared to the TPS and TPS/NC7% samples.

The $H_2PO_4^-$ ions showed an increase in leaching until week 4, followed by a stable plateau until week 9. This pattern can be explained by the unique chemical properties of P, which tends to form insoluble complexes with soil minerals, resulting in a more consistent release over time [46]. The interaction of P with the nanocomposite may not have been significantly influenced by the components, which have a more pronounced impact on the retention of soluble macronutrients like N and K. Thus, the initial availability and chemical dynamics of P in the soil may have contributed to a more stable leaching rate, as the fixation of phosphorus occurs differently compared to N and K. This is due to the transformation of phosphorus available to plants (labile) versus that which remains unavailable (non-labile), resulting from interactions with the soil structure and other ions present. This behavior contrasts with nitrogen and potassium, which were retained more efficiently and had greater availability through the nanocomposite [46].

Although the concentrations of leached NH_4^+, $H_2PO_4^-$, and K^+ ions were relatively close among the different materials, the TPS/NC7%/NL0.3% nanocomposite stood out for exhibiting lower concentrations of leached N and K throughout the experiment. The improved water absorption and retention of TPS/NC7%/NL0.3% may decrease the likelihood of N and K leaching with water, thereby increasing the efficiency of nutrient absorption and plant utilization efficiency, as Macedo *et al.* (2023)[46] observed. This behavior can be attributed to the specific composition of this nanocomposite. As an organic matrix, TPS provides a favorable environment for nutrient retention, while NC contributes a porous structure that can enhance ion absorption capacity [46]. With its bactericidal properties, NL may inhibit microbial activity that would typically release N and K into the soil, thus reducing the leaching of these macronutrients.

Furthermore, combining TPS with NC7% and NL0.3% may result in a more stable matrix that reduces solubilization and leaching of NH_4^+ and K^+ ions. The synergistic effect of these components contributes to more efficient retention of macronutrients, providing a longer-lasting source of N and K for plants. This superior performance in retaining N and K can be particularly beneficial for agricultural practices, as it improves the availability of these macronutrients to plants and reduces the need for frequent fertilization, contributing to sustainability and fertilizer use efficiency.

3.3.4. Biodegradation in soil

The materials TPS, TPS/NC7%, and TPS/NC7%/NL0.3% were evaluated for their biodegradability alongside a control sample of pure soil. Figure 6 presents the biodegradation profile of the samples monitored over 50 days, based on the cumulative release of CO_2 (Figure 6A) and the daily release of CO_2 (Figure 6B).

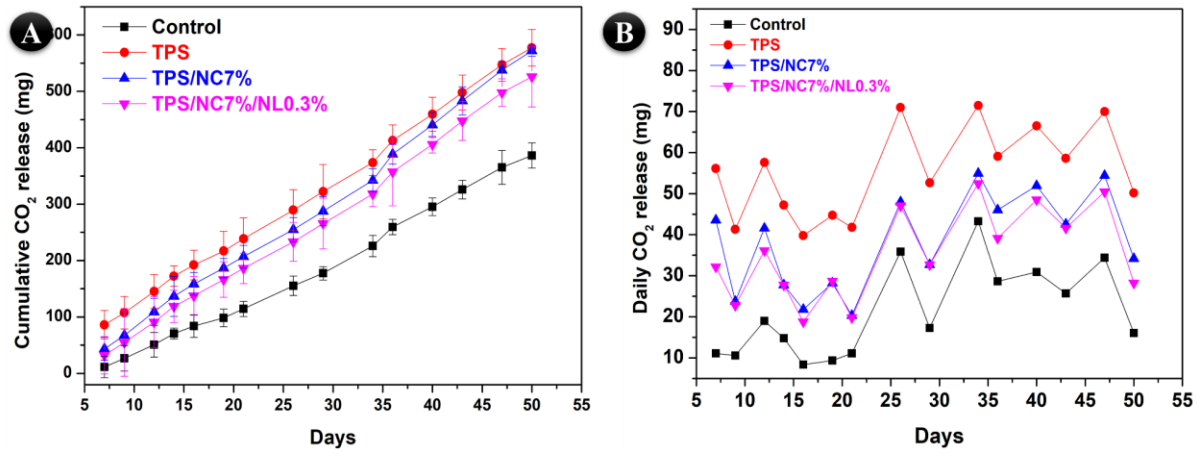

Figure 6. Biodegradation performance in soil of the samples TPS, TPS/NC7%, and TPS/NC7%/NL0.3%, (A) cumulative CO_2 release and (B) daily CO_2 release.

The cumulative CO_2 release results analysis showed a generally similar behavior among the samples regarding production. However, it is noteworthy that the TPS sample maintains the highest CO_2 release rate, followed by the TPS/NC7% and TPS/NC7%/NL0.3% samples. Nonetheless, the release rates are statistically similar among the samples at most measured points. However, a significant difference in CO_2 emissions can be observed when the sample set is compared to the control.

Thus, the TPS sample exhibits the highest CO_2 release, indicating greater biodegradability than the NC-containing samples, which show reduced capacity. This behavior has been observed in other literature. Angelo *et al.*(2021)[47] studied the biological degradation of chitosan and montmorillonite clay samples and found that the clay hinders the degradation of the polymeric matrix. They attributed this to the restriction of segmental movement at the interface, which decreases microorganism access to attack the polymer. This reduction is also correlated in other studies with the limited growth of microorganisms on clay particles, diminishing their functionality [48].

When analyzing the daily release profile, despite the oscillations in the quantities eliminated, as previously observed in the literature [47], it was possible to conclude that the TPS sample exhibited the highest CO_2 release. The samples containing NC (TPS/NC7% and TPS/NC7%/NL0.3%) showed lower biodegradability compared to TPS but higher than the control. Four distinct general behaviors could be identified over the evaluated time intervals by analyzing the curves. Between the 1^{st} and 2^{nd} days, the control sample showed a maximum CO_2 release of 19 mg, but most daily releases were close to 10 mg. The TPS sample showed a maximum release of 57 mg, while the NC-containing samples released approximately 40 mg. On the 25^{th} day, all samples experienced a significant but proportional increase in CO_2 elimination. Between the 35^{th} and 47^{th} days, there was a stabilization in CO_2 release, followed by a sharp decline on the 50^{th} day, marking the end of the analysis.

These behavioral phases can be attributed to the diffusion of NPK through the polymer matrix, as the nutrient is released from the material's structure, primarily from the TPS network. This also explains its higher biodegradation rate, as water molecules and microorganisms have more sites to interact with the polymer matrix [47]. It was observed that between the 14^{th} and 21^{st} days, this coincides with the highest release of $H_2PO_4^-$ ions (Figure 5A), and K^+ ions (Figure 5B), which remained elevated until the 25^{th} day, a high CO_2 release. The sustained high elimination after this period aligns with the phase of increased NH_4^+ release (Figure 5C), as

microorganisms benefit from the nitrogen, promoting their growth. This suggests that the availability of NPK significantly impacts the biodegradation process, as seen by the corresponding peaks in CO_2 release, driven by microbial activity feeding off the nitrogen and other nutrients during the experiment.

3.4 Soil Conditioner Effectiveness in Red Cherry Tomato Cultivation

The effectiveness of the soil conditioners prepared in this study was tested through a field study with the cultivation of red cherry tomatoes. Seedling development was monitored weekly over 9 weeks (2 months), recording the number of leaf stems and measuring seedling height from seed planting. Figure 7A shows the results for stem counts, where it was observed that the first seedlings to emerge as early as the first week of monitoring were from the control group, with no treatment applied to the soil before planting. In the following week, the TPS/NC7%/NL0.3% treated seedlings began to sprout, followed by the TPS and TPS/NC7% treatments, which developed in the third week. The seedlings in the soil fertilized with commercial NPK, without the soil conditioners, were the last to emerge, only sprouting after 4 weeks. The delay of the other treatments compared to the control can be attributed to the dormancy effect caused by the NPK fertilizer. In this complex biomolecular phenomenon, seeds delay germination until the environment reaches optimal conditions. This result aligns with the fact that the NPK sample was the last to emerge overall, as it released the fertilizer more uncontrolled and directly into the soil.

This effect was also reduced over time in the other samples, especially in TPS/NC7%/NL0.3%, which emerged in half the time of NPK, indicating that this composite established a suitable medium more quickly. Over the weeks, the number of stems per sample showed overall stability, increasing between weeks 6 and 7, likely due to the ion leaching peak observed in Figure 5. The NPK and TPS treatments exhibited similar stem counts, while the control aligned with TPS/NC7% during the last three weeks. TPS/NC7%/NL0.3% showed the highest overall stem count.

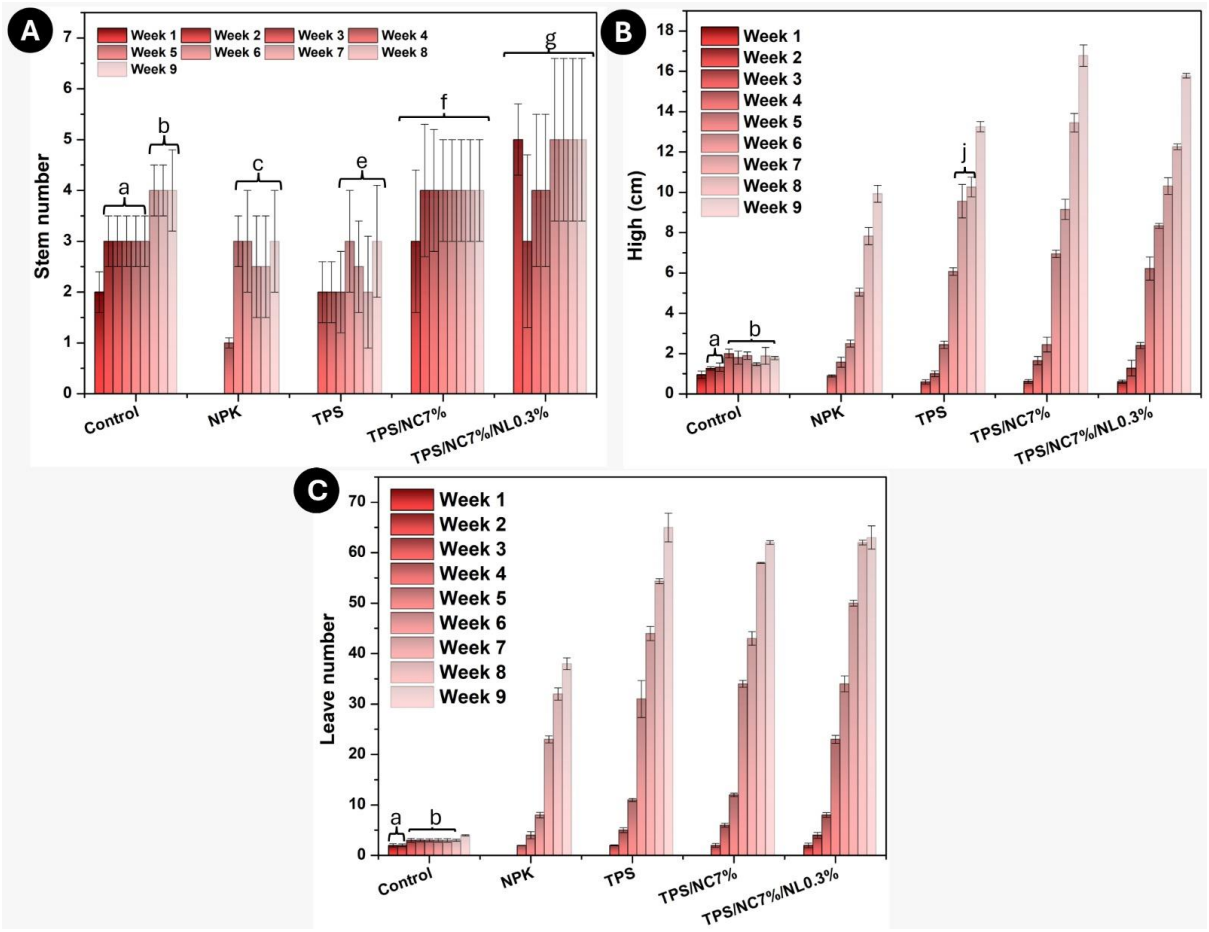

Figure 7. Weekly monitoring of red cherry tomato seedling development over 9 weeks. (A) stem number, (B) seedling high, and (C) leaf number. Statistically similar samples (a-g) of the same sample, analyzed over different weeks.

Height and leaf count (Figures 7B and 7C) showed similar behavior across the samples. The control remained without significant increases in these parameters. At the same time, NPK, TPS, TPS/NC7%, and TPS/NC7%/NL0.3% followed a similar exponential pattern, with TPS/NC7% showing the most significant average height and TPS the highest average leaf count. Despite being the first to germinate, the control sample was quickly surpassed by the other samples, even under identical growth conditions. However, as observed in Figure 7B, its growth was significantly lower than that of the different samples, and its leaves showed a slightly yellowish hue (Figure 8), suggesting that a lack of water may have been a critical factor in its stagnation [49].

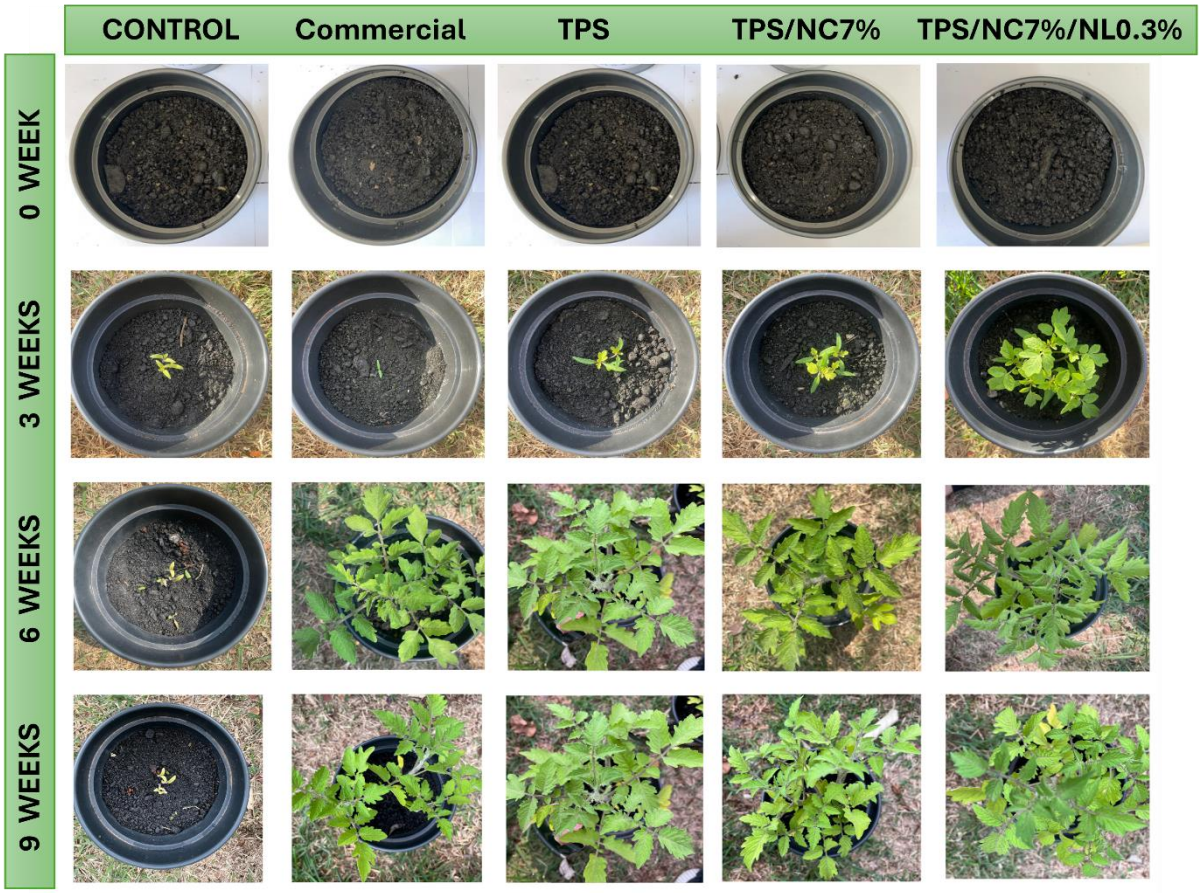

Figure 8. Photographic records showing the visual monitoring of red cherry tomato seedling development, taken weekly over a 9-week period. Weeks (vertical) and control, commercial, TPS, TPS/NC7%, and TPS/NC7%/NL0.03% (horizontal), respectively.

All samples were watered daily with 100 mL of water, but this stagnation, combined with leaf yellowing, may be attributed to the nanocomposites acting as a hydrogel. As liquid NPK was released into the soil, the polymeric network swelled with water, which was then gradually released into the soil. The occurrence of this phenomenon in week 8 indicates a possible correlation with the leaching behavior of the composites in Figure 5, where, after the peak of fertilizer release, the composites disintegrated, making it challenging to meet the water demands of the tomato seedlings. In the case of the NPK sample, leaf yellowing was not observed as early as week 8, likely because it was the last to germinate, resulting in a lower water demand than the others.

Thus, overall, the TPS/NC7%/NL0.3% sample showed the best results, with the highest number of stems. Although it had a slightly lower height compared to TPS/NC7% and slightly fewer leaves than TPS, the lignin-containing nanocomposite stands out overall, as the presence of more stems increases its surface area for photosynthesis, potentially boosting the plant's energy production and, consequently, the production of flowers and fruits [50]. Additionally,

due to the earlier breaking of seed dormancy, it can produce these resources more quickly than the other composites, making TPS/NC7%/NL0.3% the standout in the cultivation test. Nonetheless, all the composites produced showed superior results compared to the control and the commercial fertilizer.

4. Conclusion

In conclusion, this study demonstrated that combining NL, NC, and TPS as soil conditioners offers a promising approach to improving soil properties and enhancing agricultural sustainability. The analysis of the nanocomposites revealed that including 7% NC and 0.3% NL significantly enhanced the cation exchange capacity, water retention, and UV-C degradation resistance of TPS while promoting efficient nutrient absorption and reducing NPK ion leaching. Tests conducted on cherry tomatoes confirmed the practical effectiveness of these nanocomposites, demonstrating their ability to improve plant growth and soil health under real cultivation conditions. The synergy between NL and NC represents a significant advancement in soil conditioner formulation, optimizing their physicochemical properties and amplifying direct benefits for sustainable agriculture. This study fills a gap in existing literature and opens new perspectives for applying nanocomposites in innovative and efficient agricultural practices.

Acknowledgments

This research was partially funded by the São Paulo State Research Foundation (FAPESP - #2023/06505-9 (M.F.), #2024/01872-6 (L.F.), #2024/14149-0 (A.F), #2023/00335-4 (J.R), #2017/21004-5 (L.F.), CEPID CBioClima #2021/10639-5). Also, to Project 14805 – FINEP 01.22.0179.00 (MARTMA), as well as by the National Council for Scientific and Technological Development (CNPq) through grant #153850/2024-8 and the National Institute of Science and Technology in Nanotechnology for Sustainable Agriculture (MCTI-CNPq - INCTNanoAgro #405924/2022-4 and CAPES-MEC #88887.953443/2024-00) and the National Institute of Science and Technology in Organic Electronics (INEO #2014/50869-6)).

References

[1] S.H. Muhie, Novel approaches and practices to sustainable agriculture, J. Agric. Food Res. 10 (2022) 100446.

[2] S. Sabzevari, J. Hofman, A worldwide review of currently used pesticides' monitoring in agricultural soils, Sci. Total Environ. 812 (2022) 152344. https://doi.org/10.1016/j.scitotenv.2021.152344.

[3] M. Babla, U. Katwal, M.T. Yong, S. Jahandari, M. Rahme, Z.H. Chen, Z. Tao, Value-added products as soil conditioners for sustainable agriculture, Resour. Conserv. Recycl. 178 (2022) 106079. https://doi.org/10.1016/j.resconrec.2021.106079.

[4] J. Zhang, S. Wang, X. Wang, W. Jiao, M. Zhang, F. Ma, A review of functions and mechanisms of clay soil conditioners and catalysts in thermal remediation compared to emerging photo-thermal catalysis, J. Environ. Sci. (China). 147 (2025) 22–35. https://doi.org/10.1016/j.jes.2023.11.006.

[5] A. Aynehband, A. Gorooei, A.A. Moezzi, Vermicompost: An Eco-Friendly Technology for Crop Residue Management in Organic Agriculture, Energy Procedia. 141 (2017) 667–671. https://doi.org/10.1016/j.egypro.2017.11.090.

[6] Melanie Kah, C. Sabliov, Y. Wang, J. White, Nanotechnology as a foundational tool to combat global food insecurity, One Earth. 6 (2023) 772–775. https://doi.org/https://doi.org/10.1016/j.oneear.2023.06.011.

[7] D.K. Rajak, D.D. Pagar, R. Kumar, C.I. Pruncu, Recent progress of reinforcement materials: A comprehensive overview of composite materials, J. Mater. Res. Technol. 8 (2019) 6354–6374. https://doi.org/10.1016/j.jmrt.2019.09.068.

[8] A. de S.M.A.P.B. da S.L.S.M.I.A.N.N.K.C.V.S. de F.N.B. dos S.A.P.L. Freitas, Thermoplastic starch nanocomposites_ sources, production and applications – a review, (2022) 46. https://doi.org/https://doi.org/10.1080/09205063.2021.2021351.

[9] J.S. Rodrigues, A. de S.M. de Freitas, H.S.M. Lopes, A.A.F. Pires, A.P. Lemes, M. Ferreira, V.R. Botaro, Improvement of UV stability of thermoplastic starch matrix by addition of selected lignin fraction - Photooxidative degradation, Int. J. Biol. Macromol.

230 (2023) 1–12. https://doi.org/10.1016/j.ijbiomac.2023.123142.

[10] T.A. Lerma, M. Palencia, E.M. Combatt, Soil polymer conditioner based on montmorillonite-poly(acrylic acid) composites, J. Appl. Polym. Sci. 135 (2018) 1–8. https://doi.org/10.1002/app.46211.

[11] L.D. da Silva Neto, A. Maged, R. Gabriel, P.V.S. Lins, N.H. Haneklaus, M.W. Hlawitschka, L. Meili, Nanoclays in water treatment: Core concepts, modifications, and application insights, J. Water Process Eng. 67 (2024). https://doi.org/10.1016/j.jwpe.2024.106180.

[12] P. G, S. AS, J.S. Jayan, A. Raman, A. Saritha, Lignin based nano-composites: Synthesis and applications, Process Saf. Environ. Prot. 145 (2021) 395–410. https://doi.org/10.1016/j.psep.2020.11.017.

[13] A. de S. M. de Freitas, J.S. Rodrigues, C.C. Maciel, A.A.F. Pires, A.P. Lemes, M. Ferreira, V.R. Botaro, Improvements in thermal and mechanical properties of composites based on thermoplastic starch and Kraft Lignin, Int. J. Biol. Macromol. 184 (2021) 863–873. https://doi.org/10.1016/j.ijbiomac.2021.06.153.

[14] H. Sadeghifar, A. Ragauskas, Lignin as a UV Light blocker-a review, Polymers (Basel). 12 (2020) 1134. https://doi.org/10.3390/POLYM12051134.

[15] M.M. Delavari, I. Stiharu, Preparing and Characterizing Novel Biodegradable Starch/PVA-Based Films with Nano-Sized Zinc-Oxide Particles for Wound-Dressing Applications, Appl. Sci. 12 (2022). https://doi.org/10.3390/app12084001.

[16] L.P. Canellas, F.L. Olivares, Physiological responses to humic substances as plant growth promoter, Chem. Biol. Technol. Agric. 1 (2014) 1–11. https://doi.org/10.1186/2196-5641-1-3.

[17] M. Parit, P. Saha, V.A. Davis, Z. Jiang, Transparent and Homogenous Cellulose Nanocrystal/Lignin UV-Protection Films, ACS Omega. 3 (2018) 10679–10691. https://doi.org/10.1021/acsomega.8b01345.

[18] R.W. Behle, D.L. Campton, J.A. Kenar, D.I. Shapiro-Ilan, Improving Formulations for Biopesticides: Enhanced UV protection for beneficial Microbes, J. ASTM Int. 8 (2011) 10382.

[19] S.R. Yearla, K. Padmasree, Exploitation of subabul stem lignin as a matrix in controlled release agrochemical nanoformulations: a case study with herbicide diuron, Environ. Sci. Pollut. Res. 23 (2016) 18085–18098. https://doi.org/10.1007/s11356-016-6983-8.

[20] A. do E.S. Pereira, J. Luiz de Oliveira, S. Maira Savassa, C. Barbara Rogério, G. Araujo de Medeiros, L.F. Fraceto, Lignin nanoparticles: New insights for a sustainable agriculture, J. Clean. Prod. 345 (2022). https://doi.org/10.1016/j.jclepro.2022.131145.

[21] M.H. Hussin, J.N. Appaturi, N.E. Poh, N.H.A. Latif, N. Brosse, I. Ziegler-Devin, H. Vahabi, F.A. Syamani, W. Fatriasari, N.N. Solihat, A. Karimah, A.H. Iswanto, S.H. Sekeri, M.N.M. Ibrahim, A recent advancement on preparation, characterization and application of nanolignin, Int. J. Biol. Macromol. 200 (2022) 303–326. https://doi.org/10.1016/j.ijbiomac.2022.01.007.

[22] B. Abraham, V.L. Syamnath, K.B. Arun, P.M. Fathima Zahra, P. Anjusha, A. Kothakotta, Y.H. Chen, V.K. Ponnusamy, P. Nisha, Lignin-based nanomaterials for food and pharmaceutical applications: Recent trends and future outlook, Sci. Total Environ. 881 (2023) 163316. https://doi.org/10.1016/j.scitotenv.2023.163316.

[23] M. Parit, Z. Jiang, Towards lignin derived thermoplastic polymers, Int. J. Biol. Macromol. 165 (2020) 3180–3197. https://doi.org/10.1016/j.ijbiomac.2020.09.173.

[24] S.I. Hong, L.F. Wang, J.W. Rhim, Preparation and characterization of nanoclays-incorporated polyethylene/thermoplastic starch composite films with antimicrobial activity, Food Packag. Shelf Life. 31 (2022) 100784. https://doi.org/10.1016/j.fpsl.2021.100784.

[25] K.M. Dang, R. Yoksan, E. Pollet, L. Avérous, Morphology and properties of thermoplastic starch blended with biodegradable polyester and filled with halloysite nanoclay, Carbohydr. Polym. 242 (2020) 116392. https://doi.org/10.1016/j.carbpol.2020.116392.

[26] M. Morsali, A. Moreno, A. Loukovitou, I. Pylypchuk, M.H. Sipponen, Stabilized Lignin Nanoparticles for Versatile Hybrid and Functional Nanomaterials, Biomacromolecules. (2022). https://doi.org/10.1021/acs.biomac.2c00840.

[27] K. Pal, S. Pal, Development of porous hydroxyapatite scaffolds, Mater. Manuf. Process. 21 (2006) 325–328. https://doi.org/10.1080/10426910500464826.

[28] N. GONTARD, S. GUILBERT, J. -L CUQ, Edible Wheat Gluten Films: Influence of the Main Process Variables on Film Properties using Response Surface Methodology, J. Food Sci. 57 (1992) 190–195. https://doi.org/10.1111/j.1365-2621.1992.tb05453.x.

[29] B. van Raij, A. Küpper, Capacidade de troca de catíons em solos: estudo comparativo de alguns métodos, Bragantia. 25 (1966) 327–336. https://doi.org/10.1590/s0006-87051966000200005.

[30] N.I.F. Himmah, G. Djajakirana, D. Darmawan, Nutrient Release Performance of Starch Coated NPK Fertilizers and Their Effects on Corn Growth, SAINS TANAH - J. Soil Sci. Agroclimatol. 15 (2018) 104. https://doi.org/10.15608/stjssa.v15i2.19694.

[31] ABNT, ABNT NBR 14283-Resíduos em solos - Determinação da biodegradação pelo método respirométrico, Assoc. Bras. Normas Técnidas - NBR. (1999) 1–8.

[32] S.P. Bangar, W.S. Whiteside, A.O. Ashogbon, M. Kumar, Recent advances in thermoplastic starches for food packaging: A review, Food Packag. Shelf Life. 30 (2021) 100743. https://doi.org/10.1016/j.fpsl.2021.100743.

[33] A. Zare Shahrabadi, A. Kargari, A. Tayebi, Evaluation of the effectiveness of poly (phenyl sulfone) / nanoclay mixed matrix membranes for carbon dioxide/methane separation, Int. J. Greenh. Gas Control. 121 (2022) 103792. https://doi.org/10.1016/j.ijggc.2022.103792.

[34] O. Levana, J. Hoon Jeong, S. Sik Hur, W. Seo, M. Lee, K. Mu Noh, S. Hong, J. Hong Park, J. Hun Lee, C. Choi, Y. Hwang, Development of nanoclay-based nanocomposite surfaces with antibacterial properties for potential biomedical applications, J. Ind. Eng. Chem. 120 (2023) 448–459. https://doi.org/10.1016/j.jiec.2022.12.052.

[35] O.V. Kharissova, L.M. Torres-Martnez, B.I. Kharisov, Nanomaterials and Nanocomposites for Energy and Environmental Applications, 2021. https://doi.org/10.1007/978-3-030-36268-3.

[36] M. El Moustaqim, A. El Kaihal, M. El Marouani, S. Men-la-yakhaf, Thermal and thermomechanical analyses of lignin, Sustain. Chem. Pharm. 9 (2018) 63–68. https://doi.org/10.1016/j.scp.2018.06.002.

[37] H. Yang, R. Yan, H. Chen, D.H. Lee, C. Zheng, Characteristics of hemicellulose,

cellulose and lignin pyrolysis, Fuel. 86 (2007) 1781–1788. https://doi.org/10.1016/j.fuel.2006.12.013.

[38] D. Muscat, M.J. Tobin, Q. Guo, B. Adhikari, Understanding the distribution of natural wax in starch-wax films using synchrotron-based FTIR (S-FTIR), Carbohydr. Polym. 102 (2014) 125–135. https://doi.org/10.1016/j.carbpol.2013.11.004.

[39] A.C. Bertolini, C. Mestres, J. Raffi, A. Buléon, D. Lerner, P. Colonna, Photodegradation of cassava and corn starches, J. Agric. Food Chem. 49 (2001) 675–682. https://doi.org/10.1021/jf0010174.

[40] M. Kanidi, N. Loura, A. Frengkou, T.K. Milickovic, A.F. Trompeta, C. Charitidis, Inductive Thermal Effect on Thermoplastic Nanocomposites with Magnetic Nanoparticles for Induced-Healing, Bonding and Debonding On-Demand Applications, J. Compos. Sci. 7 (2023). https://doi.org/10.3390/jcs7020074.

[41] A.G. Morena, T. Tzanov, Antibacterial lignin-based nanoparticles and their use in composite materials, Nanoscale Adv. 4 (2022) 4447–4469. https://doi.org/10.1039/d2na00423b.

[42] Q. Zheng, P.O. Osei, S. Shi, S. Yang, X. Wu, Green fabrication of nanocomposite films using lignin nanoparticles and PVA: Characterization and application, Food Biosci. 59 (2024) 104022. https://doi.org/10.1016/j.fbio.2024.104022.

[43] A.C. Albuquerque, J.S. Rodrigues, A.S.M. De Freitas, G.T. Machado, V.R. Botaro, Renewable Source Hydrogel as a Substrate of Controlled Release of NPK Fertilizers for Sustainable Management of Eucalyptus urograndis: Field Study, ACS Agric. Sci. Technol. 2 (2022) 1251–1260. https://doi.org/10.1021/acsagscitech.2c00215.

[44] H. Liu, R. Wang, X.T. Lü, J. Cai, X. Feng, G. Yang, H. Li, Y. Zhang, X. Han, Y. Jiang, Effects of nitrogen addition on plant-soil micronutrients vary with nitrogen form and mowing management in a meadow steppe, Environ. Pollut. 289 (2021) 117969. https://doi.org/10.1016/j.envpol.2021.117969.

[45] A.M. Carswell, P.W. Hill, D.L. Jones, M.S.A. Blackwell, P.J. Johnes, E.R. Dixon, D.R. Chadwick, Impact of microbial activity on the leaching of soluble N forms in soil, Biol. Fertil. Soils. 54 (2018) 21–25. https://doi.org/10.1007/s00374-017-1250-9.

[46] J.R. Macedo, S.G. Moreira, F.A. de Moraes, D. de S.R. Junior, D.S. Peixoto, B.M. Silva, J.C.R. Silva, The management of phosphate fertilization affects soil phosphorus and yield of autumn/winter crops, Acta Sci. - Agron. 45 (2023). https://doi.org/10.4025/actasciagron.v45i1.57336.

[47] L.M. Angelo, D. França, R. Faez, Biodegradation and viability of chitosan-based microencapsulated fertilizers, Carbohydr. Polym. 257 (2021) 1–9. https://doi.org/10.1016/j.carbpol.2021.117635.

[48] G.F. Perotti, T. Kijchavengkul, R.A. Auras, V.R.L. Constantino, Nanocomposites based on cassava starch and chitosan-modified clay: Physico mechanical properties and biodegradability in simulated compost soil, J. Braz. Chem. Soc. 28 (2017) 649–658. https://doi.org/10.21577/0103-5053.20160213.

[49] S. Fahad, A.A. Bajwa, U. Nazir, S.A. Anjum, A. Farooq, A. Zohaib, S. Sadia, W. Nasim, S. Adkins, S. Saud, M.Z. Ihsan, H. Alharby, C. Wu, D. Wang, J. Huang, Crop production under drought and heat stress: Plant responses and management options, Front. Plant Sci. 8 (2017) 1–16. https://doi.org/10.3389/fpls.2017.01147.

[50] P.A. Magallanes-Cruz, P.C. Flores-Silva, L.A. Bello-Perez, Starch Structure Influences Its Digestibility: A Review, J. Food Sci. 82 (2017) 2016–2023. https://doi.org/10.1111/1750-3841.13809.

Designing Sustainable Soil Conditioners: Nanocomposite-Based Thermoplastic Starch for Enhanced Soil Health and Crop Performance

Jéssica S. Rodrigues[a1], Amanda S. M de Freitas[a,b1], Henrique O. S. Vieira[b], Lívia S. Emidio[b], Stefanny F. Amaro[b], Mariana A. Azevedo[b], Iolanda C. S. Duarte[b], Vagner R. Botaro[b], Leonardo F. Fraceto[a], Marystela Ferreira[b]

[a]Institute of Science and Technology of Sorocaba, São Paulo State University (UNESP), Av.Três de Março 511, 18087-180, Sorocaba, SP, Brazil.

[b] Science and Technology Center for Sustainability (CCTS), Federal University of São Carlos (UFSCar), João Leme dos Santos, km 110, 18052-780, Sorocaba, SP, Brazil.

[1] These authors contributed equally to the manuscript

Corresponding author: marystela@ufscar.br

ABSTRACT

The growing demand for sustainable solutions in agriculture, driven by global population growth and increasing soil degradation, has intensified the search for sustainable soil conditioners. This study investigated the impact of adding nanoclay (NC) and nano lignin (NL) to thermoplastic starch (TPS) on its physical, chemical, and thermal properties, its effectiveness as a soil conditioner, and its resistance to UV-C degradation. TPS nanocomposites were prepared with varying NC (3%, 5%, 7%) and NL (0.3%, 0.5%, 0.7%) proportions and characterized by FTIR (Fourier Transform Infrared Spectroscopy), SEM (Scanning Electron Microscopy), TGA (Thermogravimetric Analysis), and DSC (Differential Scanning Calorimetry). Swelling tests, phosphate buffer solubility, cation exchange capacity (CEC), and UV-C degradation resistance were evaluated. Results indicated that incorporating 7% NC (TPS/NC7%) significantly improved TPS's CEC and swelling properties. Conversely, adding 0.3% NL (TPS/NC7%/NL0.3%) improved photodegradation resistance and thermal stability. The TPS/NC7%/NL0.3% nanocomposites also demonstrated superior water retention in soil, efficient absorption and controlled release of nitrogen, phosphorus and potassium (NPK) fertilizer, significant reduction in the leaching of NH_4^+, $H_2PO_4^-$, and K^+ ions, and antimicrobial activity against both Gram-positive and Gram-negative bacteria, highlighting their biodegradability and potential as soil conditioners to promote agricultural sustainability. Additionally, tests conducted on cherry tomatoes confirmed the effectiveness of these nanocomposites under real cultivation conditions, with improved seedling development when using the TPS/NC7%/NL0.3% soil conditioner.

Keywords: Soil water retention, NPK absorption, UV-C degradation resistance, sustainable agriculture.

1. Introduction

The rapid population growth and increasing demand for agricultural land drive the need for higher food production, particularly as the global population reaches 8 billion [1,2]. This puts significant pressure on agricultural systems, creating major challenges for global food security while negatively impacting soils, with severe consequences for human health and ecosystem sustainability [3]. In this context, seeking innovative and efficient techniques to mitigate these damages becomes crucial, with the conversion of waste into soil conditioners emerging as a highly effective approach [1,2].

Soil conditioners are crucial in promoting plant growth, enhancing soil health, and reducing the need for chemical fertilizers [4]. Recently, a notable effort has been to incorporate microorganisms into soil conditioners to boost carbon sequestration. Using living organisms, such as earthworms, to produce vermicompost - a nutrient-rich organic fertilizer - has emerged as a beneficial approach [5]. At the same time, nanotechnology has gained traction in agriculture, showing promising results [6], suggesting that nanoscale materials can be effective agents in soil conditioners. Materials such as starch, lignin, and clay are now recognized as innovative and accessible solutions to enhance agricultural productivity. Beyond their critical role in agriculture, these composites are applied across various sectors, including aerospace, construction, sports, marine, and personal protection [7].

Thermoplastic starch (TPS) is a promising biopolymer that can replace conventional polymers, mainly when derived from cassava starch combined with a selected plasticizer [8,9]. This material can absorb fluids, respond readily to water, and excel in soil moisture retention. Meanwhile, clay, an essential element for soil fertility, plays a pivotal role in sustainable soil management [10]. Its cation exchange capacity (CEC) influences ion exchange, pollutant migration, and nutrient availability. In this context, nanoclay (NC) enhances the properties of traditional clay. These nanoscale, one-dimensional particles can be modified to form clay complexes compatible with organic monomers and polymers [11], offering benefits such as significant improvements in modulus, mechanical strength, flame resistance, heat resistance, and barrier properties.

In addition, lignin can be used as a soil conditioner due to its physical, chemical, thermal, and biological properties, greatly enhancing plant growth and development [12,13]. It improves soil structure by increasing its porosity and water retention capacity. Additionally, lignin's functional groups, such as carboxyl and phenolic, enhance the soil's CEC. This helps improve the availability of essential nutrients like potassium, calcium, and magnesium while reducing nutrient leaching. Lignin achieves this by forming complexes with these nutrients,

preventing them from being rapidly washed away by irrigation or rainwater [14]. Lignin can also serve as a substrate for beneficial soil microorganisms, as its gradual decomposition increases the organic matter content in the soil, which is essential for soil fertility. Furthermore, lignin acts as a biostimulant, promoting root growth and enhancing the plant's ability to absorb water and nutrients. This improvement can be attributed to several factors. Lignin acts as a biostimulant, promoting root growth and increasing root surface area, which improves soil exploration and nutrient uptake [15].

Additionally, lignin derivatives can enhance soil structure, improve water retention and facilitating root access to nutrients. Its bioactive compounds, such as phenolics, stimulate enzymatic and metabolic activities in plants, optimizing absorption processes [16]. Its antioxidant properties also play a crucial role in protecting plants from oxidative stress caused by adverse conditions such as drought, salinity, or pathogen attacks [17].

Lignin's role as a UV blocker has shown positive results in protecting certain groups of microorganisms and promoting their growth [9]. Studies have demonstrated that lignin can protect bacteria, fungi, and specific viruses used in pest control when added to pesticide formulations [18]. Lignin also preserves *Pichia anomala* (strain K) and other antagonistic yeasts used as biocontrol agents against post-harvest diseases from UV radiation. Furthermore, adding lignin, especially in its nanostructured form, plays a vital role in protecting *Escherichia coli* from UV-induced mortality, with enhanced results when nano lignin are employed [19].

Nanoscale materials, such as nano lignin (NL), have garnered significant interest from researchers due to their unique properties and ability to enhance particle reactivity through a high surface area [20]. This improved availability of reactive sites makes processes more efficient, enabling the use of smaller quantities of material and reducing costs. In addition to its well-known applications, nano lignin has recently been used as a reinforcing agent in composites and hybrid nanocomposites across a wide range of applications. Its ability to bind tightly with various biopolymers significantly improves materials' thermal and mechanical properties [21].

This study investigated the combined effects of TPS, NC, and NL as soil conditioners. Previous studies had demonstrated the individual benefits of TPS when combined with NL and NC, highlighting enhancements in mechanical and thermal strength, increased water retention capacity, and good biodegradability [22–25]. However, more research is needed to address the synergistic interaction of these three components in a single nanocomposite and their combined impact on soil quality. The simultaneous inclusion of NL, known for its antioxidant, antimicrobial, and UV-blocking properties, along with NC, which enhances CEC, offered

substantial potential to optimize soil conditioners' physical and chemical properties and improve nutrient availability and soil aeration. Moreover, the effectiveness of these nanocomposites was tested on red cherry tomatoes, providing proof of concept in greenhouse conditions. Thus, this study sought valuable insights into how these nanocomposites could improve soil quality and contribute to more sustainable agricultural practices.

2. Materials and methods

2.1 Materials

The lignin used in this research was extracted from *Eucalyptus urograndis* through the kraft process in the production of cellulose and paper, supplied by the company Suzano, located in the state of São Paulo, Brazil. The soluble starch (ACS), ammonium acetate ($NH_4C_2H_3O_2$), barium chloride ($BaCl_2$), and potassium hydroxide (KOH) were provided by Êxodo Científica. Anidrol supplied the glycerol ($C_3H_8O_3$). The NC used was hydrophilic bentonite (Montmorillonite), and potassium chloride (KCl) were obtained from Sigma-Aldrich. Acetone (C_3H_6O), hydrochloric acid (HCl), and phenolphthalein ($C_{20}H_{14}O_4$) were sourced from Synth. The NPK fertilizer used in the soil conditioner evaluation was Fertilizante Mineral Misto 10-10-10+micros (Boron (0.06%), Sulfur (1%), Iron (0.03%), Magnesium (0.03%), and Zinc (0.10%)) from Dimy®, and the soil used was from Forth®. The red cherry tomato seeds were obtained from Feltrin Sementes®. Mueller Hinton Broth was supplied by Difco.

2.2 Lignin Nanoparticles Synthesis

NL was synthesized using the antisolvent precipitation method, as detailed by Morsali *et al.* (2022)[26]. Initially, 0.5 g of pre-dried kraft lignin (KL) was dissolved in a solution containing 30 g of acetone and 10 g of deionized water under constant stirring for 3 h at room temperature. The solution was filtered through a 0.45 μm pore membrane (Millipore) to remove undissolved solids. To form a colloidal dispersion of KL, 120 g of deionized water was added to the stirring solution. Finally, the acetone was removed using a rotary evaporator under reduced pressure at a temperature of 40°C.

2.3 Sample Preparation

A mixture of 110 g of ultrapure water, 30 g of soluble starch, and 10 g of glycerol was heated under stirring until it reached approximately 80°C. This condition was maintained for 5 min to prepare the TPS sample. The exact composition was used to prepare the TPS/NC nanocomposites, but with the addition of 3%, 5%, and 7% (w/w) of NC relative to the starch mass, respectively. The addition of NC was strategically performed to enhance cation exchange capacity, soil structure stability, and controlled nutrient release. The most effective TPS/NC

(7%) composition was selected to prepare nanocomposites with NL, termed TPS/NC/NL, in proportions of 0.3%, 0.5%, and 0.7% of NL relative to the starch mass.

The solutions were transferred into Falcon tubes, each filled to approximately one-third of their total volume (~15 mL). The tubes were sealed and placed in a freezer at -18°C for 24 h. After freezing, the samples were lyophilized using a bench-top freeze dryer, Enterprise IB model from Terroni®, for 24 h at a pumping speed of 250 L/min and a temperature of -55°C. Once removed from the lyophilizer, the samples were ground using a mortar and pestle and then sieved.

2.4 Nanocomposites Characterization

Structural and Morphological Analysis: Structural characterization of the nanocomposites was performed using a Nicolet Summit IR 200 spectrometer in Attenuated Total Reflectance (ATR) mode, with 126 scans, a nominal resolution of 4.0 cm^{-1}, and a range of 4000 to 400 cm^{-1}. Morphological analysis was conducted using a Field Emission Gun Scanning Electron Microscope (JSM 7200F Japan Electron Optics Ltd.), operating in InLens mode, with an emission energy beam of 2 kV and a working distance of approximately 7 mm. The samples were coated with iridium via sputtering.

Thermal Analysis: Thermal characterization of the composites was carried out using a Perkin Elmer Pyris1 TGA with a constant heating rate of 20 °C/min up to 900°C, maintained in an inert atmosphere with a nitrogen flow rate of 20 mL/min. Thermal measurements were also conducted using a Differential Scanning Calorimeter (DSC), model Q10 from TA Instruments, USA, equipped with a RCS 40 cooling system. The samples were preheated to 100°C with a 5-minute isothermal hold to eliminate thermal history. They were then cooled to -10°C, followed by a second heating to 200°C at a rate of 20 °C/min. All measurements were performed under a 250 mL/min nitrogen flow, with sample masses maintained around 4-7 mg. Thermal events were identified and quantified during the second heating scan for DSC analyses, supported by TRIOS® software.

2.4.1 Physical Properties

Swelling: The swelling capacity in the buffer was assessed according to a method adapted from PAL and PAL (2006)[27]. Approximately 0.1 g of the nanocomposite was added to 10 mL beakers containing 5 mL of phosphate buffer solution (pH 5, 7, and 9) for 30 min. Initially, the samples were weighed dry (Ws, dry mass). After each immersion period, the samples were carefully removed, dried with absorbent paper, and weighed again (Wu, wet weight). The immersion, removal, drying, and weighing process was repeated in triplicate for each time interval. The swelling capacity was calculated according to Equation 1.

$$Swelling\ (\%) = \frac{Wu - Ws}{Ws}\ x\ 100 \qquad \text{(Equation 1)}$$

Soluble Fraction Determination: The determination of the soluble fraction of the samples in phosphate buffer solutions (pH 5.0, 7.0, and 9.0) was performed following the method of Gontard, Guilbert, and Cuq (1992)[28], with some adaptations. Initially, the dry matter percentage of the samples was determined by weighing them after drying in an oven at 70°C for 2 h. The samples were then immersed in 20 mL of phosphate buffer solution (pH 5.0, 7.0, and 9.0) and maintained under slow agitation at 38°C for 24 h. After this period, each solution was filtered, and the retained material was dried in an oven at 70°C for 24 h until a constant mass was achieved. The amount of non-soluble dry matter was determined using Equation 2

$$Soluble\ Fraction\ (\%) = \frac{Wi - Wf}{Wf}\ x\ 100 \qquad \text{(Equation 2)}$$

Where: Wi = initial mass of dry material and Wf = final mass of non-solubilized dry material.

2.4.2. Cation Exchange Capacity

The study of CEC was conducted following the Ammonium Acetate Method established by the Instituto Geográfico Agustín Codazzi.[29] 1 g of the nanocomposite was mixed with 15 mL of ammonium acetate solution (1.0 M), agitated for 20 min, and allowed to stand for 16 h to initiate cation exchange reactions. After this period, the sample was filtered and washed with a diluted ammonium acetate solution (0.01 M). Subsequently, 15 mL of KCl extraction solution (1.0 M) was added, agitated vigorously for 1 h, and filtered again. The amount of exchanged ammonium was then determined by titration with HCl (0.1 M).

2.4.3. UV-C Exposure

Photodegradation tests of the nanocomposites were conducted to assess their degradation behavior under UV-C radiation. The materials were exposed to UV-C radiation in a lab-made chamber. The lamps used were fluorescent, germicidal, 15 W in power, with a maximum emission wavelength of 254 nm, and an incident energy of 610 ± 10 μW/cm². The distance between the sample and the lamp was 20 cm for 21 days. Degradation was monitored through FTIR analyses, with measurements taken at the beginning and end of the exposure period (0 and 21 days).

2.5. Soil Conditioner Evaluation Tests

2.5.1. Soil Water Retention

To calculate water retention, 10 g of characterized soil (Supplementary Information - S1) was initially used, dried at 105°C for 24 h, and screened through a 2 mm sieve to ensure homogeneity. The soil was mixed with 2.5 g of nanocomposite (TPS, TPS/NC7%, and TPS/NC7%/NL0.3%), maintaining a ratio of 75% soil and 25% nanocomposite (V_{s+n}). This mixture was placed in a 200 mL system made from recycled PET bottles (Polyethylene Terephthalate), with drainage holes at the bottom and perforations at the top to allow airflow. Water was gradually added until the mixture was completely saturated, and the excess water drained was collected and measured. After drainage, the bottles were weighed to determine the saturated soil mass (S_s). The samples were then dried at 105°C for 24 h and weighed again to obtain the mass of the dry soil (D_s). The water retention capacity was calculated using Equation 3. The results were compared with pure soil samples to assess the effectiveness of the nanocomposites in water retention.

$$Water\ retention\ (\%) = \frac{Ss - Ds}{Vs+n}\ x\ 100 \qquad \text{(Equation 3)}$$

2.5.2 Evaluation of NPK Ion by Leaching

Leaching tests were conducted in triplicate at room temperature and neutral pH, adapting the method described by Himmah *et al.*[30] This method aimed to simulate real soil leaching conditions using the soil-film systems mentioned in Section 3.5.2. Over 9 weeks, the concentrations of N (NH_4^+), P ($H_2PO_4^-$), and K (K^+) ions present in the leaching systems were monitored. Weekly, 50 mL of distilled water was poured onto the tops of the PETs, and the collected leachate was analyzed using UV-vis spectrophotometry. A flame photometer was used for K ion release. Additional details can be found in Supplementary Files S2.

2.5.3 Soil Biodegradation

Accelerated biodegradation tests were conducted using Bartha respirators. Each unit contained 50 g of soil and 0.5 g of nanocomposites. To capture the carbon dioxide (CO_2) produced from aerobic microbial activity, 10 mL of 0.2 M KOH solution was placed in the side arm of each respirator. At least three times a week, the KOH solution from the side arm was carefully removed, transferred to an Erlenmeyer flask, and mixed with 1 mL of $BaCl_2$ (1 M) solution to precipitate the carbonate formed. The remaining KOH in the flask was titrated with a standardized HCl (0.1 M) solution to quantify the captured CO_2. Before refilling the side arm

with fresh KOH solution, it was rinsed with 10 mL of CO_2-free deionized water. The biodegradation of the materials was monitored over 50 days at 28°C, following NBR 14283 [31], with samples analyzed in triplicate and results compared to blank triplicates to measure background CO_2 levels.

2.5.4 Antimicrobial Activity

The bacterial viability was evaluated by assessing the growth of Gram-positive and Gram-negative strains, Staphylococcus aureus (ATCC 6538) and Escherichia coli (ATCC 25922), respectively, in the presence of the synthesized hybrid composites. To conduct this, 0.5 g of the material was added to 9.0 mL of Mueller Hinton Broth (MHB). Then, 1.0 mL of bacterial dispersion was standardized to 0.5 at an optical density of 600 nm (OD600), equivalent to 1×10^5 colony-forming units (CFU)·mL^{-1}, and added to the MHB. The mixtures were incubated for 24 h at 35°C. Finally, the quantification of CFU in each experimental batch was determined using a spectrophotometer (OD600). All experiments were conducted in triplicate.

2.6 Effectiveness of Soil Conditioners in Red Cherry Tomato Cultivation

To evaluate the effectiveness of soil conditioners in NPK release, five distinct compositions were tested in 1 L pots using red cherry tomatoes as the model crop. The nanocomposites evaluated were: TPS, TPS/NC7%, and TPS/NC7%/NL0.3%. A total of 6 g of each nanocomposite was swollen with 12 mL of liquid NPK solution (10-10-10). Additionally, two control groups were included: one consisting of only soil (Control) and another with soil plus 12 mL of commercial liquid NPK. Two red cherry tomato seeds were planted in pots containing 500 g of pre-homogenized soil. Each pot received one of the treatments as specified, ensuring all plants were subjected to similar conditions, except for the different soil conditioners applied. To ensure reproducibility, each treatment was replicated in six pots.

Throughout the experiment, plants were monitored weekly to assess their growth, development, and the effectiveness of soil conditioners. Measurements of plant height, number of leaves, and fruit development were recorded weekly. Plant health was observed, including any signs of nutritional deficiencies or stress. Irrigation was controlled to ensure all plants received the same amount of water, avoiding variations that could affect the results.

2.7 Statistical Data Analysis

Statistical analysis was performed on the numerical results obtained from some of the analyses to compare sets of results and identify significant differences between the studied populations. The one-way ANOVA test was used, a variance analysis technique to compare means of multiple independent populations. Among the results from the test, the p-value was used to determine significant statistical differences between sample sets, with significance set at 5% ($p<0.05$). For p-values less than 0.05, a Tukey's Honest Significant Difference test was subsequently conducted to identify significant differences between pairs of sample sets.

3. Results and Discussions

3.1. TPS/NC Characterization

Initially, the effects of adding different concentrations of NC (3, 5, and 7%) on the swelling properties of TPS were examined. Figure 1A presents the FTIR analysis conducted to characterize the structural components of the nanocomposites, both with and without the addition of NC, and to verify the interaction between these materials. In the spectrum attributed to TPS (Figure S3), we observed O-H stretching vibrations at approximately 3300 cm^{-1}. The 2931 and 2881 cm^{-1} bands were assigned to C-H axial deformation. The band at 1632 cm^{-1} is characteristic of OH angular deformation in water and appeared in the samples with the addition of NC. Additionally, the spectrum showed bands at 1409 and 1331 cm^{-1}, related to COH groups, characteristic of TPS. At 995 cm^{-1}, a band corresponding to C-O deformation was observed, where an increase in intensity in the TPS spectrum was noted due to interactions between the plasticizer glycerol and the starch [9,32].

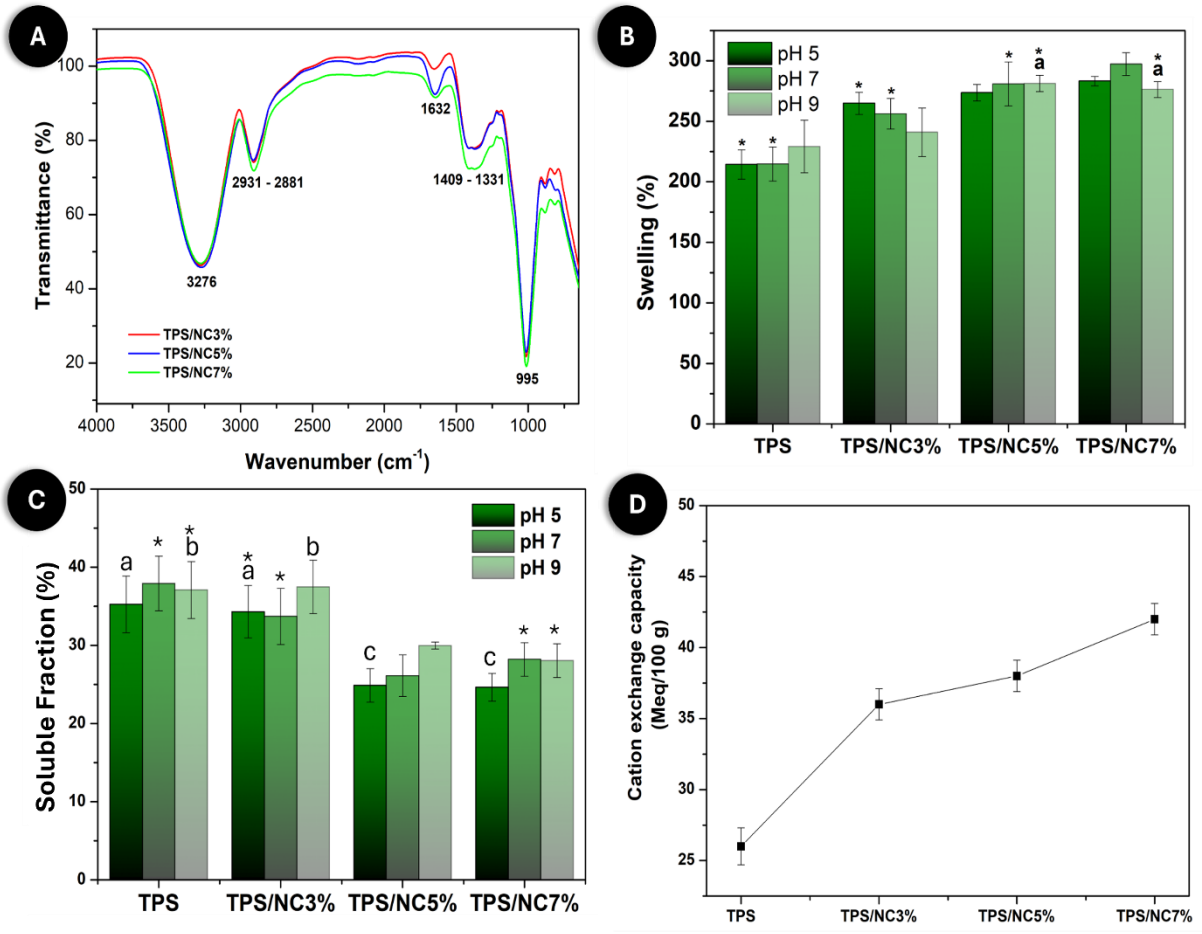

Figure 1. A. FTIR Spectrum. B. Swelling vs. pH Variation (5, 7, and 9). C. Soluble Fraction vs. pH Variation (5, 7, and 9). D. Cation Exchange Capacity for the TPS, TPS/NC3%, TPS/NC5%, and TPS/NC7%. Statistically similar samples: $^{a\text{-}c}$ for the same pH value among different samples; * for the same sample at various pH values.

For the spectrum attributed to NC (Figure S3), characteristic bands were observed between 3600 and 3300 cm^{-1}, corresponding to the stretching vibrations of hydroxyl groups in the silicate layers of NC. In a study by Mert *et al.*[12], where NC was incorporated into macroporous polymers modeled in emulsion (PolyHIPEs), a band between 2230 and 2150 cm^{-1} was attributed to surface groups of NC. This explains the 2359 cm^{-1} band in NC, linked to asymmetric C–H (aliphatic) stretches from surface-modifying groups, absent in the TPS samples. At 1632 cm^{-1}, associated with OH angular deformation in water, NC had a more intense peak than TPS. The TPS/NC7% spectrum closely resembled that of NC, suggesting changes in bonding and structure with increased NC content.

Additionally, the band at 995 cm^{-1}, indicative of C-O deformation, was stronger in NC, possibly due to the vibration of Si-O groups in the NC [33]. The spectra of TPS/NC nanocomposites showed similarities to pure TPS, particularly in the 3300 to 2881 cm^{-1} range, corresponding to O-H stretching and C-H axial deformations, and in the 1409 to 1331 cm^{-1}

range, linked to COH groups. The prominent peaks at 1632 cm^{-1} across the TPS/NC nanocomposites (Figure 1A) and NC may be due to water between the NC layers, with ammonium bromide possibly intercalated between the silicate layers, showing more intensely in the NC spectrum. Furthermore, the 995 cm^{-1} band, besides being related to C-O deformation, may result from the stretching vibration of Si-O groups within the NC.

Adding NC to the nanocomposites enhanced their swelling properties (Figure 1B), attributed to the unique characteristics of this clay, particularly its capacity for expansion and ion exchange. Bentonite, the montmorillonite type, can swell upon contact with water, forming a sandwich-like structure where water molecules are trapped between the clay layers [34]. This considerable expansion significantly increased the volume of the nanocomposite, thereby improving its swelling properties. Based on statistical analysis, no significant difference in swelling was observed for the same sample across different pH levels. It was also noted that increasing the NC content further improved the swelling properties (TPS/NC7% > TPS/NC5% > TPS/NC3% > TPS).

Figure 1C presents soluble fraction analysis vs. pH variation (5, 7, and 9) for TPS and TPS/NC samples (3, 5, and 7%), revealing a behavior opposite to swelling. As the NC concentration in the nanocomposites increased, the soluble fraction decreased. This pattern aligns with NC's water retention ability, as Kharissova *et al.* (2021)[35] highlighted, suggesting that its inclusion in TPS protects the material from dissolution. Notably, samples composed solely of TPS showed significant soluble fraction due to its high affinity for water, which is attributed to the intermolecular hydrogen bonds present in its main components: amylose, characterized by α-(1-4) glycosidic bonds and amylopectin, with α-(1-6) glycosidic bonds [4]. Statistical analysis of the results across different pH levels for the same sample showed no clear behavioral trend, with most groups exhibiting statistically similar samples. TPS and TPS/NC3% had statistically similar soluble fractions for the same pH, while the samples with 5% and 7% NC were also quite similar, particularly at pH 5.

The increase in NC percentage was directly proportional to the rise in CEC, as shown in Figure 1D. Montmorillonite clay exhibits high CEC due to its layered crystalline structure [24]. Cations in the solution surrounding the nanocomposite can move in and out of these layers, allowing for even more significant material expansion. Additionally, CEC influences the interactions between water molecules and clay particles, contributing to the enhanced swelling properties depicted in Figure 1B. These results emphasize the importance of adding montmorillonite to improve the desired properties of the nanocomposites, making them more effective for various applications [4].

The samples exhibited pH levels of 5.7±0.4, 6.9±0.1, 6.5±0.1, 6.6±0.3, and 6.7±0.1 for TPS, NC TPS/NC3%, TPS/NC5%, and TPS/NC7%, respectively. The data showed a trend toward neutral pH, with values ranging between 6 and 7, except for TPS, which was slightly more acidic. This difference can be attributed to the chemical composition of the materials used. NC, being neutral, tends to raise the pH of the samples, while TPS, with its intrinsic acidity, has the opposite effect, lowering the pH. This pH neutrality is important because it allows nanocomposites to be applied across various soil types, regardless of the soil's initial pH [3].

3.2 Nanocomposite added with NL

The TPS/NC7% was selected for its reduced water solubility, which helps minimize the likelihood of leaching, and for exhibiting greater swelling capacity and better CEC compared to the other tested nanocomposites (Figure 1D). In the second phase, the effects of adding different concentrations of NL (0.3%, 0.5%, and 0.7%) on the properties of TPS/NC7% were explored. This approach aims to develop a more effective soil conditioner by leveraging NL's antioxidants, UV-blocking, antimicrobial, and other potential benefits.

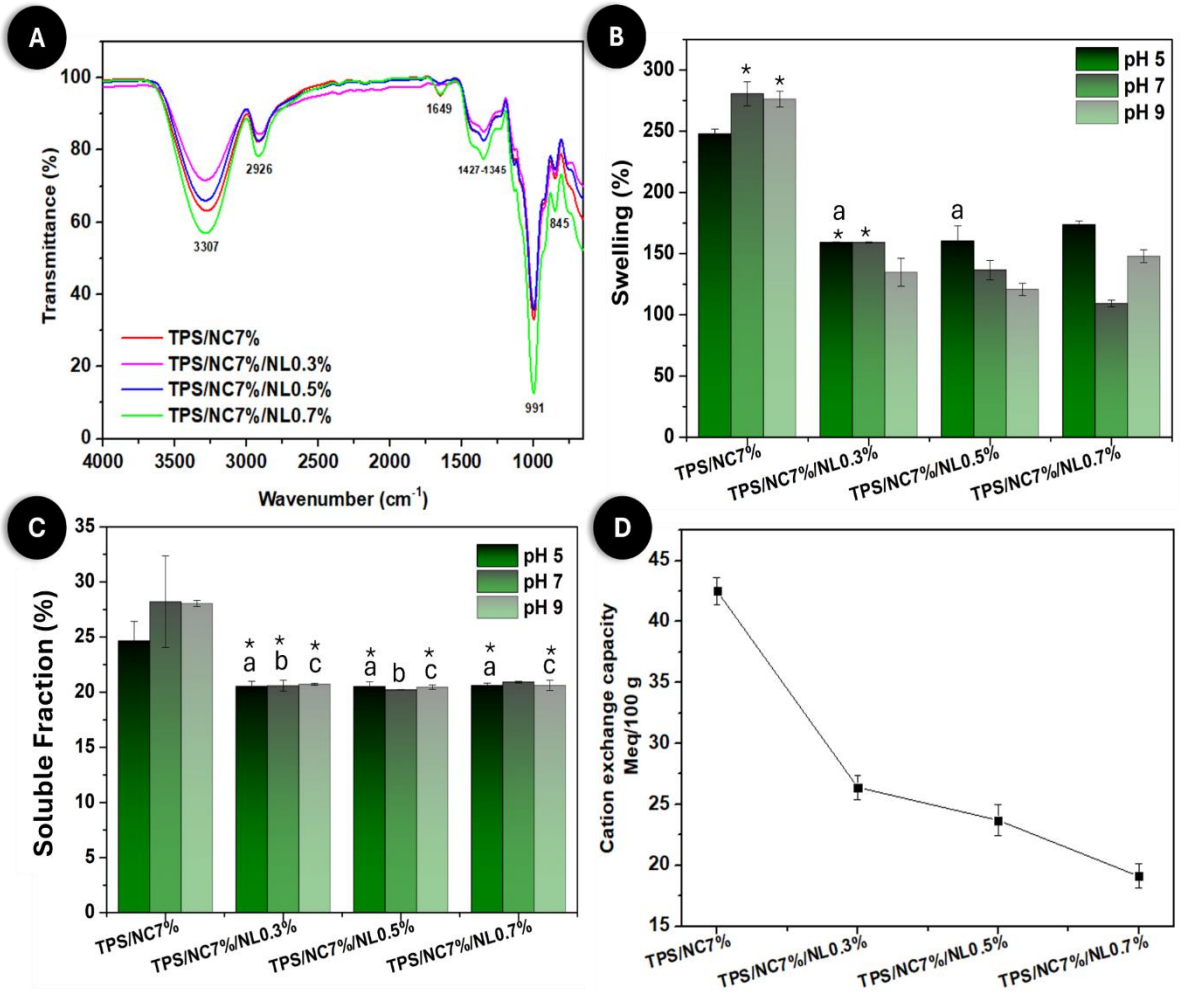

Figure 2. A. FTIR spectrum; B. Swelling vs. pH variation (5, 7, and 9); C. soluble fraction vs. pH variation (5, 7, and 9); and D. Cation exchange capacity for the samples TPS/NC7% and TPS/NC7%/NL (0.3, 0.5, and 0.7%). Statistically similar samples: $^{a\text{-}c}$ for the same pH value among different samples; * for the same sample at various pH values.

Figure 2A presents the FTIR spectra for the three different concentrations of NL. The analysis revealed interactions among the components, indicating that the spectra of the NL-added nanocomposites tend to maintain structures like those of pure TPS and NL (Figure S3). This suggests that these components strongly influence the structure and bonding of the nanocomposite. The band at 2926 cm^{-1} exhibits characteristics like pure TPS, attributed to the axial deformation of C-H, while the band at 1649 cm^{-1} resembles the spectrum of pure NL, corresponding to the vibrations of C=C benzene rings typical of lignin structure. In the case of the TPS/NC7%/NL0.7% nanocomposite, a higher peak is observed, indicating a greater concentration of NL in its composition. The other bands align with those of TPS and NL, except for the band at 991 cm^{-1}, characteristic of NC, which shows a more pronounced peak, especially for TPS/NC7%/NL0.7%. This can be attributed to C-O deformation, stretching vibrations of Si-O groups present in NC, and/or specific structures from NL [13,33].

Figure 2B shows that pH 5 was the most effective for the expansion of materials with NL, with swelling increasing as the concentration of NL rose, where the samples with 0.3% and 0.5% NL were statistically similar. In contrast, at pH 7, there was a trend of decreasing swelling as the concentration of NL increased. At pH 9, a slight decrease in swelling was observed, followed by an increase, remaining relatively constant. In summary, the addition of NL reduced the swelling properties of the nanocomposite compared to TPS/NC7%. This effect can be attributed to NC charges' excellent dispersion and interaction with the TPS matrix. The bonds between TPS, and the various added nanoparticles decreased the polymer chains' mobility, hindering the aqueous medium's permeability through the material. The graph in Figure 2C displayed a soluble fraction trend of around 20% for all samples at the three tested pH levels. Notably, there was a reduction in soluble fraction for all composites compared to the TPS/NC7% sample, indicating lower soluble fraction due to the addition of NL, as anticipated in the literature [21]. This reduction in soluble fraction suggests greater resistance to dissolution in aqueous environments, resulting in more effective protection against leaching. Due to the low mass of NL added, which was less than 1% of the total, the variations in soluble fraction among the different concentrations were minimal.

Figure 2D shows the CEC for the composites TPS/NC7%/NL0.3%, TPS/NC7%/NL0.5%, and TPS/NC7%/NL0.7%. The values indicate a decreasing trend in CEC with increasing NL concentration in the composite. This may be attributed to the greater proportion of NL in the nanocomposite, reducing the available surface area for cations. The pH test revealed values of 6.57±0.06, 5.63±0.02, and 6.25±0.06 for the samples TPS/NC7%/NL0.3%, TPS/NC7%/NL0.5%, and TPS/NC7%/NL0.7%, respectively. These data suggest that the addition of NL, due to its acidic nature, slightly lowered the pH of the samples, except for the composite with 0.5% NL, which had a more acidic pH than the others. However, the overall neutral character was maintained compared to the TPS/NC7% nanocomposites, with pH values ranging from 5.5 to 7. This neutrality makes the TPS/NC7%/NL composites suitable for application in various soils.

3.2.1 Thermal properties

The data from the TGA (Figure 3A) and the DTG (Figure 3B) are compiled in Table 1. This table includes information such as the initial degradation temperature ($T_{5\%}$), which indicates the temperature at which 5% of the initial mass of the analyte was lost; the maximum degradation temperature (T_{max}), obtained from the first derivative of the TGA curves; the mass loss index (Δm), representing the percentage of mass degraded during T_{max}; the final

temperature (T_f), derived from the TGA curves; the decomposition temperature range (ΔT), calculated as the difference between T_f and $T_{5\%}$; and the char residue at 600°C ($R_{600°C}$).

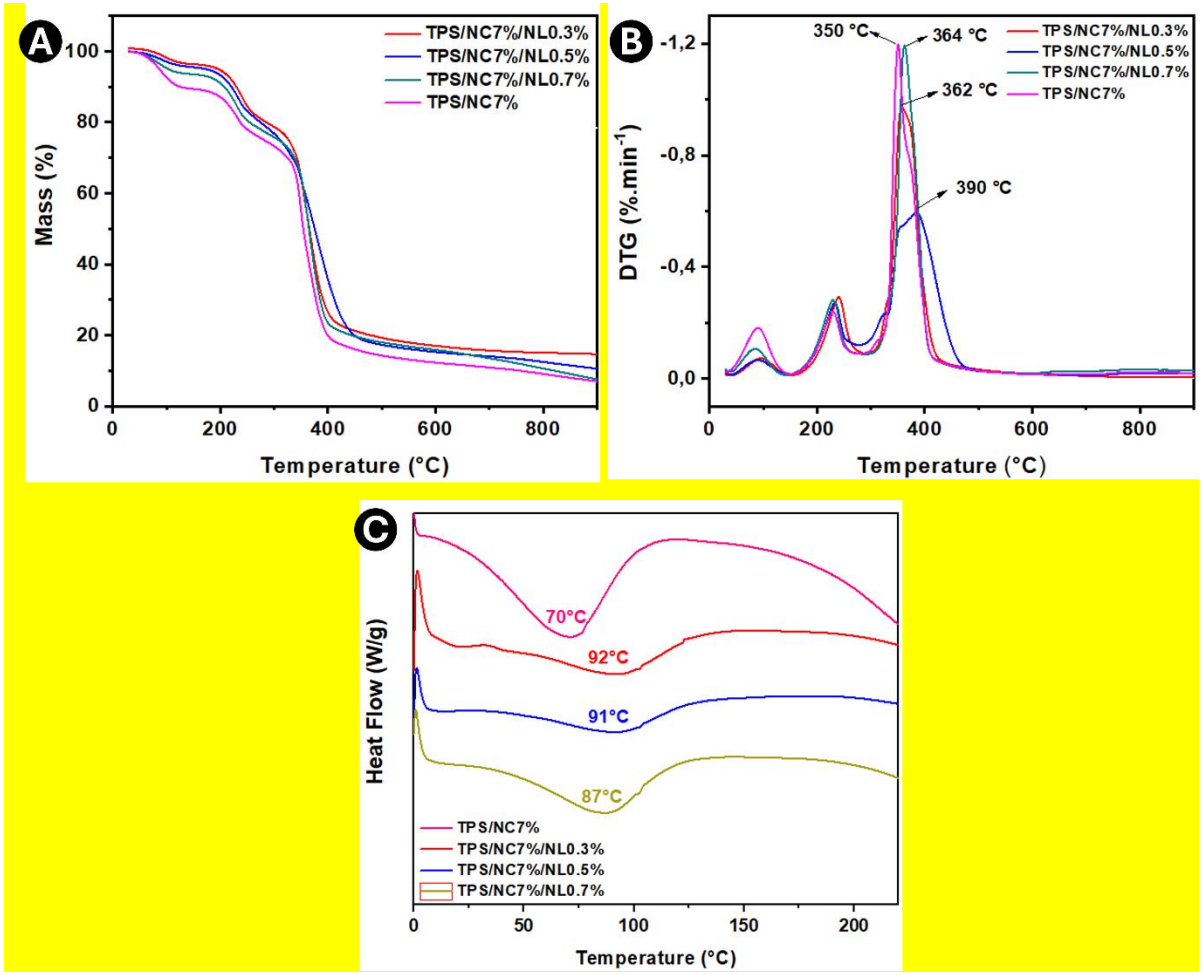

Figure 3. (A) Thermogravimetric (TGA) curves, (B) First Derivative of Thermogravimetric Curves (DTG), and (C) Differential Scanning Calorimetry (DSC) for the samples of TPS/NC7% and TPS/NC7%/NL (0.3, 0.5, and 0.7%).

The variability observed in the $T_{5\%}$ values, as shown in Table 1, is attributed to the complexity of the thermal decomposition process in these composite systems. The interaction between TPS, NC, and NL introduces multiple decomposition mechanisms influenced by the proportion of each component. While the sample with 0.3% NL displayed the highest $T_{5\%}$ (190°C), indicating improved initial thermal resistance, the samples with 0.5% and 0.7% NL exhibited lower values (165°C and 98°C, respectively). This lack of a consistent trend can be explained by potential phase segregation or non-uniform dispersion of the nanoaditives in the matrix, which could reduce the effectiveness of thermal stabilization in some cases. This is consistent with findings in similar systems, where optimal properties are often achieved at specific additive concentrations due to balanced interactions within the composite matrix [36].

T_{max} also varied among the samples, reflecting thermal resistance during decomposition. The TPS/NC7% sample showed a Tmax of 350°C, while the NL-added samples exhibited values of 362°C (TPS/NC7%/NL0.3%), 390°C (TPS/NC7%/NL0.5%), and 364°C (TPS/NC7%/NL0.7%). The highest T_{max} was observed in TPS/NC7%/NL0.5%, indicating superior thermal resistance, possibly due to greater interaction between the polymer matrix and the nanoaditives [13]. Δm at T_{max} also displayed variations. The TPS/NC7% sample experienced a mass loss of 49%, while the NL-containing samples showed losses of 47% (TPS/NC7%/NL0.3%), 59% (TPS/NC7%/NL0.5%), and 52% (TPS/NC7%/NL0.7%). The high mass loss observed in the sample TPS/NC7%/NL0.5% might indicate that at this specific composition, the thermal decomposition is dominated by the degradation of NL, which is consistent with its higher T_{max}.

The T_f was derived from the TGA curves, with the TPS/NC7% sample showing the highest T_f of 542°C. The modified samples showed slightly lower T_f values: 539°C for TPS/NC7%/NL0.3%, 532°C for TPS/NC7%/NL0.5%, and 511°C for TPS/NC7%/NL0.7%. These reductions indicate that the presence of nanocomposites can influence the temperature at which decomposition ends. The ΔT varied from 458°C for TPS/NC7% to 342°C for TPS/NC7%/NL0.3%, 370°C for TPS/NC7%/NL0.5%, and 414°C for TPS/NC7%/NL0.7%. The TPS/NC7% sample exhibited the largest ΔT, indicating a broader decomposition range, while adding NL resulted in narrower decomposition ranges. Finally, the $R_{600°C}$ was higher in the samples containing NL, with values of 17% (TPS/NC7%/NL0.3%), 16% (TPS/NC7%/NL0.5%), and 15% (TPS/NC7%/NL0.7%), compared to 12% for the TPS/NC7% sample. This suggests that NL promotes the formation of a stable carbonaceous structure, likely due to its aromatic composition, which resists complete degradation.

Table 1. Thermal parameters result in TPS/NC7%, TPS/NC7%/NL0.3%, TPS/NC7%/NL0.5%, and TPS/NC7%/NL0.7%.

Samples	$T_{5\%}$ (°C)[a]	$T_{máx}$ (°C)[b]	Δ_m (%)[c]	T_f (°C)[d]	Δ_T (°C)[e]	$R_{600°C}$ (%)[f]
TPS/NC7%	83	350	49	542	458	12
TPS/NC7%/NL0.3%	190	362	47	539	342	17
TPS/NC7%/NL0.5%	165	390	59	532	370	16
TPS/NC7%/NL0.7%	98	364	52	511	414	15

[a]Initial degradation temperature; [b]Temperature of the maximum degradation; [c]Mass loss index up to Tmax; [d]Final degradation temperature; [e]Decomposition temperature range; [f]The amount at the end of degradation process at 600°C.

In the DSC curve (Figure 3C) of TPS/NC7%, a temperature peak at 70°C was identified, associated with the glass transition of starch, suggesting a change in the molecular structure at this point. In the other samples aditivated with NL, only peaks were observed at 92°C for TPS/NC7%/NL0.3%, 91°C for TPS/NC7%/NL0.5%, and 87°C for TPS/NC7%/NL0.7%. These peaks likely represent a combination of phase transitions and specific degradation events related to the interaction between NC and NL in the polymer matrix.

Thus, the addition of NL to TPS/NC7% significantly improved the material's thermal stability. The combination of 7% NC with 0.3% NL exhibited the best results regarding increased initial degradation temperature and amount of charcoal residue, indicating a potential synergy between the components that confers greater thermal resistance to the material. The presence of NC and NL promoted new intermolecular interactions in the composite, with the latter characterized by a complex, highly branched aromatic structure, contributing to the considerable thermal stability of the samples [37].

3.2.2. Impact of UV-C Exposure on the Stability and Photodegradation of the Nanocomposite

It was possible to observe in Figure S4-A that for the samples without UV-C exposure, that is, at 0 days, the higher the percentage of NL added, the greater the intensity of the absorptions at bands 3276 and 2931 cm^{-1} (both corresponding to O-H stretching and C-H axial deformations), 1400 cm^{-1} (associated with COH groups), and 995 cm^{-1} (related to C-O deformation) [32,38,39]. In other words, the concentration of NL is proportional to the increase in band intensity. After 21 days, the TPS and TPS/NC7%/NL0.3% samples exhibited similar UV-C degradation behavior, while the TPS/NC7%/NL0.5% and TPS/NC7%/NL0.7% samples showed improved resistance to photodegradation, indicating that the higher NL concentrations provided better protection against UV-C exposure.

In the bands shown in Figure S4-B, there was a reduction in intensity as the amount of NL added to the sample increased. However, the samples TPS/NC7%/NL0.5% and TPS/NC7%/NL0.7% showed a more significant reduction compared to the TPS and TPS/NC7%/NL0.3% samples. Overall, there is a subtle modification in the samples after exposure to UV-C light due to the low percentage variation ($<1\%$) of NL analyzed. Thus, there is no predictable behavior for the relationship between NL and photoprotection. Future work aims to conduct this study with higher concentrations of NL.

3.3. Evaluation of the Nanocomposite as a Soil Conditioner

The TPS/NC7%/NL0.3% nanocomposite was selected for soil conditioner evaluation tests due to its superior performance in terms of thermal stability. Additionally, its soluble fraction remained consistent across all tested samples, and it exhibited less variation in swelling at the different pH levels analyzed.

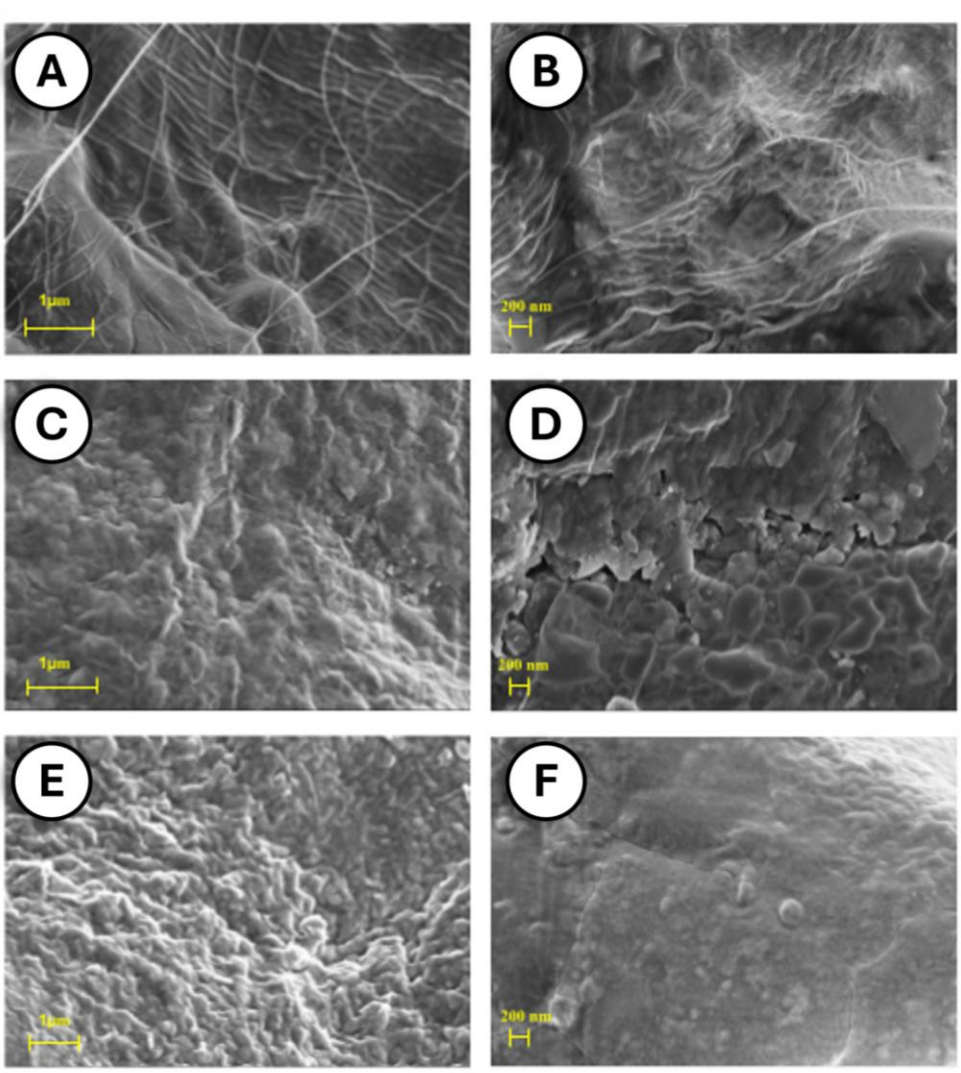

Figure 4. SEM microscopy with the magnification of 35,000 x (right column) and 50,000 x (left column) of the samples TPS (A-B), TPS/NC7% (C-D), and TPS/NC7%/NL0.3% (E-F), respectively.

The SEM micrographs obtained for the samples of TPS (Figures 4A-B), TPS/NC7% (Figures 4C-D), and TPS/NC7%/NL0.3% (Figures 4E-F) were presented at scales of 1 µm and 200 nm. In the micrographs, long filaments characteristic of TPS were identified, reflecting its intrinsic polymeric structure and tendency to form continuous chains [40]. However, with the addition of NC, these filaments were fragmented, resulting in a significantly rougher surface

and a more fragile structural matrix, as evidenced by the formation of tiny pores. This behavior suggests that NC acted as a disruptive agent, interfering with the continuity of the TPS matrix and contributing to a more heterogeneous texture.

The incorporation of NL further intensified the surface roughness of the composite while simultaneously reducing the observed porosity. This decrease in porosity may be attributed to the filling effect of NL, as reported in the literature [40], which possibly infiltrated the existing pores, promoting a compacting effect within the matrix. In the micrographs of the TPS/NC7%/NL0.3% composite (Figures 4E-F), individual components could not be visually distinguished, suggesting strong adhesion and interaction between TPS, NC, and NL. This result indicates an efficient integration of the materials, likely due to robust intermolecular interactions that enhanced the cohesion of the composite structure, corroborating the FTIR analyses.

3.3.1. Antimicrobial Activity

The impact of the soil conditioner on the bacterial growth of *S. aureus* and *E. coli* is illustrated in Figure S5. A more significant bacteriostatic effect was observed for *S. aureus*, with inhibition rates of 68.5% for TPS, 70.76% for TPS/NC7%, and 73.8% for TPS/NC7%/NL0.3%. In the case of *E. coli* (Figure S5), TPS inhibited growth by 38.25%, TPS/NC7% by 59.36%, and TPS/NC7%/NL0.3% by 70.15%. For *S. aureus*, the soil conditioners showed significant differences compared to the control, but there were no significant differences among the treatments themselves. For *E. coli*, significant differences were found between the control and the soil conditioners and between TPS and the other treatments. However, the difference between TPS/NC7% and TPS/NC7%/NL0.3% was insignificant.

The study by Levana *et al.* (2023)[34] with clay-based nanocomposites reported similar inhibition results. The bacteriostatic effect can be attributed to the composition of the soil conditioner. NC is known for its high antibacterial activit. Also, NL has been shown to cause greater inhibition against *S. aureus* than *E. coli*. [41] Overall, the results demonstrated that the soil conditioners have an inhibitory effect on the tested microorganisms.

3.3.2. Water retention in soil

In Figure S6, the control soil, without additives (Control), showed an initial water retention of around 160%, which was used as a reference. The addition of TPS to the soil increased this retention to approximately 180%, which was attributed to the hygroscopic nature

of TPS. The polar groups in TPS strongly interacted with water molecules, forming hydrogen bonds and enhancing water absorption [13]. When NC were added (TPS/NC7%), water retention slightly decreased, reaching around 170%. This suggested that the presence of NC influenced the composite structure, making it denser and reducing its ability to hold moisture, as it became less effective at retaining water.

When NL was added (TPS/NC7%/NL0.3%), water retention was further reduced, down to approximately 150%. This effect was explained by the hydrophobic properties of lignin, which hindered water absorption by the starch and nanoclay matrix [42]. NL acted as an additional barrier, reducing the water retention of the composite by decreasing its ability to absorb and retain moisture.

3.3.4. Leaching of NH_4^+, $H_2PO_4^-$, and K^+ ions

The ability to absorb essential macronutrients, such as N, P, and K, is a crucial parameter for evaluating the effectiveness of nanocomposites in agricultural and environmental applications [43]. Figure 5 presents the graphs of the concentrations of NH_4^+ (Figure 5A), $H_2PO_4^-$ (Figure 5B), and K^+ (Figure 5C) ions, leached weekly, obtained through UV-VIS analysis. This data provided valuable insights into the leaching dynamics of macronutrients and allowed for a critical assessment of the nanocomposite's performance in retaining and releasing these ions. A significant portion of the samples showed statistically similar results over the weeks, such as the control sample, and the graphs highlight the statistically distinct samples for each week among the different compositions.

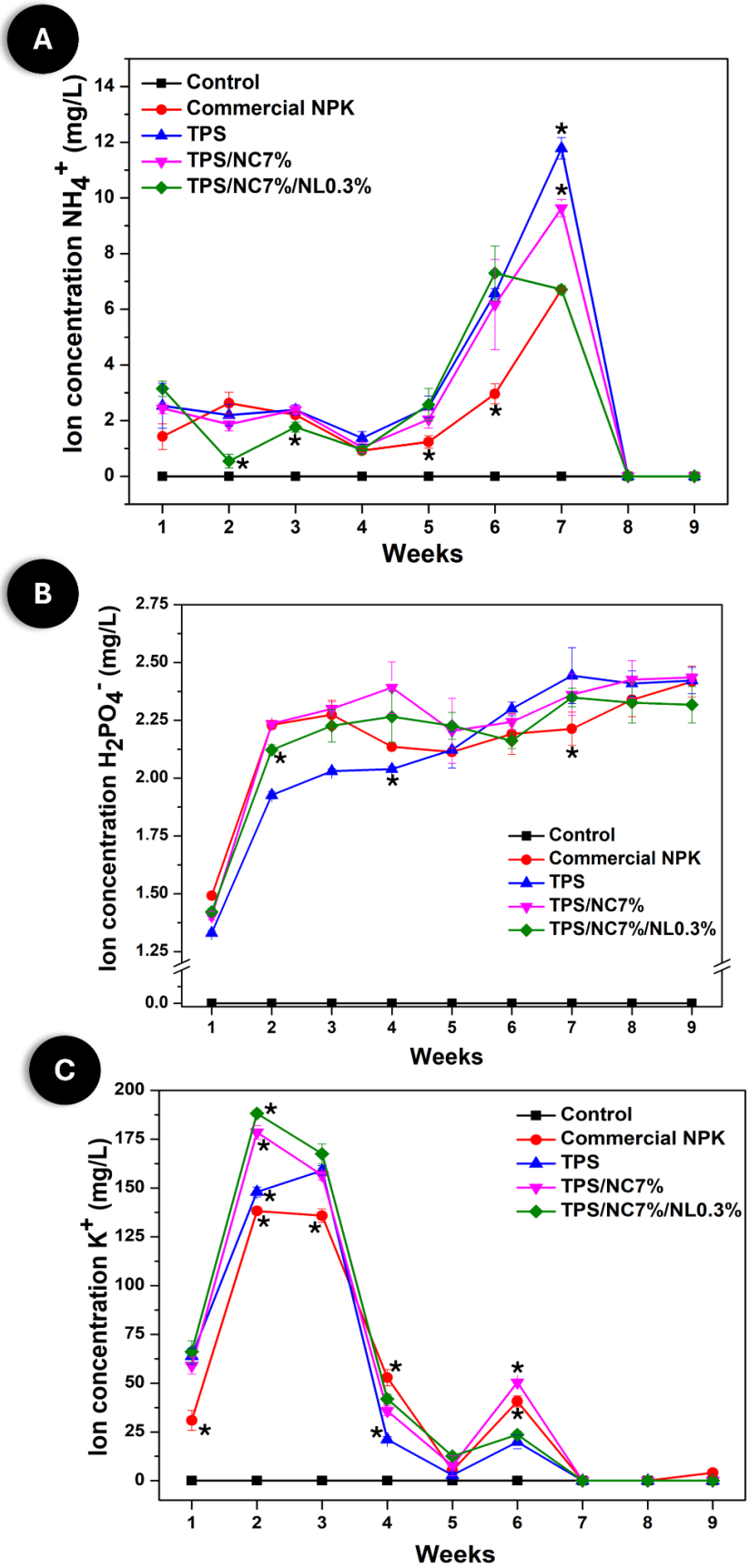

Figure 5. Concentration of NH_4^+ (A), $H_2PO_4^-$ (B), and K^+ (C) ions after leaching in soil. *Statistically distinct samples from the set of samples within the same week interval.

Figure 5A revealed that the leaching behavior of NH_4^+ ions was relatively linear until the fifth week. Overall, the behavior of the samples was quite similar, except for the control, as expected, with the TPS/NC7%/NL0.3% sample being the most statistically distinct, showing lower N leaching compared to the others. From this point, the concentration of ions increased significantly in the sixth week, with the behavior of the nanocomposites being statistically similar. Week 7 saw the maximum leaching, followed by a sharp decline to zero in week 8, which remained consistent throughout week 9. This increase in NH_4^+ leaching can be attributed to microbial activity releasing nitrogenous compounds into the soil [44,45]. The monitoring of leaching for K^+ ions is shown in Figure 5C, where the leached concentration increased significantly by the second week, with statistical differences among all samples. Between weeks 3 and 5, the leached amount drastically decreased, reaching values close to zero by the fifth week, followed by a slight increase in week 6, remaining statistically similar for the TPS and TPS/NC7%/NL0.3% samples. In the final weeks (7, 8, and 9), leaching was zeroed out, considering the measurement error. The behavior observed for K^+ leaching in week 6 may also be related to microbial activity influencing potassium release into the soil.

After the sixth week, only the TPS and TPS/NC7% samples showed an increase in nitrogen leaching, while the nanocomposite TPS/NC7%/NL0.3% exhibited a reduction. This difference can be explained by the fact that TPS served as a food source for microorganisms, whereas NL inhibited microbial activity with its bactericidal properties. This hypothesis was confirmed by the antimicrobial activity test results, which demonstrated a greater inhibitory capacity against bacteria for the TPS/NC7%/NL0.3% compared to the TPS and TPS/NC7% samples.

The $H_2PO_4^-$ ions showed an increase in leaching until week 4, followed by a stable plateau until week 9. This pattern can be explained by the unique chemical properties of P, which tends to form insoluble complexes with soil minerals, resulting in a more consistent release over time [46]. The interaction of P with the nanocomposite may not have been significantly influenced by the components, which have a more pronounced impact on the retention of soluble macronutrients like N and K. Thus, the initial availability and chemical dynamics of P in the soil may have contributed to a more stable leaching rate, as the fixation of phosphorus occurs differently compared to N and K. This is due to the transformation of phosphorus available to plants (labile) versus that which remains unavailable (non-labile), resulting from interactions with the soil structure and other ions present. This behavior contrasts with nitrogen and potassium, which were retained more efficiently and had greater availability through the nanocomposite [46].

Although the concentrations of leached NH_4^+, $H_2PO_4^-$, and K^+ ions were relatively close among the different materials, the TPS/NC7%/NL0.3% nanocomposite stood out for exhibiting lower concentrations of leached N and K throughout the experiment. The improved water absorption and retention of TPS/NC7%/NL0.3% may decrease the likelihood of N and K leaching with water, thereby increasing the efficiency of nutrient absorption and plant utilization efficiency, as Macedo *et al.* (2023)[46] observed. This behavior can be attributed to the specific composition of this nanocomposite. As an organic matrix, TPS provides a favorable environment for nutrient retention, while NC contributes a porous structure that can enhance ion absorption capacity [46]. With its bactericidal properties, NL may inhibit microbial activity that would typically release N and K into the soil, thus reducing the leaching of these macronutrients.

Furthermore, combining TPS with NC7% and NL0.3% may result in a more stable matrix that reduces solubilization and leaching of NH_4^+ and K^+ ions. The synergistic effect of these components contributes to more efficient retention of macronutrients, providing a longer-lasting source of N and K for plants. This superior performance in retaining N and K can be particularly beneficial for agricultural practices, as it improves the availability of these macronutrients to plants and reduces the need for frequent fertilization, contributing to sustainability and fertilizer use efficiency.

3.3.4. Biodegradation in soil

The materials TPS, TPS/NC7%, and TPS/NC7%/NL0.3% were evaluated for their biodegradability alongside a control sample of pure soil. Figure 6 presents the biodegradation profile of the samples monitored over 50 days, based on the cumulative release of CO_2 (Figure 6A) and the daily release of CO_2 (Figure 6B).

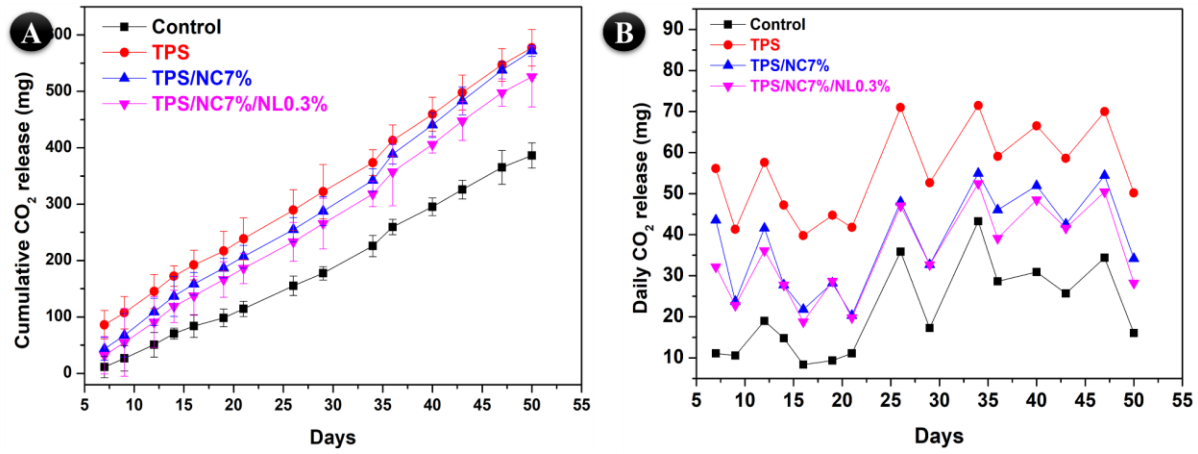

Figure 6. Biodegradation performance in soil of the samples TPS, TPS/NC7%, and TPS/NC7%/NL0.3%, (A) cumulative CO_2 release and (B) daily CO_2 release.

The cumulative CO_2 release results analysis showed a generally similar behavior among the samples regarding production. However, it is noteworthy that the TPS sample maintains the highest CO_2 release rate, followed by the TPS/NC7% and TPS/NC7%/NL0.3% samples. Nonetheless, the release rates are statistically similar among the samples at most measured points. However, a significant difference in CO_2 emissions can be observed when the sample set is compared to the control.

Thus, the TPS sample exhibits the highest CO_2 release, indicating greater biodegradability than the NC-containing samples, which show reduced capacity. This behavior has been observed in other literature. Angelo *et al.*(2021)[47] studied the biological degradation of chitosan and montmorillonite clay samples and found that the clay hinders the degradation of the polymeric matrix. They attributed this to the restriction of segmental movement at the interface, which decreases microorganism access to attack the polymer. This reduction is also correlated in other studies with the limited growth of microorganisms on clay particles, diminishing their functionality [48].

When analyzing the daily release profile, despite the oscillations in the quantities eliminated, as previously observed in the literature [47], it was possible to conclude that the TPS sample exhibited the highest CO_2 release. The samples containing NC (TPS/NC7% and TPS/NC7%/NL0.3%) showed lower biodegradability compared to TPS but higher than the control. Four distinct general behaviors could be identified over the evaluated time intervals by analyzing the curves. Between the 1^{st} and 2^{nd} days, the control sample showed a maximum CO_2 release of 19 mg, but most daily releases were close to 10 mg. The TPS sample showed a maximum release of 57 mg, while the NC-containing samples released approximately 40 mg. On the 25^{th} day, all samples experienced a significant but proportional increase in CO_2 elimination. Between the 35^{th} and 47^{th} days, there was a stabilization in CO_2 release, followed by a sharp decline on the 50^{th} day, marking the end of the analysis.

These behavioral phases can be attributed to the diffusion of NPK through the polymer matrix, as the nutrient is released from the material's structure, primarily from the TPS network. This also explains its higher biodegradation rate, as water molecules and microorganisms have more sites to interact with the polymer matrix [47]. It was observed that between the 14^{th} and 21^{st} days, this coincides with the highest release of $H_2PO_4^-$ ions (Figure 5A), and K^+ ions (Figure 5B), which remained elevated until the 25^{th} day, a high CO_2 release. The sustained high elimination after this period aligns with the phase of increased NH_4^+ release (Figure 5C), as

microorganisms benefit from the nitrogen, promoting their growth. This suggests that the availability of NPK significantly impacts the biodegradation process, as seen by the corresponding peaks in CO_2 release, driven by microbial activity feeding off the nitrogen and other nutrients during the experiment.

3.4 Soil Conditioner Effectiveness in Red Cherry Tomato Cultivation

The effectiveness of the soil conditioners prepared in this study was tested through a field study with the cultivation of red cherry tomatoes. Seedling development was monitored weekly over 9 weeks (2 months), recording the number of leaf stems and measuring seedling height from seed planting. Figure 7A shows the results for stem counts, where it was observed that the first seedlings to emerge as early as the first week of monitoring were from the control group, with no treatment applied to the soil before planting. In the following week, the TPS/NC7%/NL0.3% treated seedlings began to sprout, followed by the TPS and TPS/NC7% treatments, which developed in the third week. The seedlings in the soil fertilized with commercial NPK, without the soil conditioners, were the last to emerge, only sprouting after 4 weeks. The delay of the other treatments compared to the control can be attributed to the dormancy effect caused by the NPK fertilizer. In this complex biomolecular phenomenon, seeds delay germination until the environment reaches optimal conditions. This result aligns with the fact that the NPK sample was the last to emerge overall, as it released the fertilizer more uncontrolled and directly into the soil.

This effect was also reduced over time in the other samples, especially in TPS/NC7%/NL0.3%, which emerged in half the time of NPK, indicating that this composite established a suitable medium more quickly. Over the weeks, the number of stems per sample showed overall stability, increasing between weeks 6 and 7, likely due to the ion leaching peak observed in Figure 5. The NPK and TPS treatments exhibited similar stem counts, while the control aligned with TPS/NC7% during the last three weeks. TPS/NC7%/NL0.3% showed the highest overall stem count.

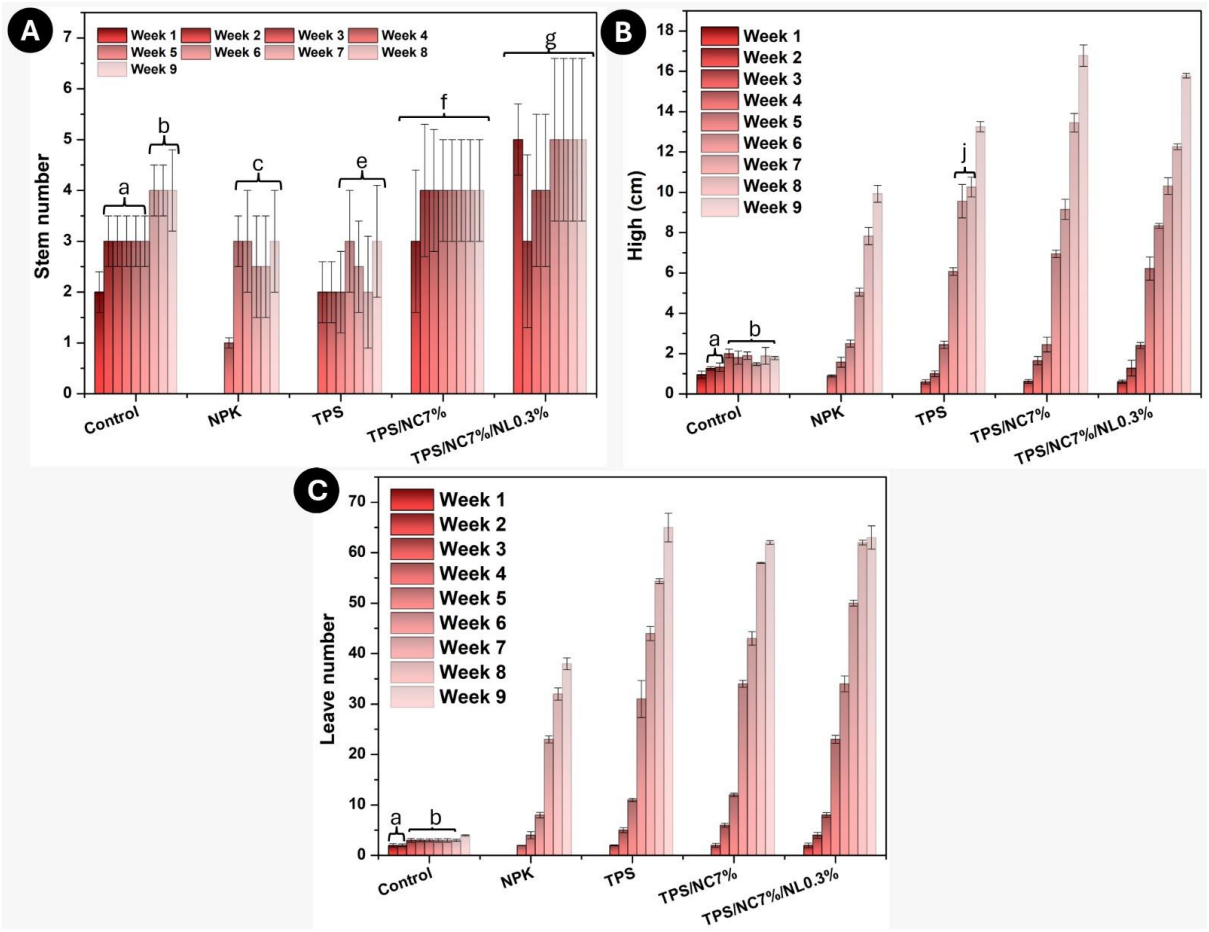

693

694 **Figure 7.** Weekly monitoring of red cherry tomato seedling development over 9 weeks. (A)
695 stem number, (B) seedling high, and (C) leaf number. Statistically similar samples (a-g) of the
696 same sample, analyzed over different weeks.
697

698 Height and leaf count (Figures 7B and 7C) showed similar behavior across the samples.
699 The control remained without significant increases in these parameters. At the same time, NPK,
700 TPS, TPS/NC7%, and TPS/NC7%/NL0.3% followed a similar exponential pattern, with
701 TPS/NC7% showing the most significant average height and TPS the highest average leaf
702 count. Despite being the first to germinate, the control sample was quickly surpassed by the
703 other samples, even under identical growth conditions. However, as observed in Figure 7B, its
704 growth was significantly lower than that of the different samples, and its leaves showed a
705 slightly yellowish hue (Figure 8), suggesting that a lack of water may have been a critical factor
706 in its stagnation [49].

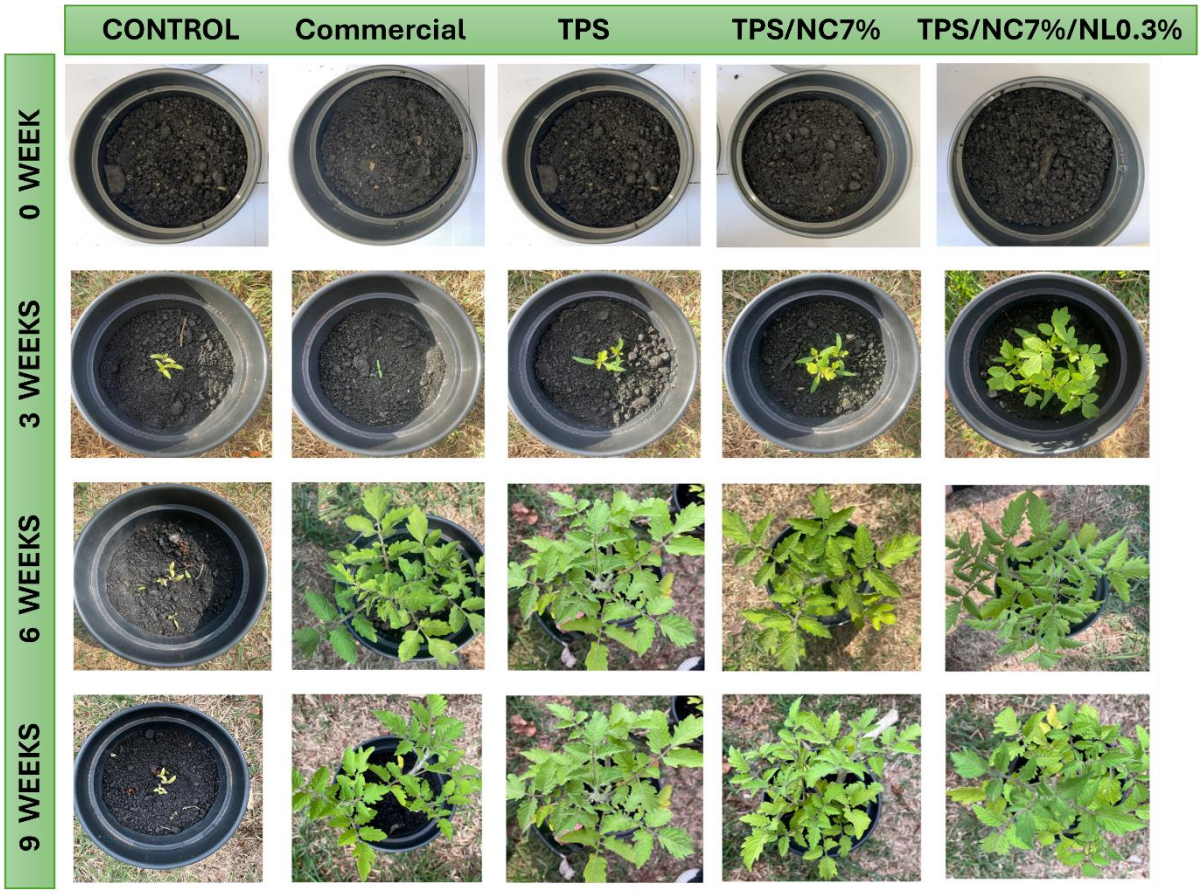

Figure 8. Photographic records showing the visual monitoring of red cherry tomato seedling development, taken weekly over a 9-week period. Weeks (vertical) and control, commercial, TPS, TPS/NC7%, and TPS/NC7%/NL0.03% (horizontal), respectively.

All samples were watered daily with 100 mL of water, but this stagnation, combined with leaf yellowing, may be attributed to the nanocomposites acting as a hydrogel. As liquid NPK was released into the soil, the polymeric network swelled with water, which was then gradually released into the soil. The occurrence of this phenomenon in week 8 indicates a possible correlation with the leaching behavior of the composites in Figure 5, where, after the peak of fertilizer release, the composites disintegrated, making it challenging to meet the water demands of the tomato seedlings. In the case of the NPK sample, leaf yellowing was not observed as early as week 8, likely because it was the last to germinate, resulting in a lower water demand than the others.

Thus, overall, the TPS/NC7%/NL0.3% sample showed the best results, with the highest number of stems. Although it had a slightly lower height compared to TPS/NC7% and slightly fewer leaves than TPS, the lignin-containing nanocomposite stands out overall, as the presence of more stems increases its surface area for photosynthesis, potentially boosting the plant's energy production and, consequently, the production of flowers and fruits [50]. Additionally,

due to the earlier breaking of seed dormancy, it can produce these resources more quickly than the other composites, making TPS/NC7%/NL0.3% the standout in the cultivation test. Nonetheless, all the composites produced showed superior results compared to the control and the commercial fertilizer.

4. Conclusion

In conclusion, this study demonstrated that combining NL, NC, and TPS as soil conditioners offers a promising approach to improving soil properties and enhancing agricultural sustainability. The analysis of the nanocomposites revealed that including 7% NC and 0.3% NL significantly enhanced the cation exchange capacity, water retention, and UV-C degradation resistance of TPS while promoting efficient nutrient absorption and reducing NPK ion leaching. Tests conducted on cherry tomatoes confirmed the practical effectiveness of these nanocomposites, demonstrating their ability to improve plant growth and soil health under real cultivation conditions. The synergy between NL and NC represents a significant advancement in soil conditioner formulation, optimizing their physicochemical properties and amplifying direct benefits for sustainable agriculture. This study fills a gap in existing literature and opens new perspectives for applying nanocomposites in innovative and efficient agricultural practices.

Acknowledgments

This research was partially funded by the São Paulo State Research Foundation (FAPESP - #2023/06505-9 (M.F.), #2024/01872-6 (L.F.), #2024/14149-0 (A.F), #2023/00335-4 (J.R), #2017/21004-5 (L.F.), CEPID CBioClima #2021/10639-5). Also, to Project 14805 – FINEP 01.22.0179.00 (MARTMA), as well as by the National Council for Scientific and Technological Development (CNPq) through grant #153850/2024-8 and the National Institute of Science and Technology in Nanotechnology for Sustainable Agriculture (MCTI-CNPq - INCTNanoAgro #405924/2022-4 and CAPES-MEC #88887.953443/2024-00) and the National Institute of Science and Technology in Organic Electronics (INEO #2014/50869-6)).

References

[1] S.H. Muhie, Novel approaches and practices to sustainable agriculture, J. Agric. Food Res. 10 (2022) 100446.

[2] S. Sabzevari, J. Hofman, A worldwide review of currently used pesticides' monitoring in agricultural soils, Sci. Total Environ. 812 (2022) 152344. https://doi.org/10.1016/j.scitotenv.2021.152344.

[3] M. Babla, U. Katwal, M.T. Yong, S. Jahandari, M. Rahme, Z.H. Chen, Z. Tao, Value-added products as soil conditioners for sustainable agriculture, Resour. Conserv. Recycl. 178 (2022) 106079. https://doi.org/10.1016/j.resconrec.2021.106079.

[4] J. Zhang, S. Wang, X. Wang, W. Jiao, M. Zhang, F. Ma, A review of functions and mechanisms of clay soil conditioners and catalysts in thermal remediation compared to emerging photo-thermal catalysis, J. Environ. Sci. (China). 147 (2025) 22–35. https://doi.org/10.1016/j.jes.2023.11.006.

[5] A. Aynehband, A. Gorooei, A.A. Moezzi, Vermicompost: An Eco-Friendly Technology for Crop Residue Management in Organic Agriculture, Energy Procedia. 141 (2017) 667–671. https://doi.org/10.1016/j.egypro.2017.11.090.

[6] Melanie Kah, C. Sabliov, Y. Wang, J. White, Nanotechnology as a foundational tool to combat global food insecurity, One Earth. 6 (2023) 772–775. https://doi.org/https://doi.org/10.1016/j.oneear.2023.06.011.

[7] D.K. Rajak, D.D. Pagar, R. Kumar, C.I. Pruncu, Recent progress of reinforcement materials: A comprehensive overview of composite materials, J. Mater. Res. Technol. 8 (2019) 6354–6374. https://doi.org/10.1016/j.jmrt.2019.09.068.

[8] A. de S.M.A.P.B. da S.L.S.M.I.A.N.N.K.C.V.S. de F.N.B. dos S.A.P.L. Freitas, Thermoplastic starch nanocomposites_ sources, production and applications – a review, (2022) 46. https://doi.org/https://doi.org/10.1080/09205063.2021.2021351.

[9] J.S. Rodrigues, A. de S.M. de Freitas, H.S.M. Lopes, A.A.F. Pires, A.P. Lemes, M. Ferreira, V.R. Botaro, Improvement of UV stability of thermoplastic starch matrix by addition of selected lignin fraction - Photooxidative degradation, Int. J. Biol. Macromol.

785 230 (2023) 1–12. https://doi.org/10.1016/j.ijbiomac.2023.123142.

786 [10] T.A. Lerma, M. Palencia, E.M. Combatt, Soil polymer conditioner based on
787 montmorillonite-poly(acrylic acid) composites, J. Appl. Polym. Sci. 135 (2018) 1–8.
788 https://doi.org/10.1002/app.46211.

789 [11] L.D. da Silva Neto, A. Maged, R. Gabriel, P.V.S. Lins, N.H. Haneklaus, M.W.
790 Hlawitschka, L. Meili, Nanoclays in water treatment: Core concepts, modifications, and
791 application insights, J. Water Process Eng. 67 (2024).
792 https://doi.org/10.1016/j.jwpe.2024.106180.

793 [12] P. G, S. AS, J.S. Jayan, A. Raman, A. Saritha, Lignin based nano-composites: Synthesis
794 and applications, Process Saf. Environ. Prot. 145 (2021) 395–410.
795 https://doi.org/10.1016/j.psep.2020.11.017.

796 [13] A. de S. M. de Freitas, J.S. Rodrigues, C.C. Maciel, A.A.F. Pires, A.P. Lemes, M.
797 Ferreira, V.R. Botaro, Improvements in thermal and mechanical properties of
798 composites based on thermoplastic starch and Kraft Lignin, Int. J. Biol. Macromol. 184
799 (2021) 863–873. https://doi.org/10.1016/j.ijbiomac.2021.06.153.

800 [14] H. Sadeghifar, A. Ragauskas, Lignin as a UV Light blocker-a review, Polymers (Basel).
801 12 (2020) 1134. https://doi.org/10.3390/POLYM12051134.

802 [15] M.M. Delavari, I. Stiharu, Preparing and Characterizing Novel Biodegradable
803 Starch/PVA-Based Films with Nano-Sized Zinc-Oxide Particles for Wound-Dressing
804 Applications, Appl. Sci. 12 (2022). https://doi.org/10.3390/app12084001.

805 [16] L.P. Canellas, F.L. Olivares, Physiological responses to humic substances as plant
806 growth promoter, Chem. Biol. Technol. Agric. 1 (2014) 1–11.
807 https://doi.org/10.1186/2196-5641-1-3.

808 [17] M. Parit, P. Saha, V.A. Davis, Z. Jiang, Transparent and Homogenous Cellulose
809 Nanocrystal/Lignin UV-Protection Films, ACS Omega. 3 (2018) 10679–10691.
810 https://doi.org/10.1021/acsomega.8b01345.

811 [18] R.W. Behle, D.L. Campton, J.A. Kenar, D.I. Shapiro-Ilan, Improving Formulations for
812 Biopesticides: Enhanced UV protection for beneficial Microbes, J. ASTM Int. 8 (2011)
813 10382.

[19] S.R. Yearla, K. Padmasree, Exploitation of subabul stem lignin as a matrix in controlled release agrochemical nanoformulations: a case study with herbicide diuron, Environ. Sci. Pollut. Res. 23 (2016) 18085–18098. https://doi.org/10.1007/s11356-016-6983-8.

[20] A. do E.S. Pereira, J. Luiz de Oliveira, S. Maira Savassa, C. Barbara Rogério, G. Araujo de Medeiros, L.F. Fraceto, Lignin nanoparticles: New insights for a sustainable agriculture, J. Clean. Prod. 345 (2022). https://doi.org/10.1016/j.jclepro.2022.131145.

[21] M.H. Hussin, J.N. Appaturi, N.E. Poh, N.H.A. Latif, N. Brosse, I. Ziegler-Devin, H. Vahabi, F.A. Syamani, W. Fatriasari, N.N. Solihat, A. Karimah, A.H. Iswanto, S.H. Sekeri, M.N.M. Ibrahim, A recent advancement on preparation, characterization and application of nanolignin, Int. J. Biol. Macromol. 200 (2022) 303–326. https://doi.org/10.1016/j.ijbiomac.2022.01.007.

[22] B. Abraham, V.L. Syamnath, K.B. Arun, P.M. Fathima Zahra, P. Anjusha, A. Kothakotta, Y.H. Chen, V.K. Ponnusamy, P. Nisha, Lignin-based nanomaterials for food and pharmaceutical applications: Recent trends and future outlook, Sci. Total Environ. 881 (2023) 163316. https://doi.org/10.1016/j.scitotenv.2023.163316.

[23] M. Parit, Z. Jiang, Towards lignin derived thermoplastic polymers, Int. J. Biol. Macromol. 165 (2020) 3180–3197. https://doi.org/10.1016/j.ijbiomac.2020.09.173.

[24] S.I. Hong, L.F. Wang, J.W. Rhim, Preparation and characterization of nanoclays-incorporated polyethylene/thermoplastic starch composite films with antimicrobial activity, Food Packag. Shelf Life. 31 (2022) 100784. https://doi.org/10.1016/j.fpsl.2021.100784.

[25] K.M. Dang, R. Yoksan, E. Pollet, L. Avérous, Morphology and properties of thermoplastic starch blended with biodegradable polyester and filled with halloysite nanoclay, Carbohydr. Polym. 242 (2020) 116392. https://doi.org/10.1016/j.carbpol.2020.116392.

[26] M. Morsali, A. Moreno, A. Loukovitou, I. Pylypchuk, M.H. Sipponen, Stabilized Lignin Nanoparticles for Versatile Hybrid and Functional Nanomaterials, Biomacromolecules. (2022). https://doi.org/10.1021/acs.biomac.2c00840.

[27] K. Pal, S. Pal, Development of porous hydroxyapatite scaffolds, Mater. Manuf. Process. 21 (2006) 325–328. https://doi.org/10.1080/10426910500464826.

[28] N. GONTARD, S. GUILBERT, J. -L CUQ, Edible Wheat Gluten Films: Influence of the Main Process Variables on Film Properties using Response Surface Methodology, J. Food Sci. 57 (1992) 190–195. https://doi.org/10.1111/j.1365-2621.1992.tb05453.x.

[29] B. van Raij, A. Küpper, Capacidade de troca de catíons em solos: estudo comparativo de alguns métodos, Bragantia. 25 (1966) 327–336. https://doi.org/10.1590/s0006-87051966000200005.

[30] N.I.F. Himmah, G. Djajakirana, D. Darmawan, Nutrient Release Performance of Starch Coated NPK Fertilizers and Their Effects on Corn Growth, SAINS TANAH - J. Soil Sci. Agroclimatol. 15 (2018) 104. https://doi.org/10.15608/stjssa.v15i2.19694.

[31] ABNT, ABNT NBR 14283-Resíduos em solos - Determinação da biodegradação pelo método respirométrico, Assoc. Bras. Normas Técnidas - NBR. (1999) 1–8.

[32] S.P. Bangar, W.S. Whiteside, A.O. Ashogbon, M. Kumar, Recent advances in thermoplastic starches for food packaging: A review, Food Packag. Shelf Life. 30 (2021) 100743. https://doi.org/10.1016/j.fpsl.2021.100743.

[33] A. Zare Shahrabadi, A. Kargari, A. Tayebi, Evaluation of the effectiveness of poly (phenyl sulfone) / nanoclay mixed matrix membranes for carbon dioxide/methane separation, Int. J. Greenh. Gas Control. 121 (2022) 103792. https://doi.org/10.1016/j.ijggc.2022.103792.

[34] O. Levana, J. Hoon Jeong, S. Sik Hur, W. Seo, M. Lee, K. Mu Noh, S. Hong, J. Hong Park, J. Hun Lee, C. Choi, Y. Hwang, Development of nanoclay-based nanocomposite surfaces with antibacterial properties for potential biomedical applications, J. Ind. Eng. Chem. 120 (2023) 448–459. https://doi.org/10.1016/j.jiec.2022.12.052.

[35] O.V. Kharissova, L.M. Torres-Martnez, B.I. Kharisov, Nanomaterials and Nanocomposites for Energy and Environmental Applications, 2021. https://doi.org/10.1007/978-3-030-36268-3.

[36] M. El Moustaqim, A. El Kaihal, M. El Marouani, S. Men-la-yakhaf, Thermal and thermomechanical analyses of lignin, Sustain. Chem. Pharm. 9 (2018) 63–68. https://doi.org/10.1016/j.scp.2018.06.002.

[37] H. Yang, R. Yan, H. Chen, D.H. Lee, C. Zheng, Characteristics of hemicellulose,

cellulose and lignin pyrolysis, Fuel. 86 (2007) 1781–1788. https://doi.org/10.1016/j.fuel.2006.12.013.

[38] D. Muscat, M.J. Tobin, Q. Guo, B. Adhikari, Understanding the distribution of natural wax in starch-wax films using synchrotron-based FTIR (S-FTIR), Carbohydr. Polym. 102 (2014) 125–135. https://doi.org/10.1016/j.carbpol.2013.11.004.

[39] A.C. Bertolini, C. Mestres, J. Raffi, A. Buléon, D. Lerner, P. Colonna, Photodegradation of cassava and corn starches, J. Agric. Food Chem. 49 (2001) 675–682. https://doi.org/10.1021/jf0010174.

[40] M. Kanidi, N. Loura, A. Frengkou, T.K. Milickovic, A.F. Trompeta, C. Charitidis, Inductive Thermal Effect on Thermoplastic Nanocomposites with Magnetic Nanoparticles for Induced-Healing, Bonding and Debonding On-Demand Applications, J. Compos. Sci. 7 (2023). https://doi.org/10.3390/jcs7020074.

[41] A.G. Morena, T. Tzanov, Antibacterial lignin-based nanoparticles and their use in composite materials, Nanoscale Adv. 4 (2022) 4447–4469. https://doi.org/10.1039/d2na00423b.

[42] Q. Zheng, P.O. Osei, S. Shi, S. Yang, X. Wu, Green fabrication of nanocomposite films using lignin nanoparticles and PVA: Characterization and application, Food Biosci. 59 (2024) 104022. https://doi.org/10.1016/j.fbio.2024.104022.

[43] A.C. Albuquerque, J.S. Rodrigues, A.S.M. De Freitas, G.T. Machado, V.R. Botaro, Renewable Source Hydrogel as a Substrate of Controlled Release of NPK Fertilizers for Sustainable Management of Eucalyptus urograndis: Field Study, ACS Agric. Sci. Technol. 2 (2022) 1251–1260. https://doi.org/10.1021/acsagscitech.2c00215.

[44] H. Liu, R. Wang, X.T. Lü, J. Cai, X. Feng, G. Yang, H. Li, Y. Zhang, X. Han, Y. Jiang, Effects of nitrogen addition on plant-soil micronutrients vary with nitrogen form and mowing management in a meadow steppe, Environ. Pollut. 289 (2021) 117969. https://doi.org/10.1016/j.envpol.2021.117969.

[45] A.M. Carswell, P.W. Hill, D.L. Jones, M.S.A. Blackwell, P.J. Johnes, E.R. Dixon, D.R. Chadwick, Impact of microbial activity on the leaching of soluble N forms in soil, Biol. Fertil. Soils. 54 (2018) 21–25. https://doi.org/10.1007/s00374-017-1250-9.

[46] J.R. Macedo, S.G. Moreira, F.A. de Moraes, D. de S.R. Junior, D.S. Peixoto, B.M. Silva, J.C.R. Silva, The management of phosphate fertilization affects soil phosphorus and yield of autumn/winter crops, Acta Sci. - Agron. 45 (2023). https://doi.org/10.4025/actasciagron.v45i1.57336.

[47] L.M. Angelo, D. França, R. Faez, Biodegradation and viability of chitosan-based microencapsulated fertilizers, Carbohydr. Polym. 257 (2021) 1–9. https://doi.org/10.1016/j.carbpol.2021.117635.

[48] G.F. Perotti, T. Kijchavengkul, R.A. Auras, V.R.L. Constantino, Nanocomposites based on cassava starch and chitosan-modified clay: Physico mechanical properties and biodegradability in simulated compost soil, J. Braz. Chem. Soc. 28 (2017) 649–658. https://doi.org/10.21577/0103-5053.20160213.

[49] S. Fahad, A.A. Bajwa, U. Nazir, S.A. Anjum, A. Farooq, A. Zohaib, S. Sadia, W. Nasim, S. Adkins, S. Saud, M.Z. Ihsan, H. Alharby, C. Wu, D. Wang, J. Huang, Crop production under drought and heat stress: Plant responses and management options, Front. Plant Sci. 8 (2017) 1–16. https://doi.org/10.3389/fpls.2017.01147.

[50] P.A. Magallanes-Cruz, P.C. Flores-Silva, L.A. Bello-Perez, Starch Structure Influences Its Digestibility: A Review, J. Food Sci. 82 (2017) 2016–2023. https://doi.org/10.1111/1750-3841.13809.

Sorocaba, SP, Brazil, January 03, 2025

Dr. Mario M Martinez

Editor

International Journal of Biological Macromolecules

Ref: Revised version – IJBIOMAC-D-24-29188

The authors thank the Reviewers for their valuable comments and remarks regarding this manuscript. We have addressed all comments and suggestions adequately. The requested alterations/corrections have been inserted directly into the manuscript (significant changes are highlighted in blue) and are described below.

Yours sincerely,

Dr. Marystela Ferreira,
Corresponding author

Designing Sustainable Soil Conditioners: Nanocomposite-Based Thermoplastic Starch for Enhanced Soil Health and Crop Performance

Jéssica S. Rodrigues[a1], Amanda S. M de Freitas[a,b1], Henrique O. S. Vieira[b], Lívia S. Emidio[b], Stefanny F. Amaro[b], Mariana A. Azevedo[b], Iolanda C. S. Duarte[b], Vagner R. Botaro[b], Leonardo F. Fraceto[a], Marystela Ferreira[b]

[a]Institute of Science and Technology of Sorocaba, São Paulo State University (UNESP), Av.Três de Março 511, 18087-180, Sorocaba, SP, Brazil.

[b] Science and Technology Center for Sustainability (CCTS), Federal University of São Carlos (UFSCar), João Leme dos Santos, km 110, 18052-780, Sorocaba, SP, Brazil.

[1] These authors contributed equally to the manuscript

Corresponding author: marystela@ufscar.br

Response Letter

Reviewer #1:

1. Abstract should be more exact concerning the statements, such as "enhanced swelling properties" (line27), where it is not clear whether it should be higher or lower

Answer: The sentence was modified: “Results indicated that incorporating 7% NC (TPS/NC7%) significantly improved the CEC and the swelling properties of TPS.”

2. The abbreviation NPK is not explained.

Answer: The acronym NPK was explained as “…nitrogen, phosphorus and potassium (NPK) fertilizer.”

3. In keywords "biodegradability" is mentioned, however, this is in contradiction with some standards, requiring maximum amount of nonbiodegradable components being 5 wt %, while in all samples the montmorillojnite content is 7 wt %.

Answer: We appreciate the observation regarding the standards that limit the content of non-biodegradable components to 5% by weight. Although the 7% content exceeds the mentioned limit, the material maintains predominant biodegradability characteristics due to the biodegradable polymer matrix. However, to avoid conceptual errors, this keyword has been removed.

4. L. 52 - what is polystyreneplored?

Answer: This word doesn't make sense in the sentence; it must have been a typo. The sentence has been corrected: “Materials such as starch, lignin, and clay are now recognized as innovative and accessible solutions to enhance agricultural productivity.”

5. L. 63 - what means one-dimensional particles?

Answer: Thank you for your question about "one-dimensional particles." In this context, "one-dimensional particles" refer to materials that exhibit nanoscale dimensions in one direction while having much larger dimensions in the other two. Specifically, these particles are typically characterized by their high aspect ratio, meaning their length and width are significantly greater than their thickness.

Clay nanoparticles, such as montmorillonite, are considered one-dimensional because they exist as platelets or sheets with nanometer-scale thickness (typically 1-2 nm) but lateral dimensions in the range of several micrometers. This unique geometry allows them to interact effectively with organic monomers and polymers, creating clay-polymer nanocomposites with enhanced properties.

The term highlights their structural uniqueness, crucial for the improvements observed in modulus, mechanical strength, flame resistance, heat resistance, and barrier properties when these nanoparticles are incorporated into a polymer matrix.

6. L. 76 what is the reason for plant ability to enhanced water and nutrients abruption?

Answer: Thank you for your question about the mechanism behind the plant's increased ability to absorb water and nutrients when lignin is applied. We have inserted a paragraph to enrich this discussion due to its relevance to the manuscript. “This improvement can be attributed to several factors. Lignin acts as a biostimulant, promoting root growth and increasing root surface area, which improves soil exploration and nutrient uptake [15]. Additionally, lignin derivatives can enhance soil structure, improve water retention, and facilitate root nutrient access. Its bioactive compounds, such as phenolics, stimulate enzymatic and metabolic activities in plants, optimizing absorption processes [16].”

7. Ls 89-90, mentioning the increased reactivity is vague, in my view the reactivity is the same just the surface increase leads to an increase of reactive sites.

Answer: In fact, the term "increased reactivity" may seem vague in this context, so the text was more precisely formulated. "This enhanced availability of reactive sites makes processes more efficient, enabling the use of smaller quantities of material and reducing costs."

8. L. 123, mentioning Morsali (2022) seems as a quotation, it should be properluy numbers and inserted among the literature. I remember there was also another similar item somewhere.

Answer: All text has been reviewed and corrected in 3 different places. Thank you for noticing.

Morsali et al. (2022)[26], Kharissova *et al.* (2021)[33], Levana *et al.* (2023)[32], Macedo *et al.* (2023)[44]

9. L. 132, PD preparation, usually a kind of sheasr is applied to get thermoplastic starch.

Answer: In our study, thermoplastic starch was obtained using only heat, degreasing, and the combination of the plasticizing agent's glycerol and water. The material obtained presented the plating characteristics.

10. L. 161 Thermal events are mentioned to take as the second scan. The used sentence means that this was done also for TGA, that would be really strange to discuss TGA second run.

Answer: The sentence was modified to highlight that the second heating was used only for DSC analysis. "Thermal events were identified and quantified during the second heating scan for DSC analyses, supported by TRIOS® software."

11. L. 167 - 168, for 30 and 60 minutes until a constant mass was reached - TOTALLY UNCLEAR. Pls be more exact whemn describing the procedure.

Answer: The sentence was modified: "Approximately 0.1 g of the nanocomposite was added to 10 mL beakers containing 5 mL of phosphate buffer solution (pH 5, 7, and 9) for 30 min."

12. Solubility - total mess. First in Hnadbooks solubility of various materials is listed, in

that case usually the content of the material forming saturated solution is published, it is needed to give temperature and pressure. I guess you are determining the soluble or extractable portion, not solubility

Answer: Thank you for your observation. You are correct that our methodology evaluates the soluble or extractable fraction of the material, not the solubility in the classical sense (e.g., the concentration of the material in a saturated solution at a specific temperature and pressure). We have revised the text accordingly to clarify this distinction and avoid any potential misinterpretation. The revised term "soluble fraction determination" better describes the method and results.

Soluble Fraction Determination: The determination of the soluble fraction of the samples in phosphate buffer solutions (pH 5.0, 7.0, and 9.0) was performed following the method of Gontard, Guilbert, and Cuq (1992)[28], with some adaptations. Initially, the dry matter percentage of the samples was determined by weighing them after drying in an oven at 70°C for 2 h. The samples were then immersed in 20 mL of phosphate buffer solution (pH 5.0, 7.0, and 9.0) and maintained under slow agitation at 38°C for 24 h. After this period, each solution was filtered, and the retained material was dried in an oven at 70°C for 24 h until a constant mass was achieved. The amount of non-soluble dry matter was determined using Equation 2

$$Soluble\ Fraction\ (\%) = \frac{Wi - Wf}{Wf}\ x\ 100 \qquad \text{(Equation 2)}$$

Where: Wi = initial mass of dry material and Wf = final mass of non-solubilized dry material.

13. The data in the Table 1 seem to show interestin and perhaps important results. However, the Table is almost useless for most readers since it does not explain the individual columns, such as TR, R600, etc. In fact for all Fugures and Tables the description should enable to understand the information without necessity to read the text of the publication.

Answer: A caption has been added to the table to explain the columns and facilitate understanding of the data: "[a]Initial degradation temperature of 5%; [b]Temperature of the maximum degradation rate; [c]Mass loss rate up to Tmax; [d]Final degradation temperature; [e] Temperature difference associated with thermal transition; [f]The coal amount at the end of degradation process in 600°C."

14. In fact, insufficient explanation is given for changes of data in Table 1 with changing the concentrations. In some case it is logical, in others it is random, no trend, or even opposite regarding the expectation, e.g. for T5%.

Answer: Thank you for your observation. We have revised and expanded the section to explain better the variations in the thermal parameters presented in Table 1. The lack of a clear trend in some samples can be attributed to factors such as:

- Heterogeneity in the dispersion of the nanocomposites: The interaction between the components can vary due to differences in the compatibility and distribution of lignin (NL) in the polymer matrix.
- Trade-offs between thermal stabilization and degradation of additives: The initial increase in T5% (as observed at 0.3% NL) can be due to the formation of strong interactions between the NC, NL, and the matrix. However, higher concentrations (0.7% NL) can lead to saturation or agglomeration, impairing homogeneous heat transfer.

In the text, we have explained how intermolecular interactions and NL dispersion impact the observed thermal parameters.

"The variability observed in the $T_{5\%}$ values, as shown in Table 1, is attributed to the complexity of the thermal decomposition process in these composite systems. The interaction between TPS, NC, and NL introduces multiple decomposition mechanisms influenced by the proportion of each component. While the sample with 0.3% NL displayed the highest $T_{5\%}$ (190°C), indicating improved initial thermal resistance, the samples with 0.5% and 0.7% NL exhibited lower values (165°C and 98°C, respectively). This lack of a consistent trend can be explained by potential phase segregation or non-uniform dispersion of the nanoaditives in the matrix, which could reduce the effectiveness of thermal stabilization in some cases. This is consistent with findings in similar systems, where optimal properties are often achieved at specific additive concentrations due to balanced interactions within the composite matrix [36].

T_{max} also varied among the samples, reflecting thermal resistance during decomposition. The TPS/NC7% sample showed a Tmax of 350°C, while the NL-added samples exhibited values of 362°C (TPS/NC7%/NL0.3%), 390°C (TPS/NC7%/NL0.5%), and 364°C (TPS/NC7%/NL0.7%). The highest T_{max} was

observed in TPS/NC7%/NL0.5%, indicating superior thermal resistance, possibly due to greater interaction between the polymer matrix and the nanoadditives [13]. Δm at T_{max} also displayed variations. The TPS/NC7% sample experienced a mass loss of 49%, while the NL-containing samples showed losses of 47% (TPS/NC7%/NL0.3%), 59% (TPS/NC7%/NL0.5%), and 52% (TPS/NC7%/NL0.7%). The high mass loss observed in the sample TPS/NC7%/NL0.5% might indicate that at this specific composition, the thermal decomposition is dominated by the degradation of NL, which is consistent with its higher T_{max}.

The T_f was derived from the TGA curves, with the TPS/NC7% sample showing the highest T_f of 542°C. The modified samples showed slightly lower T_f values: 539°C for TPS/NC7%/NL0.3%, 532°C for TPS/NC7%/NL0.5%, and 511°C for TPS/NC7%/NL0.7%. These reductions indicate that the presence of nanocomposites can influence the temperature at which decomposition ends. The ΔT varied from 458°C for TPS/NC7% to 342°C for TPS/NC7%/NL0.3%, 370°C for TPS/NC7%/NL0.5%, and 414°C for TPS/NC7%/NL0.7%. The TPS/NC7% sample exhibited the largest ΔT, indicating a broader decomposition range, while the addition of NL resulted in narrower decomposition ranges. Finally, the $R_{600°C}$ was higher in the samples containing NL, with values of 17% (TPS/NC7%/NL0.3%), 16% (TPS/NC7%/NL0.5%), and 15% (TPS/NC7%/NL0.7%), compared to 12% for the TPS/NC7% sample. This suggests that NL promotes the formation of a stable carbonaceous structure, likely due to its aromatic composition, which resists complete degradation."

15. L. 456 - phase transition or specific degradation process, obviously the authors have no idea whats going on.

Answer: We appreciate the constructive critique. We have revisited this section and expanded the analysis to justify the peaks observed in the DSC curves. These peaks were associated with specific phase transitions, such as the glass transition of starch (70°C), and structural changes promoted by NL, including matrix reorganizations and potential chemical interactions. Previous studies support the notion that the presence of lignin, with its complex and highly aromatic structure, can induce additional thermal events due to its initial degradation or structural rearrangement. The revised text now clearly explains that the observed thermal events are related to the intrinsic properties of starch and the effects of varying NL concentrations.

16. L. 455 the number of decimal points is too optimistic. I wonder what is the statter of the values if you would repeat each measurement on DSC three times.

Answer: We acknowledge the reviewer's concern about the decimal points. The values in this manuscript represent the average of three measurements, and the deviation between replicates was less than 0.5°C, ensuring the reliability of the reported results. For clarity, we will simplify the decimal points to two significant figures in the revised manuscript.

17. Following statements should be made more clear

- L. 207 - sieves? Ensuer homogeneity? L. 224 tops of the PETs? L. 231-232, 273-274?

- L. 352 lower water solubility, 353 more significant awelling?

- L. 471-472 impossible to understand, shat you mean with similar behaviour?

- L. 545 Leached weakly - another puzzle?

- L. 554 – unclear

Answer: As requested, the necessary alterations were made to the text, and the changes have been highlighted in yellow for your review.

18. Concerning the effect of NL on TGA data, I recommend to run TGA of virgin NL.

Answer: We appreciate the suggestion; running TGA on virgin NL is not essential for this study. The thermal behavior of lignin, including its degradation temperature and char residue formation, has been extensively characterized in the literature and is well-documented. In this study, our focus was on understanding the impact of NL when incorporated into the TPS/NC matrix. The observed thermal improvements, such as increased T5% and Tmax, strongly suggest the formation of new interactions between the matrix and NL. These interactions, rather than the standalone thermal properties of NL, are the primary contributors to the improved thermal stability of the composites. By referring to established data for lignin, we ensured that our analysis remains focused on the synergistic effects within the composite material, aligning with the core objective of this work.

19. Whole part of 3.2.2. is based on the data in Supplementary section. In my view this is incorrect. Either put it in main text or delete whole section

Answer: Thank you for your comment. While we understand your concern regarding the reliance on Supplementary data, we would like to emphasize that we consider Section

3.2.2 to be a crucial part of the manuscript. It provides a detailed analysis of the impact of UV-C exposure on the stability and photodegradation of the nanocomposites, which is central to understanding the behavior of the materials studied. This discussion is essential for the comprehensive interpretation of the results and for the overall relevance of the study.

Therefore, we have decided to retain this section in the manuscript, with the supplementary data included, as the images and figures are essential to illustrating the conclusions discussed in this section. However, we have made efforts to ensure that the main conclusions and key findings of Section 3.2.2 are clearly explained in the main text so that readers can understand the significance of the results, even though the detailed figures are provided in the Supplementary section.

20. L.538 539, permeability and water retention are two different properties, they do not necessarily correspond and must be deiscissed independently. Pls check the definition of permeability.

Answer: Thank you for your insightful comment. Upon review, we realize that the analysis conducted in our study focused on water retention rather than permeability. Therefore, we have revised the section to discuss water retention explicitly, as this was the primary focus of the experimental setup. The revised version of the text now adequately addresses the water retention properties of the nanocomposites and removes any reference to permeability, which was not analyzed in this experiment. We believe this clarification resolves the issue.

‘In Figure S6, the control soil, without additives (Control), showed an initial water retention of around 160%, which was used as a reference. The addition of TPS to the soil increased this retention to approximately 180%, which was attributed to the hygroscopic nature of TPS. The polar groups in TPS strongly interacted with water molecules, forming hydrogen bonds and enhancing water absorption [13]. When NC were added (TPS/NC7%), water retention slightly decreased, reaching around 170%. This suggested that the presence of NC influenced the composite structure, making it denser and reducing its ability to hold moisture, as it became less effective at retaining water.

When NL was added (TPS/NC7%/NL0.3%), water retention was further reduced, down to approximately 150%. This effect was explained by the hydrophobic properties of lignin, which hindered water absorption by the starch and nano clay matrix [42]. NL

acted as an additional barrier, reducing the water retention of the composite by decreasing its ability to absorb and retain moisture."

21. English is in some parts not quite understandable, e.g. L. 68 "significantly benefit plant development".

Answer: Thank you for your comment. We have revised the sentence for clarity. The revised version reads:

"Also, lignin can be used as a soil conditioner due to its physical, chemical, thermal, and biological properties, which greatly enhance plant growth and development [12,13]."

- L. 115, glycerine and glycerol are the two different chemicals? What means P.A.?

Answer: In response to your query, glycerine and glycerol refer to the same chemical compound, $C_3H_8O_3$; sorry for the error. The term "P.A." stands for "Purissimum Analysis," which indicates that the chemical is of analytical grade, meaning it is suitable for laboratory use due to its high purity.

- L 200 Very awkward expression, perhaps something like: The distance between the sample and the lamp…

"The distance between the sample and the lamp was maintained at 20 cm for 21 days."

Answer: Other parts of the manuscript have been revised for clarity in English.

Reviewer #2: The paper's primary objective requires more nanoparticle characterization studies. Microscopy morphology studies and nanoparticle size distribution are the minimum evidence for nano approval. After that, more studies are needed about the diffusion of nanoparticles as a function of size into the crop via soil. Is there evidence that excess nanoparticles are in crops?

Comments: We appreciate your comments and suggestions. However, we would like to clarify that the primary objective of this study was to investigate the effectiveness of thermoplastic starch (TPS)-based nanocomposites with the addition of nanoclay (NC) and nanolignin (NL) as soil conditioners, focusing on their physical, chemical, and thermal properties and their resistance to UV-C degradation. While nanoparticle characterization is an important aspect for further approval in studies of their interactions with soil and

plants, the emphasis of this study was on evaluating their effectiveness under practical cultivation conditions and their impact on soil health and plant performance.

The novelty of this paper lies precisely in the practical application of nanocomposites as soil conditioners and their direct impact on plant performance and agricultural sustainability. By focusing on the effectiveness of the developed materials as soil conditioners, our results demonstrate how adding NC and NL improves key characteristics such as cation exchange capacity (CEC), water retention, UV-C degradation resistance, and controlled nutrient release. These aspects are crucial for promoting soil health and plant growth, which are the central objectives of this study.
In this context, we performed the essential characterizations for the scope of the work, including sample morphology analysis (SEM), particle size distribution (TGA and DSC), soil water retention, cation exchange capacity (CEC), UV-C degradation resistance, and NPK fertilizer absorption and controlled release tests. These tests provide a comprehensive view of how the nanocomposites influence soil structure, water retention, nutrient release, and degradation protection, which are crucial for assessing their effectiveness as soil conditioners.

Additionally, we would like to emphasize that the NC used in this study is commercial. Therefore, its characteristics have already been extensively described in the literature, making additional characterization unnecessary. As for the NL, it was developed in other studies in the literature, as mentioned in the manuscript, and its properties have been previously explored, so a further in-depth characterization of these properties was not required for this study.

Regarding the additional characterization of nanoparticles, we recognize its importance in specific research contexts. However, based on the scope of this study, we opted not to delve into the diffusion of nanoparticles in plants, as this study focused primarily on the beneficial effects of the nanocomposites on the soil and plant health without directly exploring the migration of nanoparticles to the crops. Existing literature suggests that NL and NC have properties that allow plants to modulate soil characteristics and nutrient uptake, as observed in the tomato plant tests.

Furthermore, we did not observe any evidence of adverse effects on plant development or excessive accumulation of nanoparticles in the crops tested, suggesting that the nanoparticles do not accumulate in the plants in a harmful way. A more detailed analysis of nanoparticle safety and behavior in plants can be addressed in future studies, but it was beyond the scope and objectives of the current work.

Therefore, we believe that the characterizations conducted were adequate for the objectives of this study and provided valuable insights into the potential of nanocomposites as sustainable soil conditioners. The suggestion to include more studies on nanoparticle diffusion into plants, while relevant in another context, falls outside the central theme of this study, which focuses on the application of the nanocomposites in soil and their impact on soil properties and plant growth.

Graphical Abstract

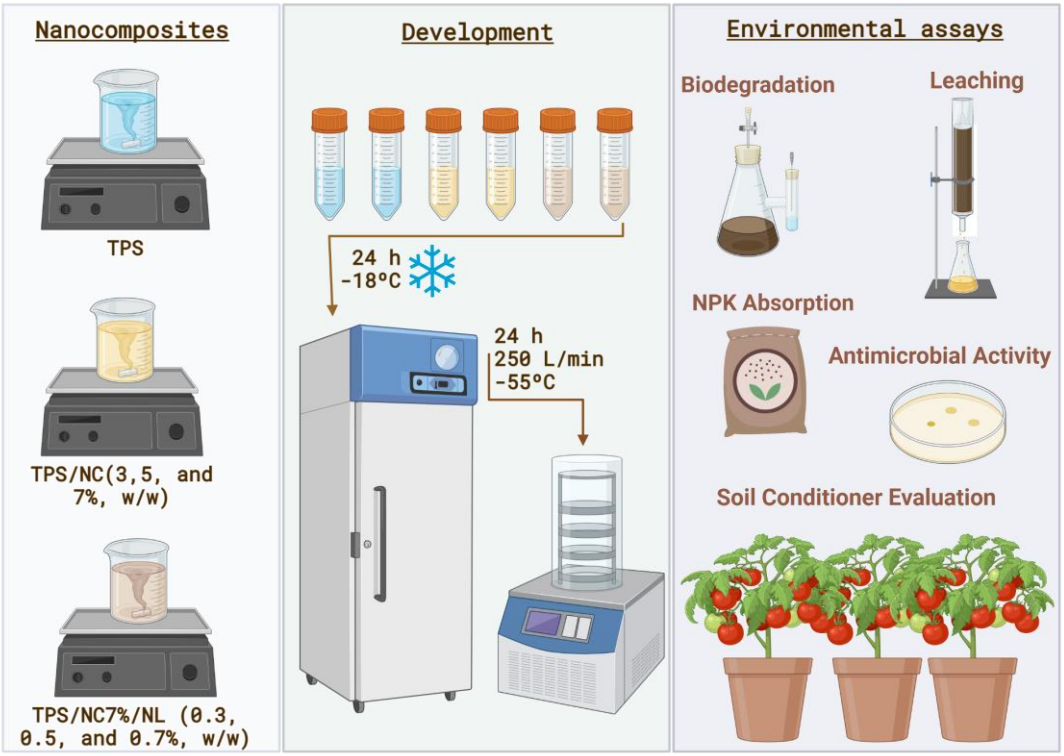

llustrative diagram of the preparation process for nanocomposites (TPS, TPS/NC, and TPS/NC/NL) and the analyses performed to evaluate the environmental behavior of the soil conditioner, including biodegradation, leaching, NPK absorption, antimicrobial activity, and performance in planting.

Designing Sustainable Soil Conditioners: Nanocomposite-Based Thermoplastic Starch for Enhanced Soil Health and Crop Performance

Jéssica S. Rodrigues[a1], Amanda S. M de Freitas[a,b1], Henrique O. S. Vieira[b], Lívia S. Emidio[b], Stefanny F. Amaro[b], Mariana A. Azevedo[b], Iolanda C. S. Duarte[b], Vagner R. Botaro[b], Leonardo F. Fraceto[a], Marystela Ferreira[b]

[a]Institute of Science and Technology of Sorocaba, São Paulo State University (UNESP), Av.Três de Março 511, 18087-180, Sorocaba, SP, Brazil.

[b] Science and Technology Center for Sustainability (CCTS), Federal University of São Carlos (UFSCar), João Leme dos Santos, km 110, 18052-780, Sorocaba, SP, Brazil.

[1] These authors contributed equally to the manuscript

Corresponding author: marystela@ufscar.br

HIGHLIGHTS

- TPS nanocomposites with nanoclay (NC) and nanolignin (NL) for soil conditioning
- Enhanced cation exchange capacity (CEC) and swelling properties with 7% NC
- Improved UV-C photodegradation resistance and thermal stability with 0.3% NL
- Superior water retention and controlled NPK release, reducing nutrient leaching
- Demonstrated antimicrobial activity against Gram-positive and negative bacteria

COVER LETTER

Dear Editor,

I am pleased to submit our manuscript entitled “Designing Sustainable Soil Conditioners: Nanocomposite-Based Thermoplastic Starch for Enhanced Soil Health and Crop Performance” for consideration in International Journal of Biological Macromolecules.

In this study, we developed and characterized nanocomposites of thermoplastic starch (TPS) with nanoclay (NC) and nanolignin (NL) as advanced soil conditioners. Our findings reveal that these materials improve soil water retention, enhance cation exchange capacity, and enable controlled nutrient release, significantly reducing fertilizer leaching. Furthermore, their resistance to UV-C degradation and antimicrobial properties highlight their durability and multifunctionality. Real cultivation tests with cherry tomatoes confirmed their effectiveness in improving plant development, showcasing their potential for scalable and sustainable agricultural practices. The manuscript provides novel insights into the development of biodegradable, biomass-based materials for soil conditioning, leveraging NC and NL as functional additives to enhance TPS performance. We believe that our work will interest researchers and practitioners seeking eco-friendly solutions for agricultural sustainability and soil management.

We affirm that this manuscript is original, has not been published elsewhere, and is not under consideration by any other journal. All authors have approved the submission and declare no conflicts of interest.

Thank you for considering our manuscript for publication in International Journal of Biological Macromolecules. We look forward to the opportunity to contribute to your esteemed journal and are available to address any questions or concerns regarding this submission.

Sincerely,

Prof. Dr. Marystela Ferreira
Federal University of São Carlos
Marystela@ufscar.br

Declaration of interests

☒ The authors declare that they have no known competing financial interests or personal relationships that could have appeared to influence the work reported in this paper.

☐The authors declare the following financial interests/personal relationships which may be considered as potential competing interests:

Designing Sustainable Soil Conditioners: Nanocomposite-Based Thermoplastic Starch for Enhanced Soil Health and Crop Performance

Jéssica S. Rodrigues[a1], Amanda S. M de Freitas[a,b1], Henrique O. S. Vieira[b], Lívia S. Emidio[b], Stefanny F. Amaro[b], Mariana A. Azevedo[b], Iolanda C. S. Duarte[b], Vagner R. Botaro[b], Leonardo F. Fraceto[a], Marystela Ferreira[b]

[a]Institute of Science and Technology of Sorocaba, São Paulo State University (UNESP), Av.Três de Março 511, 18087-180, Sorocaba, SP, Brazil.

[b] Science and Technology Center for Sustainability (CCTS), Federal University of São Carlos (UFSCar), João Leme dos Santos, km 110, 18052-780, Sorocaba, SP, Brazil.

[1] These authors contributed equally to the manuscript

Corresponding author: marystela@ufscar.br

ABSTRACT

The growing demand for sustainable solutions in agriculture, driven by global population growth and increasing soil degradation, has intensified the search for sustainable soil conditioners. This study investigated the impact of adding nanoclay (NC) and nano lignin (NL) to thermoplastic starch (TPS) on its physical, chemical, and thermal properties, its effectiveness as a soil conditioner, and its resistance to UV-C degradation. TPS nanocomposites were prepared with varying NC (3%, 5%, 7%) and NL (0.3%, 0.5%, 0.7%) proportions and characterized by FTIR (Fourier Transform Infrared Spectroscopy), SEM (Scanning Electron Microscopy), TGA (Thermogravimetric Analysis), and DSC (Differential Scanning Calorimetry). Swelling tests, phosphate buffer solubility, cation exchange capacity (CEC), and UV-C degradation resistance were evaluated. Results indicated that incorporating 7% NC (TPS/NC7%) significantly improved TPS's CEC and swelling properties. Conversely, adding 0.3% NL (TPS/NC7%/NL0.3%) improved photodegradation resistance and thermal stability. The TPS/NC7%/NL0.3% nanocomposites also demonstrated superior water retention in soil, efficient absorption and controlled release of nitrogen, phosphorus and potassium (NPK) fertilizer, significant reduction in the leaching of NH_4^+, $H_2PO_4^-$, and K^+ ions, and antimicrobial activity against both Gram-positive and Gram-negative bacteria, highlighting their biodegradability and potential as soil conditioners to promote agricultural sustainability. Additionally, tests conducted on cherry tomatoes confirmed the effectiveness of these nanocomposites under real cultivation conditions, with improved seedling development when using the TPS/NC7%/NL0.3% soil conditioner.